

AD-A125 951

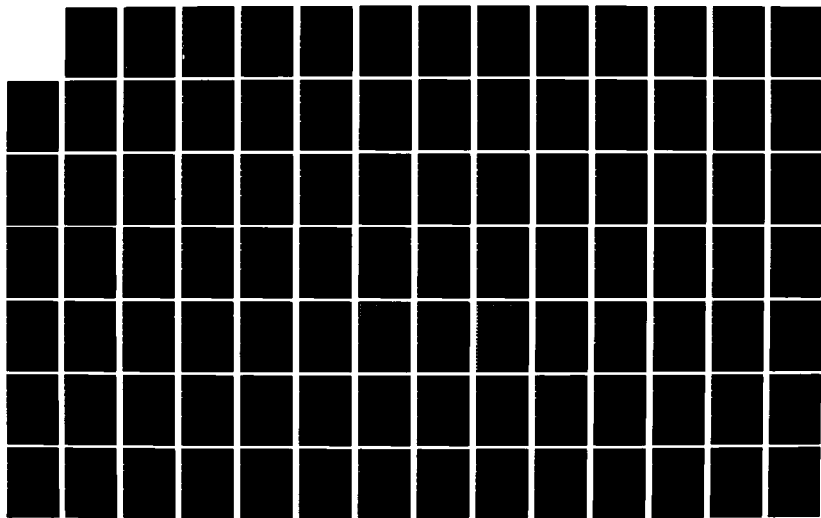
NOISE PHENOMENA IN CROSSED-FIELD ELECTRON BEAMS(U) UCA
SYSTEMS INC PALO ALTO CA G P KOOVERS ET AL. 15 APR 80
AFOSR-TR-83-0132 F49620-77-C-0061

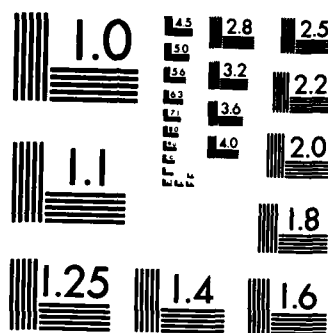
1/2

UNCLASSIFIED

F/G 9/1

NL





MICROCOPY RESOLUTION TEST CHART
NATIONAL BUREAU OF STANDARDS-1963-A

2

NOISE PHENOMENA IN
CROSSED-FIELD ELECTRON BEAMS

FINAL TECHNICAL REPORT

Submitted to:

Air Force Office of Scientific Research (AFSC)
Building 410
Bolling Air Force Base, D.C. 20332

Prepared by:

UCA Systems Inc.
701 Welch Road
Palo Alto, California 94304

Principal Investigators:

Gerald P. Kooyers Ph. 415-328-8200
Elden K. Shaw Ph. 415-328-8200

Contract:

Noise Phenomena in Crossed-Field Electron Beams

Contract F49620-77-C-0061
Period 15 February 1977 - 14 February 1980

15 April 1980

Approved for public release;
distribution unlimited.

83 03 18 078

ADA 125951

DTIC FILE COPY

DTIC
ELECTE
APR 21 1983

UNCLASSIFIED

SECURITY CLASSIFICATION OF THIS PAGE (When Data Entered)

REPORT DOCUMENTATION PAGE		READ INSTRUCTIONS BEFORE COMPLETING FORM
1. REPORT NUMBER AFOSR-TR- 83 - 0182	2. GOVT ACCESSION NO. A125957	3. RECIPIENT'S CATALOG NUMBER
4. TITLE (and Subtitle) NOISE PHENOMENA IN CROSSED-FIELD ELECTRON BEAMS		5. TYPE OF REPORT & PERIOD COVERED FINAL
		6. PERFORMING ORG. REPORT NUMBER
7. AUTHOR(s) GERALD P. KOOYERS ELDEN K. SHAW		8. CONTRACT OR GRANT NUMBER(s) F49620-77-C-0061
9. PERFORMING ORGANIZATION NAME AND ADDRESS UCA Systems Inc. 701 Welch Road Palo Alto, California 94304		10. PROGRAM ELEMENT, PROJECT, TASK AREA & WORK UNIT NUMBERS 61102F 2305/C1
11. CONTROLLING OFFICE NAME AND ADDRESS AFOSR/NE Building 410 Bolling AFB, DC 20332		12. REPORT DATE APRIL 1980
		13. NUMBER OF PAGES 113
14. MONITORING AGENCY NAME & ADDRESS (if different from Controlling Office)		15. SECURITY CLASS. (of this report) UNCLASSIFIED
		15a. DECLASSIFICATION/DOWNGRADING SCHEDULE
16. DISTRIBUTION STATEMENT (of this Report) APPROVED FOR PUBLIC RELEASE; DISTRIBUTION UNLIMITED		
17. DISTRIBUTION STATEMENT (of the abstract entered in Block 20, if different from Report)		
18. SUPPLEMENTARY NOTES		
19. KEY WORDS (Continue on reverse side if necessary and identify by block number) crossed field beams		
20. ABSTRACT (Continue on reverse side if necessary and identify by block number) In this Final Technical Report the results of a three years' research effort directed toward the theoretical study of noise in crossed-field beams is presented. The major findings of this study are: (1) The only noise growth mechanism identified by the model in the gun region of a crossed-field beam is that due to the diocotron effect. (2) In order to reduce the noise arising in the gun region of a crossed-field beam, it is important that the entire cathode be operated in the temperature limited regime with focusing and other electrodes designed to give smooth, noncycloiding beams.		

TABLE OF CONTENTS

	<u>Page</u>
1.0 INTRODUCTION	1
1.1 Research Objectives	1
1.1.1 Specific Research Tasks of the First Year's Research Effort	2
1.1.2 Specific Tasks of the Second Year's Research Effort	2
1.1.3 Specific Tasks of the Third Year's Research Effort	3
1.2 Summary of Research Accomplishments	3
1.2.1 Research Accomplishments Associated with the Two-Dimensional Model	4
1.2.2 Research Accomplishments Associated with the Three-Dimensional Model	4
1.3 Publications Resulting from the Work Performed	5
1.4 Principal Investigators	6
2.0 HISTORICAL REVIEW OF THE CROSSED-FIELD NOISE PROBLEM	7
2.1 The Problem of Noise in Crossed-Field Devices Prior to 1977	7
2.2 Comparison of AFOSR Crossed-Field Noise Studies	8
3.0 THE TWO-DIMENSIONAL NOISE MODEL	10
3.1 Simulation of the Noisy Beam at the Cathode	10
3.1.1 Emission Number	10
3.1.2 Emission Velocities	13
3.1.3 Emission Times	14
3.2 Noise Analysis Procedures	14
3.2.1 A.C. Velocity Components	16
3.2.2 Variance of the Velocity Components	16
3.2.3 A.C. Current Components	17
3.2.4 Correlation Functions and Power Spectra	18

Table of Contents (Continued)

		<u>Page</u>
4.0	TWO-DIMENSIONAL NOISE SIMULATION EXPERIMENTS	20
4.1	Noise Growth in the Gun Region	20
4.2	Noise Variation Across the Beam	20
4.3	Variation of Noise With Frequency	24
4.4	Variation of Noise with Cathode Entrance Conditions	24
5.0	THE THREE-DIMENSIONAL NOISE MODEL	28
5.1	Solving Poisson's Equation in Three Dimensions	31
5.2	Equations of Motion	34
5.3	Noise Analysis Procedures	34
5.3.1	Current Fluctuations	35
5.3.2	Velocity Fluctuations	35
5.4	Inclusion of Electrodes (Grids) in the Model	36
5.4.1	Approximate Technique Using D.C. Potentials	36
5.4.2	Exact Approach Using a Relaxation Procedure on the Space Charge	38
6.0	THREE-DIMENSIONAL NOISE SIMULATION STUDIES	40
6.1	The Long Kino Gun Test Case	40
6.1.1	Current Fluctuation Calculations	43
6.1.2	Beam Temperature Calculations	46
6.2	Three-Dimensional Studies with Grids	46
7.0	ACCURACY AND ERROR CONSIDERATIONS IN COMPUTER SIMULATIONS	50
8.0	CONCLUSIONS AND RECOMMENDATIONS	57
	REFERENCES	58
	APPENDIX A. A SURVEY OF NOISE IN CROSSED-FIELD BEAMS	
	APPENDIX B. COMPUTER AIDED DESIGN AND ANALYSIS OF ELECTRON GUNS FOR INJECTED BEAM CROSSED FIELD AMPLIFIERS	
	APPENDIX C. COMPUTER-AIDED DESIGN OF ELECTRON GUNS FOR INJECTED-BEAM CROSSED-FIELD AMPLIFIERS	
	APPENDIX D. SOLVING POISSON'S EQUATION IN THREE DIMENSIONS	

Table of Contents (Continued)

APPENDIX E. FINITE DIFFERENCE EQUATIONS OF MOTION IN THREE DIMENSIONS

APPENDIX F. SAMPLE COMPUTER CALCULATED OUTPUT FROM THE THREE-DIMENSIONAL PROGRAM

Accession For

NTIS GRA&I	<input checked="checked" type="checkbox"/>
DTIC TAB	<input type="checkbox"/>
Unannounced	<input type="checkbox"/>
Justification	<input type="checkbox"/>

A

DTIC
COPY
INSPECTED
2

A

LIST OF ILLUSTRATIONS

<u>Figure</u>		<u>Page</u>
3-1	Noise Simulation and Evaluation Flow Diagram.	11
3-2	Noise Regions in the CFA Gun Region.	15
4-1	Noise Variation with Distance for Two Cathode Temperatures.	21
4-2	Beam "Noise" as a Function of Position as Measured by Variance of the Kinetic Potential.	22
4-3	Noise Variation Across the Beam.	23
4-4	Self Power Spectral Densities for Current and Kinetic Potential Fluctuations Near the Cathode.	25
4-5	Self Power Spectral Densities for Current and Kinetic Potential Fluctuations at the Gun Exit.	26
5-1	Flow Chart Showing Major Steps in the Three-Dimensional Program.	29
5-2	Sketch Showing the Relationship of the Major Three-Dimensional Program Modules.	30
5-3	Three-Dimensional Geometry with Boundary Conditions.	32
5-4	Three-Dimensional Geometry with Modified Boundary Conditions.	33
5-5	Noise Regions Used in Noise Calculations.	37
6-1	Crossed-Field Beam Configuration to be Studied Using the Three-Dimensional Model.	41
6-2	Cathode Current in the Long Kino Gun as a Function of Iteration Number.	42
6-3	Space Charge Smoothing as a Function of Iteration Number for the Long Kino Gun.	44
6-4	Space Charge Smoothing in a Three-Dimension Crossed-Field Gun.	45
6-5	Beam Temperature in the x-z Plane.	47
6-6	Beam Temperature in the y-z Plane.	48
6-7	Beam Temperature in the x-y Plane.	49
7-1	Exact Electrode Shapes-Long Kino Gun Design.	52
7-2	A Line Charge Parallel to a Conducting Plane.	53
7-3	Electric Field Error Due to Incorrect Electrode Position.	55

LIST OF TABLES

<u>Table</u>		<u>Page</u>
I	Comparison of AFOSR Crossed-Field Noise Studies.	9

1.0 INTRODUCTION

In this Final Technical Report the results of a three years' research effort directed toward the theoretical study of noise in crossed-field beams is presented. The major findings of this study are:

- (1) The only noise growth mechanism identified by the model in the gun region of a crossed-field beam is that due to the diocotron effect.
- (2) In order to reduce the noise arising in the gun region of a crossed-field beam, it is important that the entire cathode be operated in the temperature limited regime with focusing and other electrodes designed to give smooth, noncycloiding beams.

A more complete summary of the objectives and major accomplishments of this study is given in the next two sections. In the main body of the report, more detailed discussions of the two- and three-dimensional computer models are given together with detailed discussions of the noise simulation experiments which support the major findings given above.

1.1 Research Objectives

The general research objectives as given in the contract were:
The contractor shall furnish scientific effort needed to conduct the following research:

- a. Carry out a theoretical analysis of growth of noise in cross-field microwave tubes based on solving alternately and iteratively in steps two systems of equations - one system describing the motion of each electron and the other Poisson's equation depicting the electrostatic potential corresponding to an electron concentration - with the noise identified as averages of parameters of the motion.

- b. Computer aspects of (a) are to be performed employing the most efficient computer software and hardware.

1.1.1 Specific Research Tasks of the First Year's Research Effort

- (i) Conduct a preliminary noise study using the existing two-dimensional model at cathode.
- (ii) Generalize model under (i) by introducing new boundary conditions and variable model size.
- (iii) Investigate two-dimensional noise models in parallel plane diodes.
- (iv) Generalize to investigate three-dimensional noise models.
- (v) Obtain quantitative effects on noise due to cathode length, magnetic field strength, cathode current density, feedback-to-potential-minimum noise mechanism, and the diocotron noise mechanism.
- (vi) Identify mechanisms which on the basis of the theoretical studies imply reduced noise levels.

1.1.2 Specific Tasks of the Second Year's Research Effort

- (i) Implement the three-dimensional noise model, paying special attention to program efficiency.
- (ii) Initiate preliminary studies of noise mechanisms using the three-dimensional model.
- (iii) Test validity of present approximate techniques to study arbitrary electrode shapes in the two-dimensional model.
- (iv) Continue studies to obtain further quantitative data on the noise generation and noise growth mechanisms in the two-dimensional model.

- (v) Investigate the extent of computer generated noise in the above tasks.

1.1.3 Specific Tasks of the Third Year's Research Effort

- (i) Perform a detailed study of noise mechanisms using the three-dimensional model.
- (ii) Improve the program efficiency of the three-dimensional model developed under this contract by coding portions of the program in assembly language.
- (iii) Include and study the effect of grids in the three-dimensional model.
- (iv) Study any noise reduction techniques resulting from the study of noise mechanisms.

1.2 Summary of Research Accomplishments

The research accomplishments associated with the one- and two-dimensional models are listed below. All of the specific tasks required in the first, second, and third years' effort were completed with the exception of 1.1.3 (ii), where time did not permit coding of the program in assembly language to improve program efficiency, and 1.1.3 (iii), where time constraints only made it possible to study the effects of grids in one three-dimensional gun geometry. The study of more three-dimensional gun configurations with grids included would certainly have been desirable.

It should be noted that the two- and three-dimensional computer models are not only capable of giving information about the noise generated in a crossed-field beam but can also be used to analyze and design crossed-field guns in order to obtain optimum optics and other beam characteristics.

1.2.1 Research Accomplishments Associated with the Two-Dimensional Model

- (1) An existing self-consistent two-dimensional model was successfully modified and extended to permit the study of noise in two-dimensional crossed-field geometries.
- (2) A long Kino type crossed-field gun was studied using the two-dimensional model. The steady state characteristic of the gun agreed closely with the theoretical values predicted by the Kino gun theory.
- (3) Noise studies of the two-dimensional Kino gun led to the following conclusions:
 - Shot noise at the cathode is the most important contributor to gun noise.
 - The noise is concentrated on the upper edge of the beam as it exits the gun region.
 - Designing guns with good beam optics appears to be most important in reducing beam noise.
 - The noise increases in the gun region at an exponential rate consistent with the diocotron growth mechanism.

1.2.2 Research Accomplishments Associated with the Three-Dimensional Model

- (1) A three-dimensional computer model was developed with the following important characteristics:
 - The model is self-consistent and convergent.
 - The model includes the effects of variable magnetic fields in all three dimensions.
 - The model includes the effects of space charge.

- The model is capable of handling a variety of boundary conditions.
 - The effect of grids can be taken into account in the model.
- (2) In addition to verifying the conclusions of the two-dimensional work, three-dimensional noise studies of parallel plane diode and Kino type guns have led to the following conclusions:
- A small magnetic field perpendicular to the cathode does not decrease beam noise.
 - The smoothing effects of the space charge minimum at the cathode are present and are consistent with the results obtained by Harker. ⁽¹⁾

1.3 Publications Resulting from the Work Performed

As a result of the work performed under this contract, a paper was presented at the IEDM Meeting on December 7, 1977 in Washington, D.C. A modified version of this paper was published in the IEEE Transactions on Electron Devices. Both papers are listed below.

- (1) E. K. Shaw and G. P. Kooyers, "Computer Aided Design and Analysis of Electron Guns for Injected Beam Crossed Field Amplifiers," presented at the International Electron Devices Meeting, Wash., D.C., 1977. Published in the Technical Digest of the IEDM, p. 440, 1977. (See Appendix B of this report for the complete text)
- (2) E. K. Shaw and G. P. Kooyers, "Computer Aided Design and Analysis of Electron Guns for Injected Beam Crossed Field Amplifiers," IEEE Transactions on Electron Devices, Vol. ED-26, No. 7, p. 1100, July 1979. (See Appendix C of this report for the complete text)

1.4 Principal Investigators

- (1) Gerald P. Kooyers, President of UCA Systems Inc., Palo Alto, California.
- (2) Elden K. Shaw, Senior Research Scientist, UCA Systems Inc., Palo Alto, California, and Professor of Electrical Engineering, San Jose State University, San Jose, California.

2.0 HISTORICAL REVIEW OF THE CROSSED-FIELD NOISE PROBLEM

In the first section below the state-of-the-art of crossed-field noise studies prior to 1977 is discussed, and the limitations and problems associated with these studies are pointed out. In the subsequent section a comparison of the studies sponsored by the Air Force Office of Scientific Research is given based on 1978-1979 annual reports and verbal communication with the other researchers.

2.1 The Problem of Noise in Crossed-Field Devices Prior to 1977

Although a considerable amount of experimental and some theoretical work was done on noise in crossed-field devices prior to 1977, many of the fundamental noise mechanisms were not well understood. Almost no quantitative results were available for predicting the amount of noise generated, and no definitive experiments had been made which showed how to reduce the noise. The justification for the above conclusions is given in Appendix A, where a review of the noise problems in crossed-field beams is given.

Ultimately almost all the noise in crossed-field beams can be traced to fluctuations in velocity, position, and emission time of the electrons emitted off the cathode surface. A study of noise thus must begin at the cathode surface. If these noise fluctuations generated at the cathode did not grow as the electrons move downstream, the problem of noise in crossed-field beams would be greatly reduced. However, as discussed in Appendix A, two mechanisms of noise growth have been identified,^(2,3) and others may exist when the three-dimensional nature of the beam is considered.⁽⁴⁾ In fact, one of these noise mechanisms (feedback to the potential minimum⁽²⁾) leads to a prediction of instability for the "long" crossed-field guns now in use. Any attempt to model and predict noise must then include a reasonable downstream portion of the beam and must not be limited to the small signal regime.

The statistical or Monte Carlo approach to the study of noise in crossed-field guns was used by Wadhwa and Rowe,⁽⁵⁾ Pollack and Whinnery,⁽⁶⁾ and most recently by Lele and Rowe.⁽⁷⁾ Basically each of these approaches

is the same: the beam is approximately simulated by rods of charge (two-dimensional analyses only) which are emitted off the cathode according to the random emission processes at the cathode (with, in general, some approximations). The motion of these rods of charge is then followed in time with the motion governed by the Lorentz Force Law with the electric fields obtained from a solution of Poisson's Equation.

Unfortunately, there are two problems associated with each of these previous models which drastically limited the applicability and usefulness of the results obtained. The first problem has to do with the choice of beams studied. Only "short" guns with relatively low current density were modeled. One of the most important noise mechanisms, feedback to the potential minimum, thus was not studied and high current densities which turn out to be desirable for essentially all present CFA's were not treated at all. The second problem in each previous Monte Carlo approach has to do with computer time, and thus cost. Because the computer code for the solution of each case took a relatively long time to run, only a very limited number of cases was studied. The variation of beam noise as various parameters change is not available from these previous studies.

2.2 Comparison of AFOSR Crossed-Field Noise Studies

In Table I a comparison of the four noise studies sponsored by AFOSR is presented. This table is based on 1978-1979 reports ^{(1), (8), (9)} and private communications from the researchers ^{(10), (11)} involved in the studies. The comparison is not meant to be comprehensive. Rather, only the basic methods of approach and preliminary results are compared.

TABLE I
COMPARISON OF AFOSR CROSSED-FIELD NOISE STUDIES

	Shaw & Kooyers UCA Systems	Fontana MacGregor & Rowe Harris SAI	Harker & Crawford Stanford Univ.	Shkarofsky MPB Technologies
APPROACH	Lagrangian (particle)	Eulerian (fluid) Lagrangian (particle) ⁽¹⁾	Eulerian (fluid)	Eulerian (fluid)
Two-Dimensional Model - Completed	Yes	Yes	Yes	Yes
Three-Dimensional Model - Completed	Yes	-	No	No
Self Consistent Approach	Yes	Yes	No ⁽²⁾	No ⁽²⁾
Two-Dimensional Noise Calculations	Yes	No	Yes ⁽³⁾	Yes ⁽⁴⁾
Verified Space Charge Smoothing	Yes	-	Yes	Yes
Verified Diocotron Growth Mechanism	Yes	-	-	-
Capable of Modeling Grids	Yes	Yes	No	No
Detected Feedback to Potential Min. Instab.	No	-	No	No
Capable of Modeling Entire Gun Region	Yes	Yes	No	No
Useful as a Design Tool for CFA Guns	Yes	-	No	No
Three-Dimensional Noise Calculations	Yes	No	No	No

- NOTES: (1) Fontana used a fluid approach in the two-dimensional model which gave unsatisfactory results.
(2) Both Harker and Shkarofsky assumed a parabolic d.c. potential at the cathode.
(3) Harker solved for current fluctuations only.
(4) Shkarofsky solved for velocity fluctuations only.

3.0 THE TWO-DIMENSIONAL NOISE MODEL

In the first year's study a two-dimensional model which was originally used as a design tool for crossed-field guns was refined and modified for the study of noise in crossed-field guns. The details of this two-dimensional model are given in Appendices B and C of this report. In Fig. 3.1 a flow diagram is presented of the overall approach used in both the one- and two-dimensional studies.

The method of simulating the noisy beam at the cathode and the method of calculating noise from the beam characteristics are discussed in detail below since these topics are not discussed in detail in the Appendices.

3.1 Simulation of the Noisy Beam at the Cathode

Since, as previously stated, the ultimate source of nearly all the noise is due to random processes of electron emission at the cathode surface, it is very important that the emission properties of the cathode are modeled as accurately as possible. The cathode emission is completely specified by the following:

- (1) The number of electrons emitted in a time interval Δt
- (2) The emission velocities of the electrons
- (3) The time of emission of the electrons.

The method for calculating each of the above three quantities is summarized below.

3.1.1 Emission Number

It can be shown⁽¹²⁾ that the probability that exactly S electrons are emitted from a given cathode spot of length Δy during the time interval Δt is given by

$$f(S) = \frac{e^{-\lambda \Delta y} (\lambda \Delta y)^S}{S!} \quad (3-1)$$

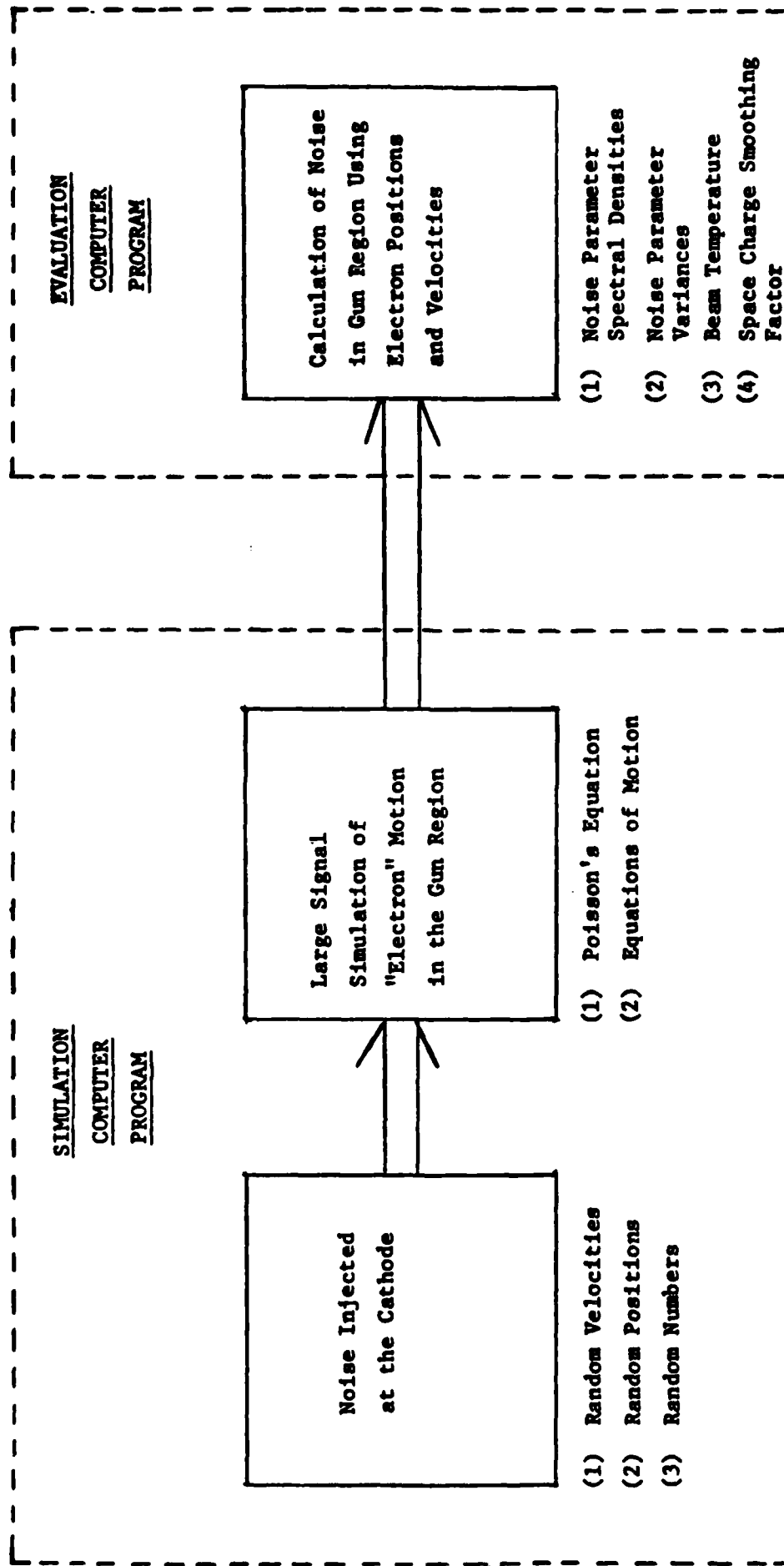


Figure 3-1. Noise Simulation and Evaluation Flow Diagram.

where λ is the average number of electrons emitted in each Δt . This is recognized to be the Poisson Distribution.

The probability that S or fewer electrons are emitted in the time interval Δt is given by the cumulative distribution function

$$F(S) = \sum_{S=0}^S f(S) \quad (3-2)$$

and

$$0 < F(S) \leq 1 \quad (3-3)$$

To determine the number of electrons emitted in a time interval, Δt , a uniformly distributed random number, R , between 0 and 1 is generated. The number of electrons emitted is S if

$$F(S-1) < R \leq F(S) \quad (3-4)$$

When $R \leq F(0)$ no electrons are emitted.

For computational purposes, the following procedure is then followed:

- (1) The maximum number, N_m , of electrons allowed to be emitted from the area $\Delta y \Delta z$ and in any Δt is selected.
- (2) $f(S)$ is then calculated for each value of S between 0 and N_m .
- (3) $F(S)$ and $F(S-1)$ are then calculated for each S between 0 and N_m using the calculated density functions $f(S)$ and are then stored in a table containing S , $F(S)$, and $F(S-1)$.
- (4) Random number R is then generated.

- (5) Knowing R , the pair of values $F(S-1)$ and $F(S)$ that bracket R are found from the table and the corresponding value of S is then known.

Initially a value of 20 was chosen for N_m . This value was used by O'Flynn⁽¹³⁾ and Kooyers⁽¹⁴⁾ for similar problems.

3.1.2 Emission Velocities

A half-Maxwellian distribution is assumed for the x component of emission velocity. The x velocity is then given by⁽⁷⁾

$$\dot{x} = \frac{2kT}{m}^{1/2} (-\ln R_x)^{1/2} \quad (3-5)$$

where R_x is a random number uniformly distributed between 0 and 1, T is the cathode temperature, k is Boltzmann's constant, and m is the electron mass.

A full-Maxwellian distribution is assumed for electron velocities in the y direction (for the two-dimensional case) and the y and z directions (for the three-dimensional case). The relation giving these velocities is

$$\dot{y} = \frac{2kT}{m}^{1/2} \text{erf}^{-1}(R_y) \quad (3-6)$$

and

$$\dot{z} = \frac{2kT}{m}^{1/2} \text{erf}^{-1}(R_z) \quad (3-7)$$

where R_y and R_z are random numbers uniformly distributed between 0 and 1. In order to simulate these velocities efficiently, an approximate formula is used for the error functions.⁽¹⁵⁾

3.1.3 Emission Times

In order to avoid calculating the positions of the electrons above the cathode for random emission times, we assume that all S of the electrons in a given Δy are emitted at the same time but with a random distribution over the Δy . The emission points are then given by

$$y = y_0 \pm R_y \frac{\Delta y}{2} \quad (3-8)$$

$$z = z_0 \pm R_z \frac{\Delta y}{2} \quad (\text{three-dimensional case}) \quad (3-9)$$

where R_y is a random number between 0 and 1 and the sign of R_y is also selected randomly. Thus, to an observer looking at one point on the cathode surface, the electrons will appear to come off that point at random times. Provided the time interval Δt is chosen to be relatively small, the degree of approximation introduced should be minor.

3.2 Noise Analysis Procedures

From the computer model we have available the positions and velocities of each electron at each discrete time $t = N_t \Delta t$ where N_t is the iteration number. In order to be useful, this information must be related to the noise. There are several different noise-related parameters which are calculated in this study.

In general we would like to be able to calculate each of these parameters at any arbitrary point (x,y,z) within the beam. However, the nature of the way we solve the problem using a finite number of electrons limits us to finding the fluctuations in some small but finite region. In order to obtain enough "electrons" in each region for reasonably good statistics, the gun region is divided into 512 noise regions which are 3×3 mesh units in size. These regions are sketched in Figure 3-2. The method used for calculating each of the parameters of interest is discussed below.

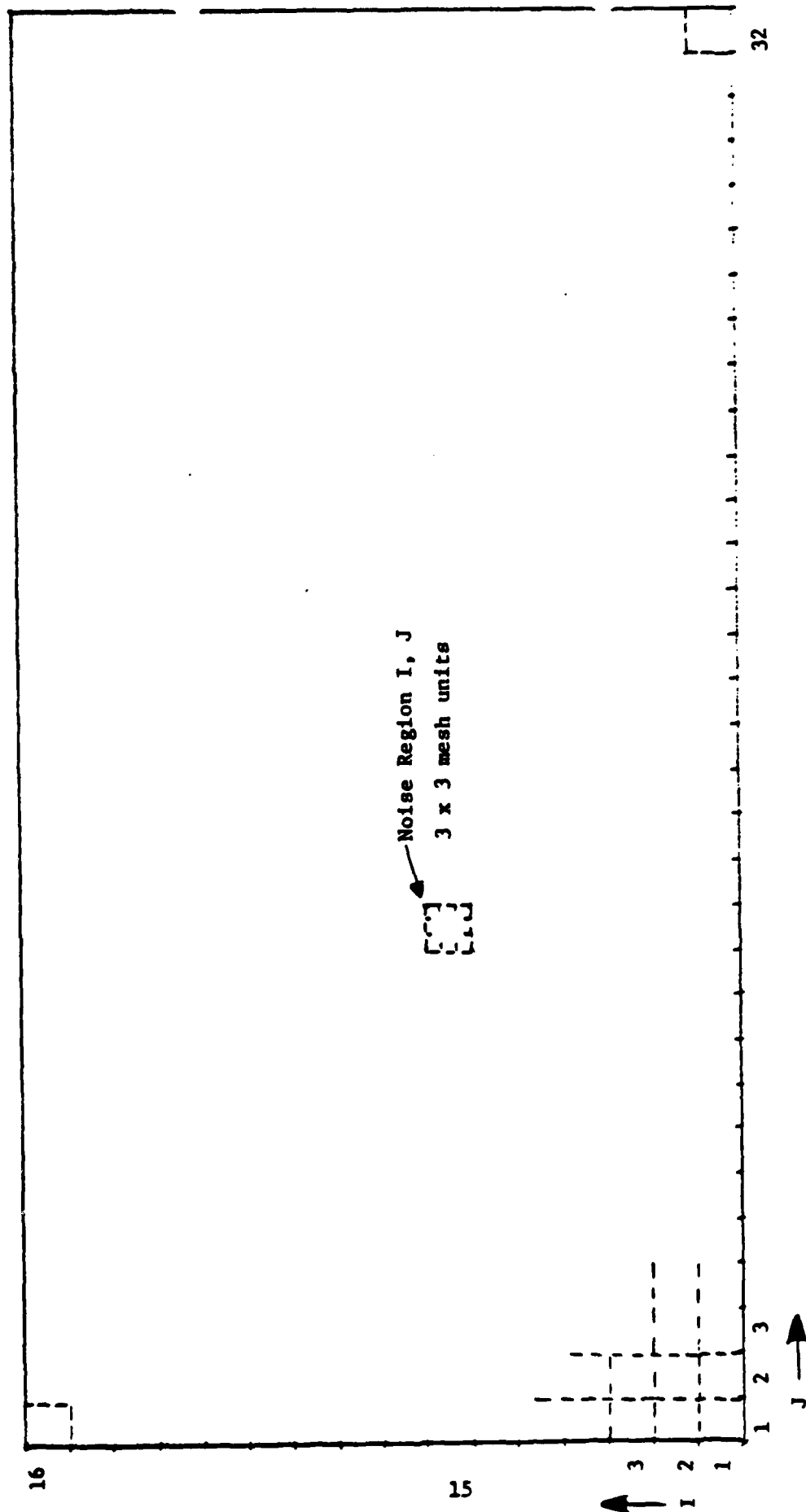


Figure 3-2. Noise Regions in the CFA Gun Region.

3.2.1 A.C. Velocity Components

In order to obtain the a.c. velocity components we first must find the average velocity. The a.c. velocity is then equal to the actual velocity minus the average velocity. The velocity averaged over one noise region at a given time t is given by

$$\langle v_{x_{i,j}}(t) \rangle = \frac{1}{N_{i,j}} \sum_{l=1}^{N_{i,j}} v_{x_{i,j}}(t, l) \quad (3-10)$$

where $v_{x_{i,j}}(t, l)$ is the x velocity of the l th electron in the i, j -th noise region. Since the equations for the other component v_y are of the same form, we carry the analysis only for the v_x component. Over the time interval $T = N_T \Delta t$ the time average velocity is given by

$$\langle v_{x_{i,j}} \rangle = \frac{1}{N_T} \sum_{m=0}^{N_T} \frac{1}{N_{i,j}} \sum_{l=0}^{N_{i,j}} v_{x_{i,j}}(t_m, l) \quad (3-11)$$

The a.c. velocity component can now be calculated at time t from

$$\tilde{v}_{x_{i,j}}(t) = \langle v_{x_{i,j}}(t) \rangle - \langle v_{x_{i,j,k}} \rangle \quad (3-12)$$

where $\tilde{v}_{x_{i,j}}(t)$ is the a.c. component of velocity in the i, j -th noise region at time t .

3.2.2 Variance of the Velocity Components

The variance of the x -velocity at time t can be found from

$$\sigma_{x_{i,j}}^2(t) = \langle v_{x_{i,j}}^2(t) \rangle - \langle v_{x_{i,j}}(t) \rangle^2 \quad (3-13)$$

where $\sigma_{x_{i,j}}^2(t)$ is the variance of the x -component of velocity in the i, j -th noise region at time t and $\langle v_{x_{i,j}}^2(t) \rangle$ is given by

$$\langle v_{x_{1,j}}^2(t) \rangle = \frac{1}{N_{1,j}} \sum_{l=1}^{N_{1,j}} v_{x_{1,j}}^2(t, l) \quad (3-14)$$

The variance of the other component of velocity can be found in a similar manner. The variance and the a.c. components of velocity are useful in that they give the relative magnitude of the fluctuations. Thus the "growth" of these fluctuations can be studied by calculating the a.c. velocity components and variances at various downstream positions in the beam. The a.c. components of velocity and their variance do not give any information about the frequency spectrum of these components.

3.2.3 A.C. Current Components

The charge density in the i, j -th noise region at time t is given by

$$\rho_{1,j}(t) = \frac{-|e| N_Q N_{1,j}}{\Delta x \Delta y} \quad (3-15)$$

where N_Q is the scaling factor for the electrons. The time averaged space charge density in the i, j -th noise region is given by

$$\langle \rho_{1,j} \rangle = \frac{-|e| N_Q}{\Delta x \Delta y \Delta z} \frac{1}{N_T} \sum_{m=0}^{N_T} N_{1,j}(t_m) \quad (3-16)$$

Now the current density at time t in the i, j -th rectangle is given by

$$J_{x_{1,j}}(t) = \rho_{1,j}(t) \dot{x}_{1,j}(t) \quad (3-17)$$

and the time average current density is given by

$$\langle J_{x_{1,j}} \rangle = \langle \rho_{1,j} \rangle \cdot \langle v_{x_{1,j}} \rangle \quad (3-18)$$

The a.c. component of the x-component of current density is thus given by

$$\tilde{J}_{x_1,j}(t) = J_{x_1,j}(t) - \langle J_{x_1,j} \rangle \quad (3-19)$$

Again, although this parameter does not tell us anything about the frequency components of the fluctuations, it is very useful in determining the relative growth rate of current fluctuations in the beam.

3.2.4 Correlation Functions and Power Spectra

Finally, in order to completely determine the noise properties of the beam, it is necessary to calculate the relative magnitudes of the various frequency components of the noise at a particular cross-section of the beam. The two quantities of interest in beginning this calculation are the a.c. kinetic potential and the a.c. current fluctuation. These two quantities may be defined for a two-dimensional beam as⁽⁷⁾

$$\tilde{V}(t) = \frac{-\vec{\mu}_0 \cdot \vec{v}(t)}{\eta} \quad (3-20)$$

and

$$\tilde{J}(t) = \frac{\vec{J}(t) \cdot \vec{J}_0}{|\vec{J}_0|} - J_0 \quad (3-21)$$

where $\tilde{V}(t)$ is the a.c. kinetic potential at time t

$\vec{\mu}_0$ is the d.c. velocity of the beam

$\vec{v}(t)$ is the a.c. component of the velocity of the beam

η is the charge-to-mass ratio of the electron

$\tilde{J}(t)$ is the a.c. current density fluctuation at time t

$\vec{J}(t)$ is the a.c. current density in the beam

\vec{J}_0 is the d.c. current density in the beam.

At this point the final problem in the spectral analysis is in relating a spectrum consisting of finite discrete data of a function $\tilde{V}(t)$ or $\tilde{J}(t)$ (each value obtained as an average over a small interval Δt) to the true spectrum of the continuous time function. Several authors have treated this subject in some detail. Results show that it is possible to calculate the Haus noise parameters $\phi(f)$, $\psi(f)$, and $\theta(f)$ from the discrete data where

$\phi(\omega)$ is the self power density spectrum of the kinetic noise voltage,

$\psi(\omega)$ is the self power density spectrum of the noise current modulation, and

$\theta(\omega)$ is the cross-power-density spectrum between the kinetic voltage and the current modulation.

For a crossed-field beam an exact relation between the noise parameters and the noise figure has not been derived. However, even without an exact expression, a study of the relative magnitudes of the various noise parameters (ϕ , ψ , and θ) as a function of position and other gun and beam parameters is very valuable in gaining an understanding of the noise mechanisms in crossed-field electron devices.

4.0 TWO-DIMENSIONAL NOISE SIMULATION EXPERIMENTS

Using the two-dimensional model, several noise simulation experiments have been carried out on a long Kino gun. The geometry and parameters of the long Kino gun are given in Appendix C. In particular, the noise growth rate, the variation of noise throughout the gun region, and the effect of changes in the beam injection conditions have been studied.

4.1 Noise Growth in the Gun Region

In Figure 4-1 the noise power spectral density due to fluctuations in the kinetic potential is plotted from the end of the cathode to where the beam exits the gun region. The noise growth appears to be approximately linear when plotted on semi-log paper, and thus the actual noise growth is exponential. For the case of Figure 4-1 a straight line approximation gives a noise growth of approximately 170 db/in which is a rather substantial growth rate. The diocotron theory also predicts an exponential growth of the noise.

4.2 Noise Variation Across the Beam

Shown in Figure 4-2 and Figure 4-3 is the variation in noise from the bottom to the top of the beam as the beam exits the gun region.

In all of these cases, noise is greater on the top edge of the beam than on the bottom edge. This may be due to the fact that the electrons on the top edge of the beam have traveled a greater distance and thus have experienced more diocotron noise growth than those electrons on the bottom edge of the beam.

Unfortunately, as the beam enters the interaction region of a CFA, the noisiest part of the beam will be nearest the slow wave circuit and thus will be more strongly coupled to the slow wave circuit.

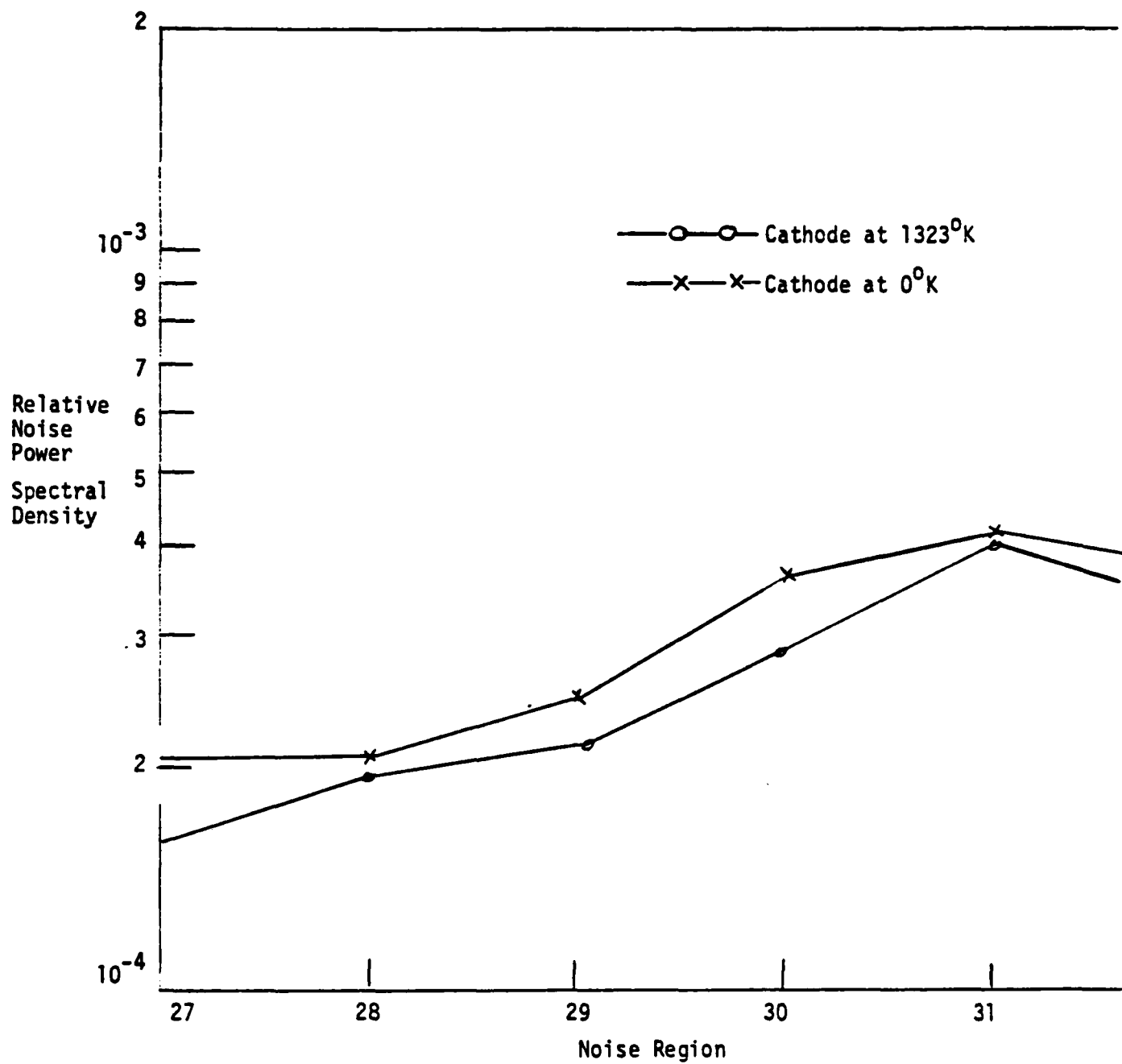


Figure 4-1. Noise Variation with Distance for Two Cathode Temperatures.

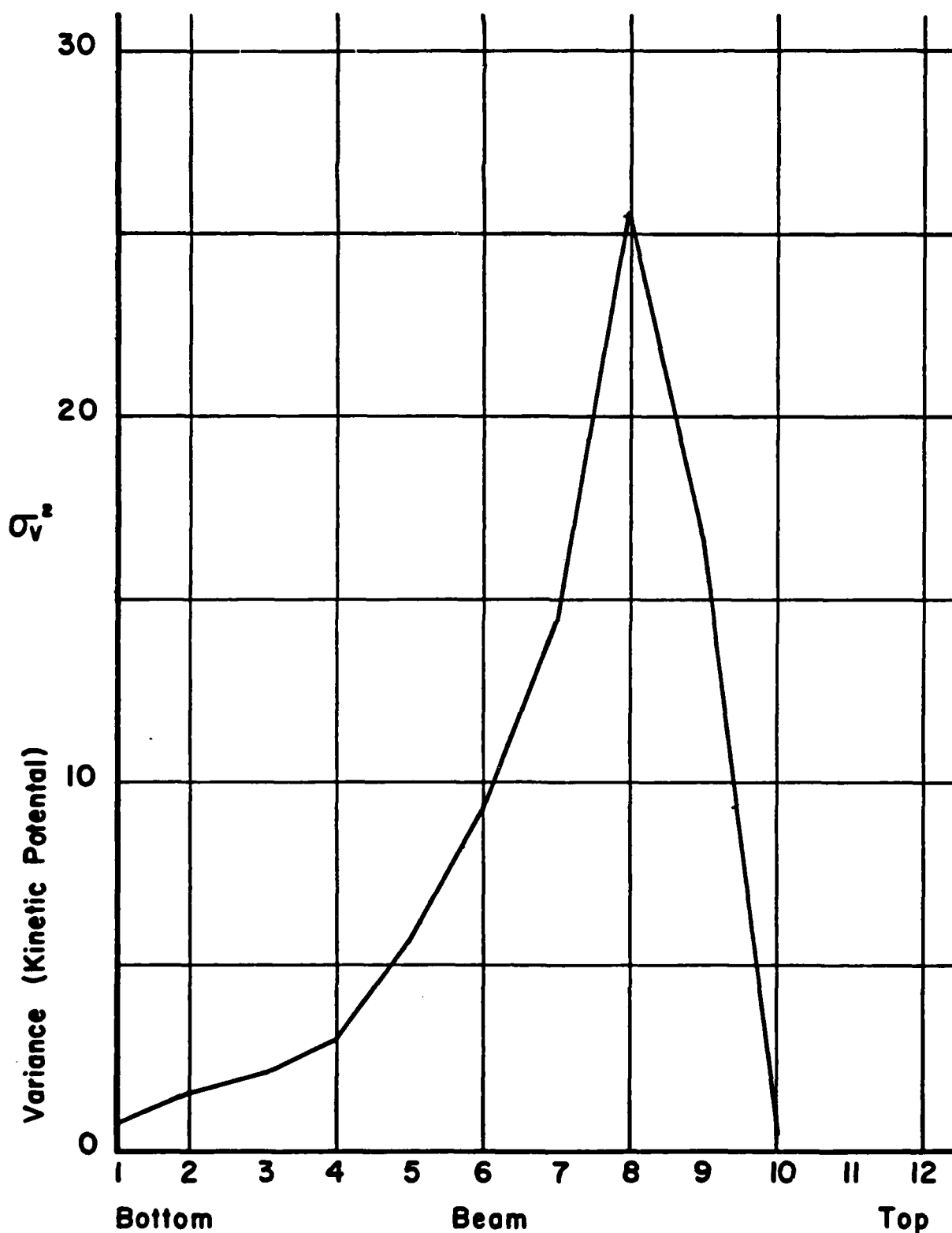


Fig. 4-2. Beam "Noise" as a Function of Position as Measured by Variance of the Kinetic Potential.

Relative
Noise
Power
Spectral
Densities
 ϕ, ψ

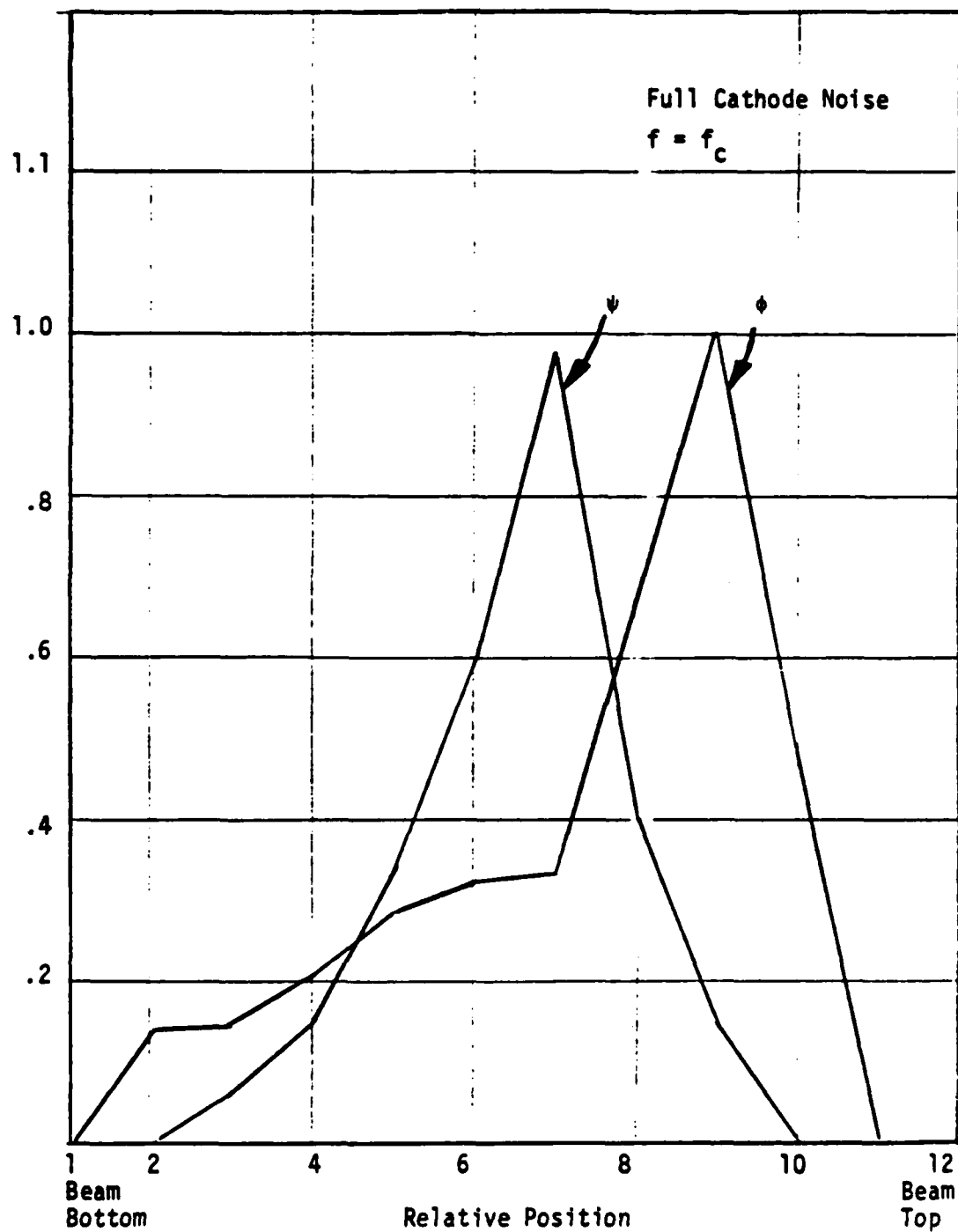


Figure 4-3. Noise Variation Across the Beam.

4.3 Variation of Noise With Frequency

Shown in Figure 4-4 and Figure 4-5 is the variation in beam noise as a function of frequency for two different positions in the beam. For Figure 4-4 the noise is sampled near the cathode; while in Figure 4-5 the noise is plotted for a noise region near the gun exit.

At the gun exit, the noise as measured by the self power spectral density, ϕ , of the kinetic potential is fairly constant with frequency, while the self power spectral density of the current density, ψ , has large peaks and valleys which roughly correspond to multiples of the cyclotron frequency.

Near the cathode both ϕ and ψ vary with frequency and have roughly the same valleys and peaks corresponding to multiples of the cyclotron frequency. The variation of noise with frequency near the cathode would be unexpected if it were not for the fact that many of the electrons near the cathode have been in the gun for a relatively long time due to two effects:

- (1) Electrons returning to the gun on a cycloidal path from further upstream
- (2) Electrons which migrate downstream while maintaining a position very close to the cathode.

In both cases noise growth mechanisms have sufficient time to affect the noise characteristics of these electrons.

4.4 Variation of Noise with Cathode Entrance Conditions

In order to study the relative effects of the various noise generation mechanisms at the cathode, computer runs were made with the following injection conditions:

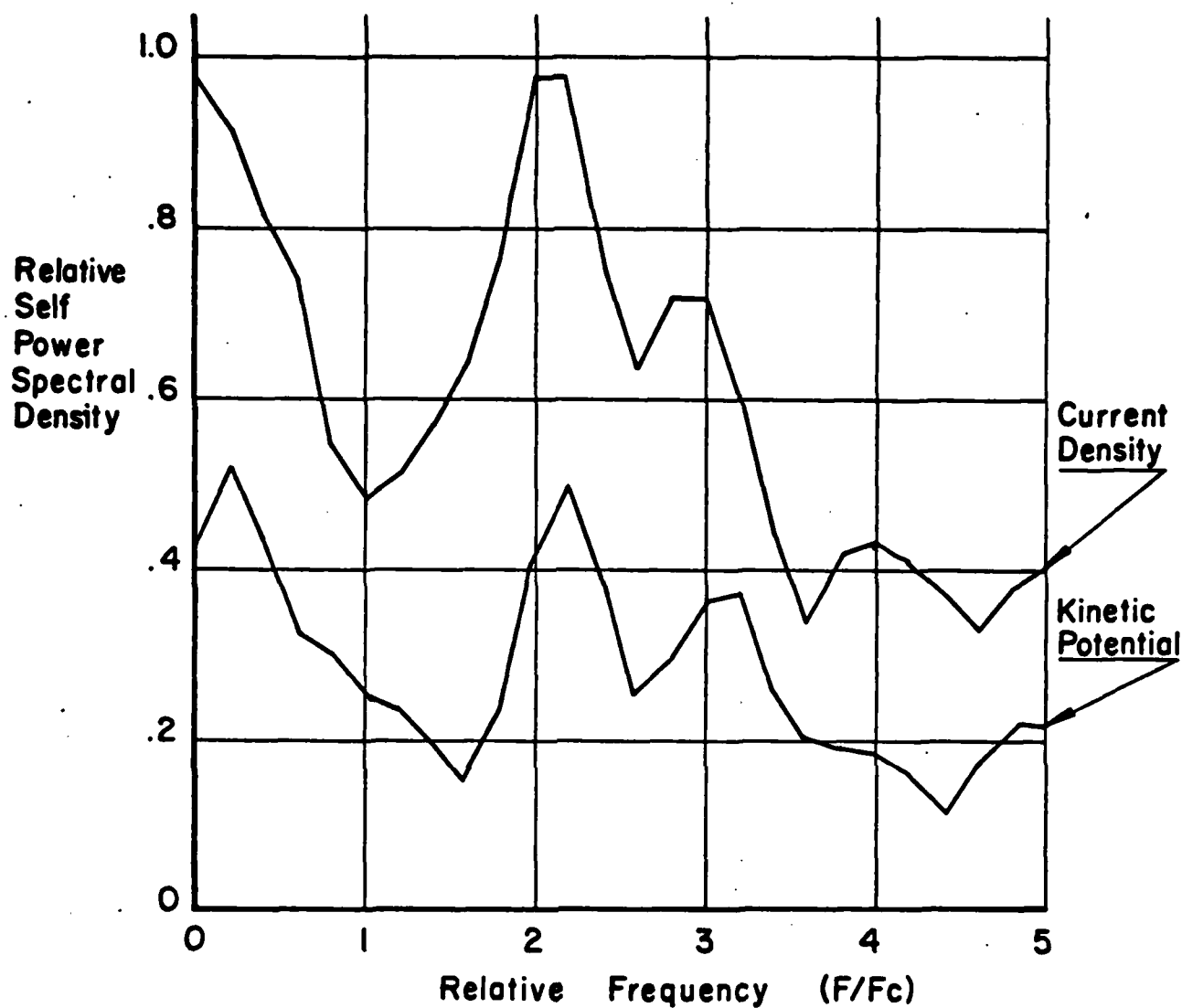


Fig. 4-4. Self Power Spectral Densities for Current and Kinetic Potential Fluctuations Near the Cathode.

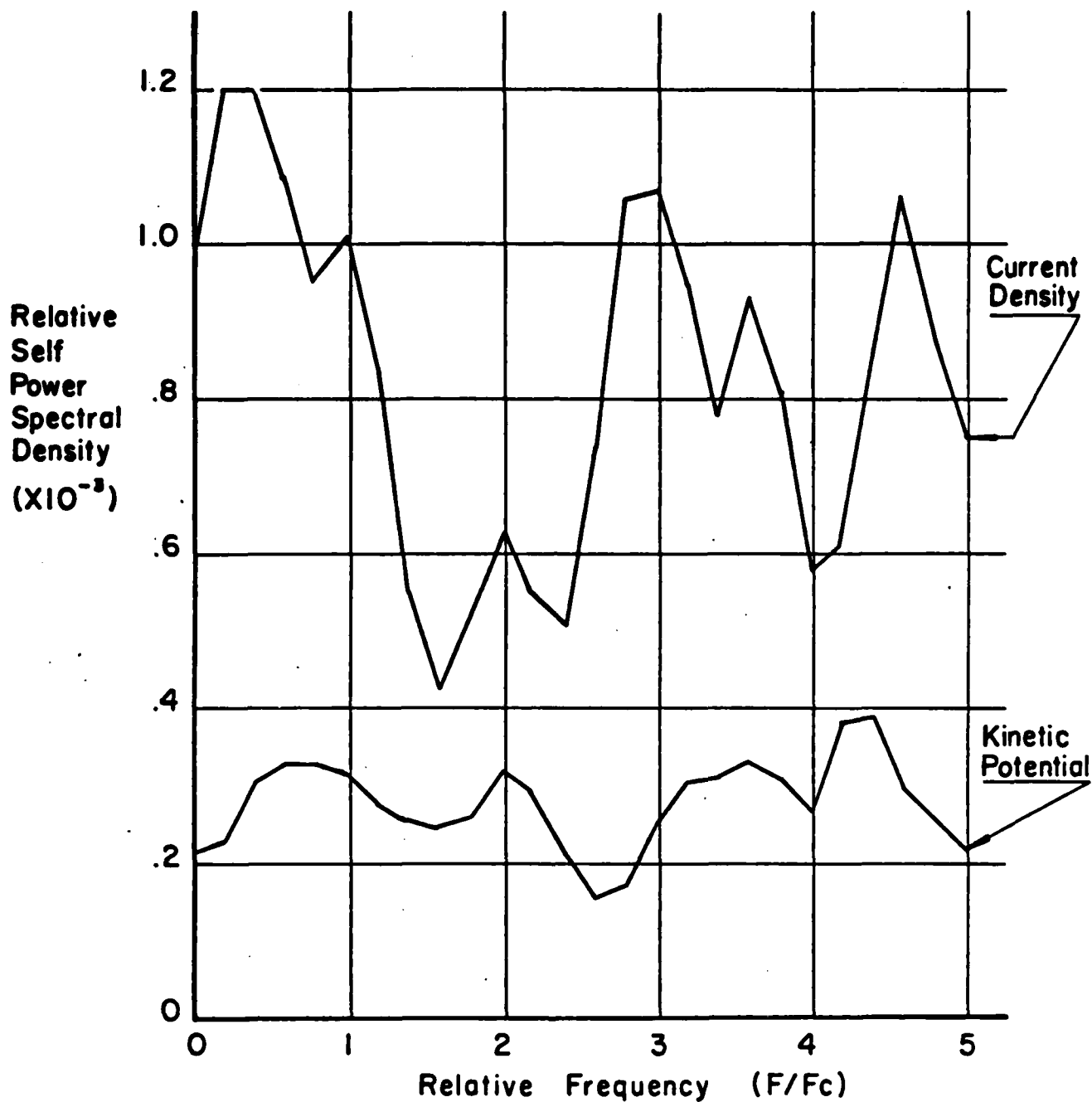


Figure 4-5. Self Power Spectral Densities for Current and Kinetic Potential Fluctuations at the Gun Exit.

- (1) Random positions and random numbers* injected but with four different injection velocities:
 - (a) Zero velocity (Temperature = 0)
 - (b) Uniform velocity
 - (c) Maxwellian velocities (Temperature = T)
 - (d) Velocities consistent with the electric fields at the cathode.

* But with constant average current emitted from the cathode surface and with the cathode space charge limited.

- (2) Random positions, random numbers injected, and Maxwellian velocities but with variable amounts of charge per "electron" from the cathode surface.

Noise outputs for the various input conditions of cases (1) above indicate that the noise is not appreciably affected by the electron injection velocities. A typical plot of noise output for simulated cathode temperatures of 0 and 1323°K is given in Figure 4-1.

In all the cases (1) above, the cathode is running in a space-charge-limited condition. If the numbers of electrons emitted from the cathode are reduced to the point where the cathode becomes temperature limited, the optics of the gun deteriorate and the noise in the beam increases dramatically.

When the total charge carried by one "electron" is increased, the shot noise is increased in direct proportion. This corresponds to the input condition of cases (2) above. Noise output from the computer simulation as measured by the velocity variance also goes up in direct proportion to the amount of charge per "electron." These results indicate that shot noise is the main contributor to beam noise in this model.

5.0 THE THREE-DIMENSIONAL NOISE MODEL

The three-dimensional noise model solves for the motion of charges in a three-dimensional rectangular geometry including the effects of static electric and magnetic fields and space charge. A computer program written in FORTRAN IV carries out the steps given in the flow chart of Figure 5-1.

A sample of the output generated by this program is given in Appendix F. Information is printed out giving cathode current density, distribution of charges in the beam, selected charge trajectory information, etc. for each time step.

Below, details are given on the potential, trajectory, and noise calculations.

The three-dimensional program consists of the major program modules shown in Figure 5-2. The function of each program module is given below:

- GUN3D - Main calling program which reads in gun data, initializes program variables, and calls other program modules.
- TRAJ3D - Solves the three-dimensional trajectory equations including variable magnetic fields in the x, y, and z directions.
- EMIT3D - Calculates particle emission numbers, positions, and velocities as they are emitted from the cathode.
- POSS3D - Solves Poisson's Equation in three dimensions using subroutines FOUR67 and PWSCRT.
- NOIS3D - Calculates current and velocity fluctuations in the beam and uses these fluctuations to calculate the space charge smoothing factor and the "temperature" of the beam at various locations within the beam.

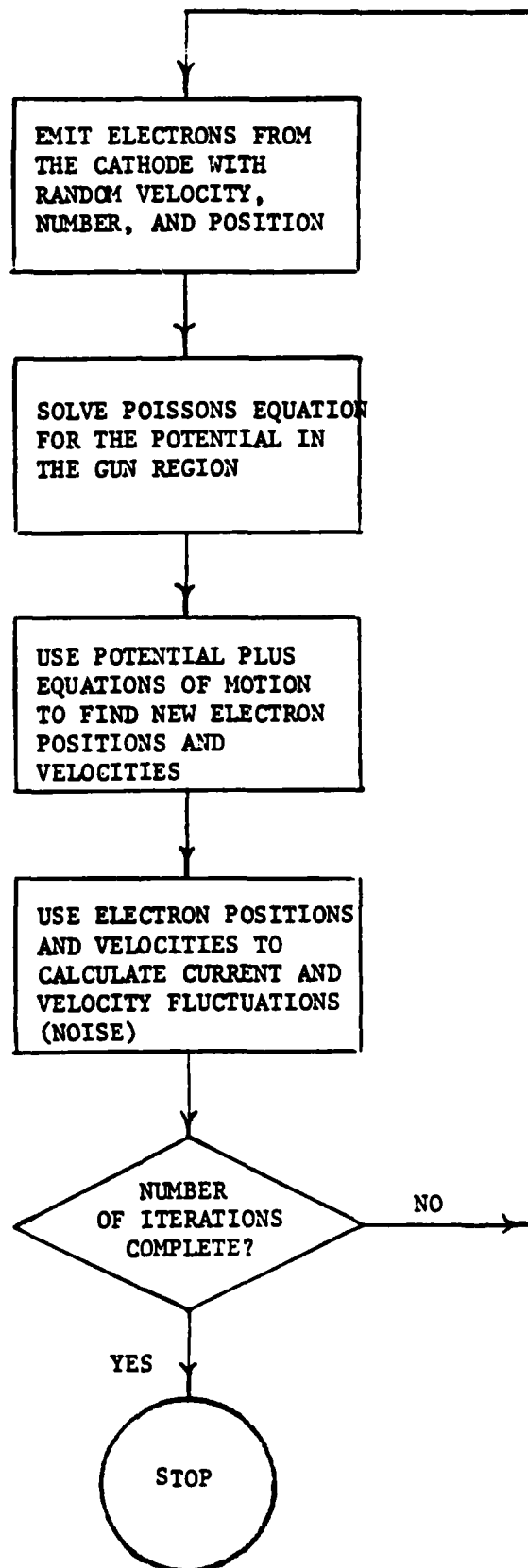


Figure 5-1. Flow Chart Showing Major Steps in the Three-Dimensional Program.

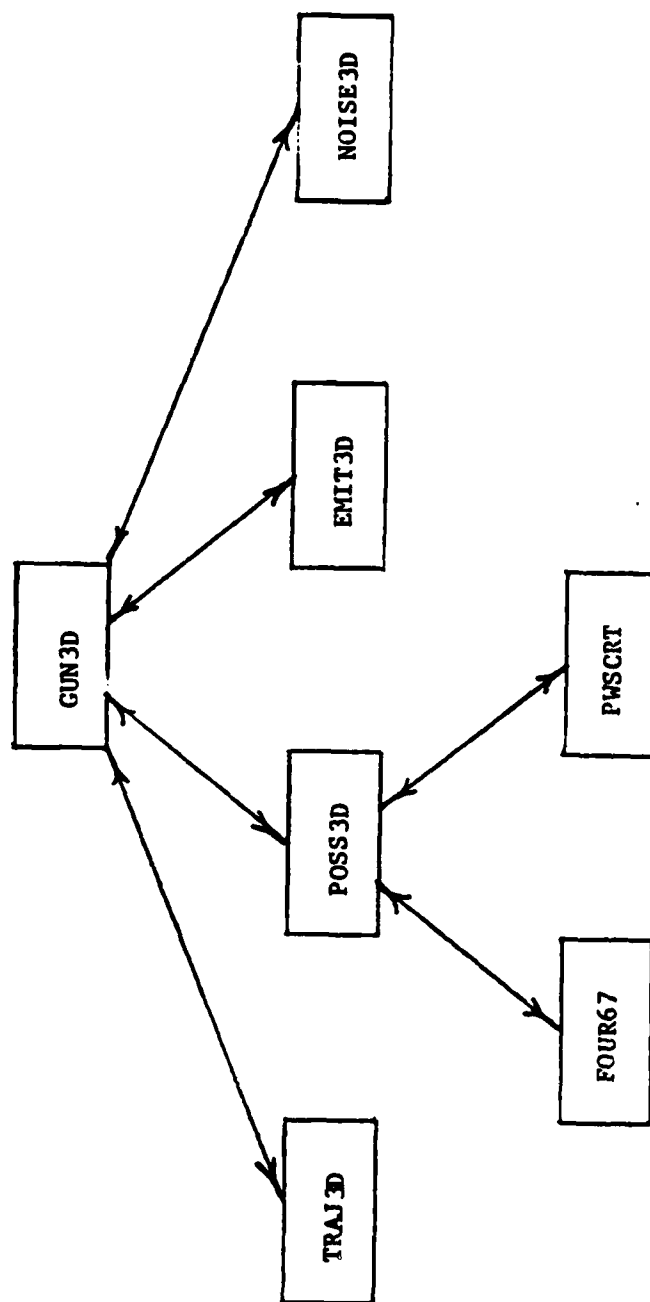


Figure 5-2. Sketch Showing the Relationship of the Major Three-Dimensional Program Modules.

5.1 Solving Poisson's Equation in Three Dimensions

In order to obtain the potentials in the three-dimensional region, it is necessary to solve the Poisson Equation

$$\frac{\partial^2 \phi}{\partial x^2} + \frac{\partial^2 \phi}{\partial y^2} + \frac{\partial^2 \phi}{\partial z^2} = -\rho/\epsilon_0 \quad (5-1)$$

in the region sketched in Figure 5-3. The boundary conditions shown in Figure 5-3 are chosen to be consistent with three-dimensional crossed-field gun geometries. Boundary conditions on the z-boundaries allow for potentials with the derivative equal to zero, periodic potentials, or constant potentials.

The finite difference techniques used in the solution are given in detail in Appendix D for the case of fixed potentials on the z-boundaries and follow a method suggested by Swartrauber and Sweet.⁽¹⁶⁾ Figure 5-4 shows the mesh geometry used in the finite difference solution. A very brief review of the technique is given below.

- (1) The finite Fourier expansion of the five point difference approximation to Poisson's Equation is taken in the z-direction using a program which performs the Fourier transform⁽¹⁷⁾ (FOUR67). This leads to n-1 two-dimensional Helmholtz equations

$$\nabla^2 \bar{\phi} + K^2 \bar{\phi} = \bar{\rho} \quad (5-2)$$

where $\bar{\phi}$ and $\bar{\rho}$ are the transformed potentials and space charge and K is a constant which depends on n . The space charge assigned to each mesh point is found by adding together the total number of particles in a cell ($h_x \times h_y \times h_z$) centered on the mesh point. This is commonly called the particle in cell (PIC) approach.

- (2) Equation (5-2) is then solved for the transformed potentials using an existing program (PWSCRT).⁽¹⁶⁾

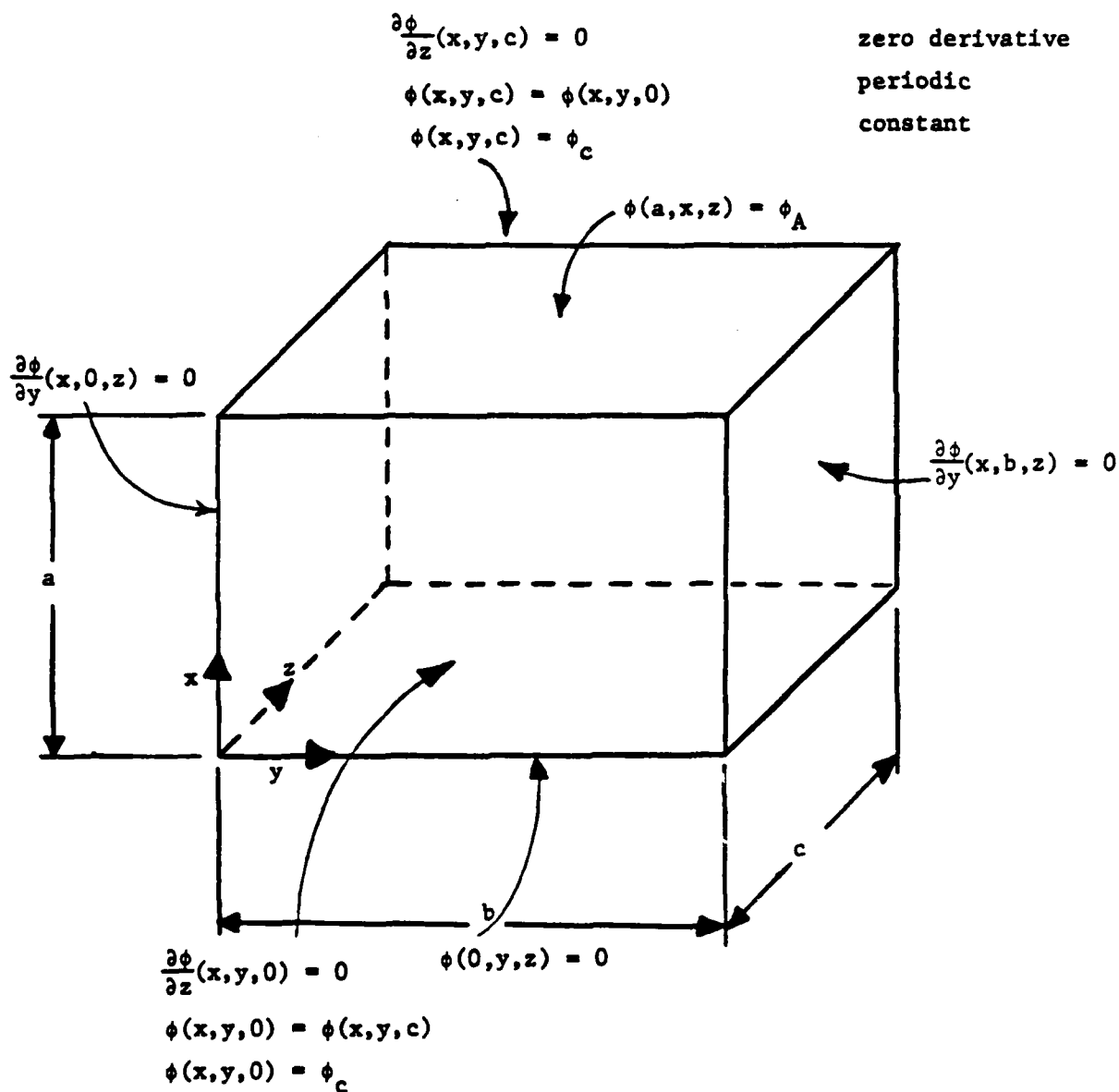


Figure 5-3. Three-Dimensional Geometry with Boundary Conditions.

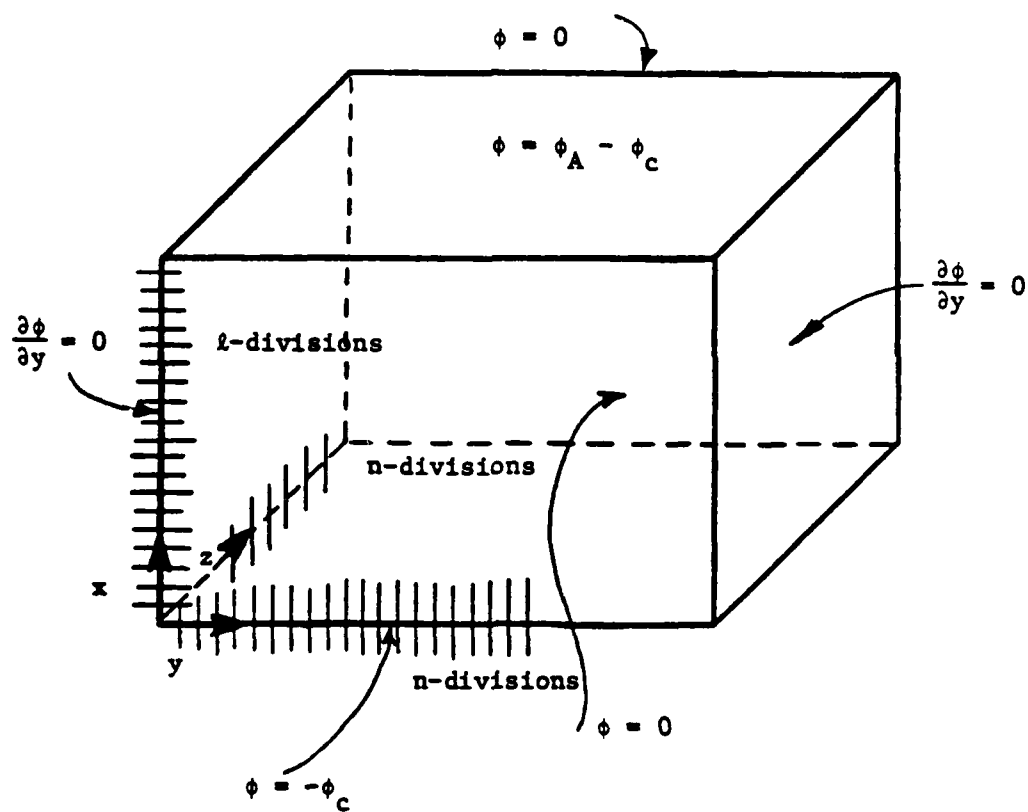


Figure 5-4. Three-Dimensional Geometry with Modified Boundary Conditions.

- (3) Given the transformed potentials a program (FOUR67)⁽¹⁷⁾ is used to obtain the actual potentials by performing the inverse Fourier Transform.

5.2 Equations of Motion

A detailed discussion of the development of the three-dimensional finite difference equations of motion is given in Appendix E. There are several facts which should be noted concerning these equations:

- (1) The finite difference equations of motion are accurate to second order and are solved in a right-handed coordinate system.
- (2) The electric field is assumed to be a slowly varying function of position (i.e., does not change much in one time step).
- (3) The magnetic field is assumed to consist of x, y, and z components which may be slowly varying functions of position.
- (4) The equations are solved in such a way as to be exact for any size time step provided the electric and magnetic fields are constant.

5.3 Noise Analysis Procedures

A separate noise analysis program (NOIS3D) has been written to perform noise analysis on the three-dimensional beam. This program calculates two parameters which are closely related to beam noise: the space charge smoothing parameter (current fluctuations) and the beam temperature (velocity fluctuations). Details of the techniques used to make these calculations are given below.

5.3.1 Current Fluctuations

In order to determine the growth of current fluctuations in the beam, the current fluctuations at the cathode are calculated using computer generated values of instantaneous cathode current, I_K , and a running average of the cathode current, $\langle I_K \rangle$. At each iteration, the current fluctuation at the cathode is calculated from

$$\tilde{I}_K = I_K - \langle I_K \rangle \quad (5-3)$$

Similarly the fluctuations in the beam current at various planes in the gun region are calculated from

$$\tilde{I}_B = I_B - \langle I_B \rangle \quad (5-4)$$

at each iteration.

A space charge smoothing factor, Γ , is then calculated by taking the r.m.s. of the ratio of the current fluctuations for the beam at a given plane within the gun to the cathode current fluctuations. The space charge smoothing factor is then defined to be

$$\Gamma = \left(\frac{\langle \tilde{I}_B^2 \rangle}{\langle \tilde{I}_K^2 \rangle} \right)^{1/2} \quad (5-5)$$

5.3.2 Velocity Fluctuations

If the beam can be considered to be in a state of equilibrium with a Maxwellian distribution of velocities, then the temperature of the beam may be calculated from

$$T = \frac{m}{3k} \langle (v - \langle v \rangle)^2 \rangle \quad (5-6)$$

where m is the electron mass, k is Boltzman's constant, and v is the instantaneous velocity. In terms of the components of velocity,

the above equation may be written as

$$T = \frac{m}{3k} (\langle \tilde{v}_x^2 \rangle + \langle \tilde{v}_y^2 \rangle + \langle \tilde{v}_z^2 \rangle - \langle \tilde{v}_x \rangle^2 - \langle \tilde{v}_y \rangle^2 - \langle \tilde{v}_z \rangle^2) \quad (5-7)$$

where the brackets, $\langle \rangle$, represent spatial averages in the region under analysis. Running averages (time averages) of the x,y,z velocities in each region under analysis are calculated at each time step and used to determine the instantaneous velocity fluctuations.

The temperature, T , is calculated in rectangular regions one mesh distance thick in the xy-plane, the xz-plane, and the yz-plane as sketched in Figure 5-5. It is thus possible to compare the beam temperature at various x, y, and z planes.

5.4 Inclusion of Electrodes (Grids) in the Model

Two approaches to the inclusion of the grids in the three-dimensional geometry are discussed below:

5.4.1 Approximate Technique Using D.C. Potentials

In this approach the principle of superposition is used to include internal electrodes in an approximate way as follows:

- (1) Using the exact geometry of the gun including grids and other internal electrodes, the potential is solved in the three-dimensional geometry neglecting space charge. In the discussion below these potentials are called the d.c. potentials.

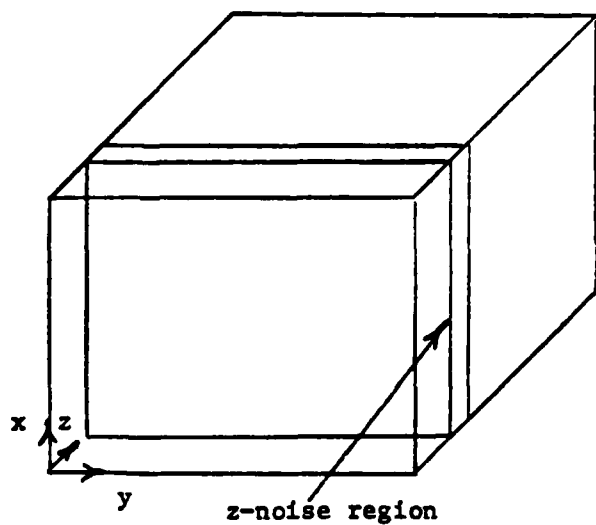
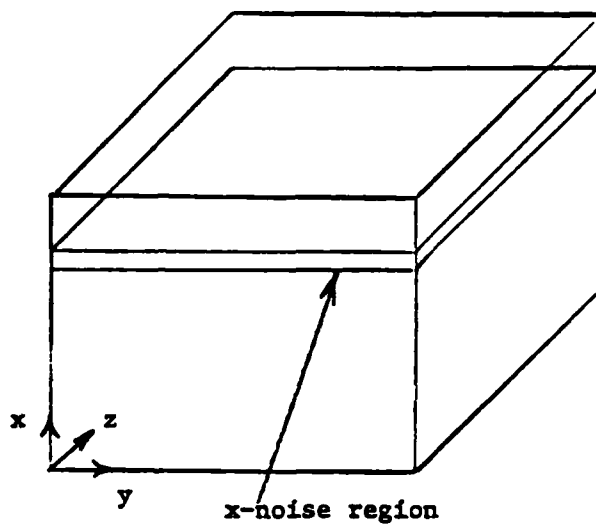
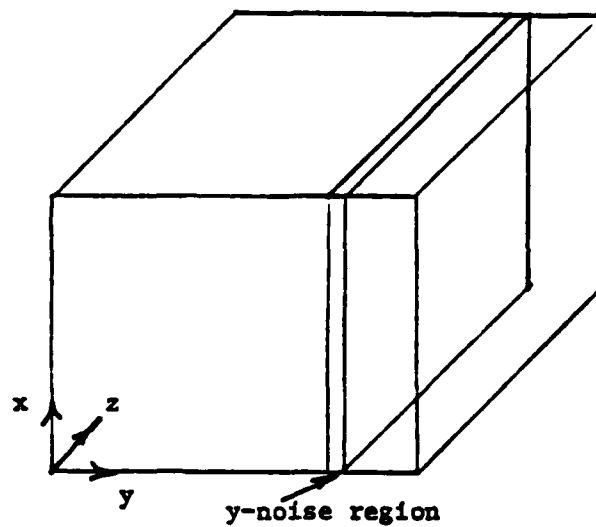


Figure 5-5. Noise Regions Used in Noise Calculations.

- (2) Poisson's Equation is solved for the potentials in a rectangular "box" (with zero potential on the electrodes) which approximates the exact gun geometry as closely as possible and the cathode exactly.
- (3) The d.c. potentials are added to the space charge potentials to obtain the potentials used in the trajectory equations.
- (4) Steps (2) and (3) are repeated for each iteration. Note that the d.c. potentials need only be calculated once and then saved.

A three-dimensional relaxation program for solving Laplace's Equation with arbitrary internal electrodes and boundary conditions has been written. The program has been tested on a three-dimensional crossed-field diode with grids in a 16 x 16 x 16 mesh convergence point system. After 50 iterations (.08 minutes CPU time) the changes in potential are less than 1% and the program appears to have converged.

This approach is approximate in that the imaging of the electrons in the grid are neglected. Since the grids are normally run at a negative potential, this error is expected to be relatively small.

5.4.2 Exact Approach Using a Relaxation Procedure on the Space Charge

Hockney⁽¹⁸⁾ has suggested several methods of including the effect of electrodes in the interior of the mesh region used for the solution of Poisson's Equation. When the number of electrode points is large, he suggests that the space charge on individual mesh points be adjusted iteratively in response to the local error in potential on that point. This approach has been programmed as a test case in the Poisson solving routines. The procedure used is outlined below:

- (1) Storage in an array is provided for the coordinates, potential, and space charge of each internal electrode point.
- (2) An initial value of charge is assigned to each internal electrode point assuming the electrode is an isolated sphere of dimension $h_x \times h_y \times h_z$.
- (3) After each iteration of Poisson's Equation a new value of charge is assigned to each electrode point according to the following relaxation formula

$$Q_{\text{new}} = Q_{\text{old}} \left[1 + R_Q \left(\frac{V_{\text{old}} - V_0}{|V_{\text{max}}|} \right) \right]$$

where R_Q is a relaxation factor ≤ 1 , V_0 is the electrode potential desired, and V_{max} is the maximum of V_{old} and V_0 .

The above technique has been tried on a parallel plane geometry test case with one interior electrode point at -100 volts. The procedure was found to converge with a relaxation factor of .25. Time did not permit the inclusion of this technique in the study of a gridded gun. Obviously, this technique will result in an increase in run-time for the computer program. However, the increase in run-time may be as small as a factor of two since the technique can be applied without a time penalty during the iterations necessary for the solution to reach a steady state. Once the steady state is reached the correction to the charges necessary to maintain the correct internal electrode potential should be small and thus easily accomplished with a few iterations.

6.0 THREE-DIMENSIONAL NOISE SIMULATION STUDIES

Using the three-dimensional model, several test cases were run to determine the correctness of the model and obtain preliminary noise information.

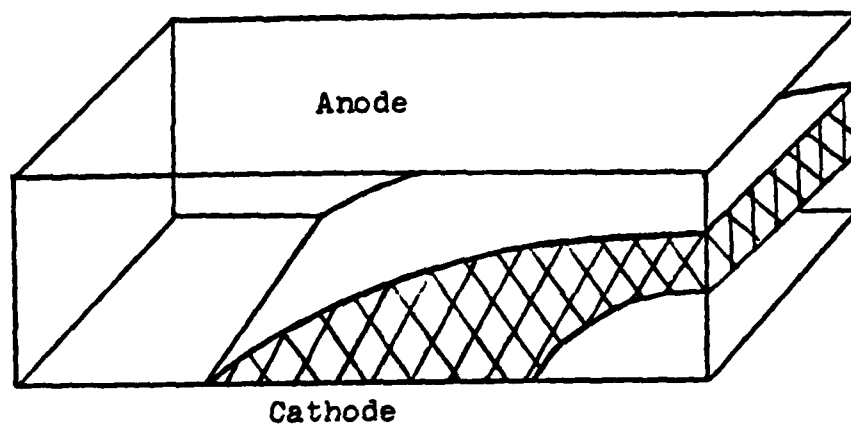
In testing the model for accuracy of potential and trajectory calculations, a 16 x 16 x 16 mesh was used in the parallel plane geometry of Fig. 6-1. For the noise calculations, a 32 x 48 x 16 mesh was used. For the larger mesh system with 16,000 charges, each case required approximately 12 minutes of computer time on the IBM 370/168. The results obtained using the larger mesh are discussed below.

6.1 The Long Kino Gun Test Case

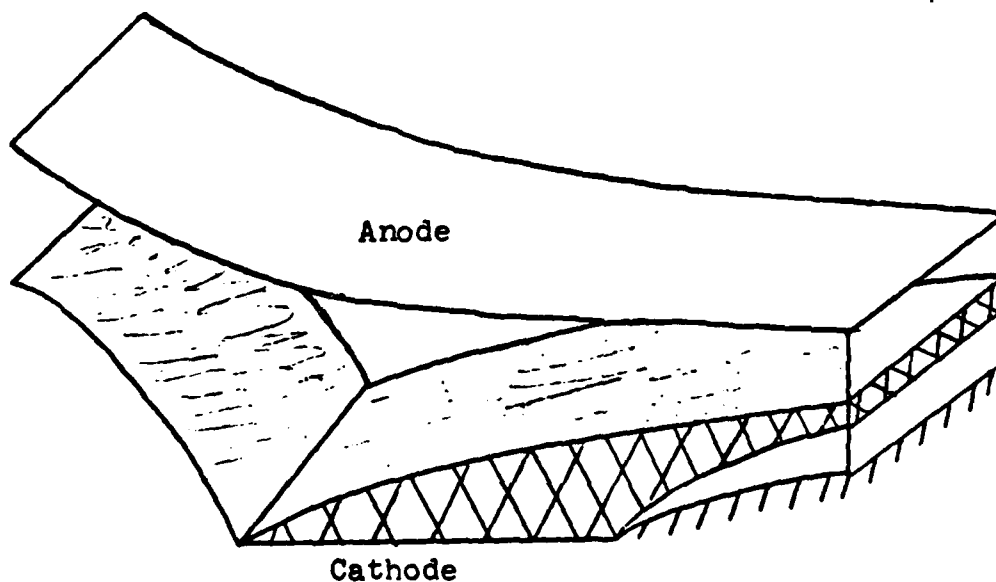
As a preliminary test case, the Long Kino Gun sketched in Figure 6-1 was approximately modeled in three dimensions using a 32 x 48 x 16 mesh system. The z-boundaries are taken to be at zero potential in order to confine the beam. The potential on the lower boundary (cathode) is taken as zero potential with the potential on the anode fixed by the potentials from the Kino gun theory. This gun has the following design parameters:

Total Beam Current	3.34 amps
Cathode Length	.150 inches
Cathode Width	.247 inches
Magnetic Field	2500 gauss
Current Density	14 amp/cm ²
Accelerator Potential	5000 volts
Normalized Cathode Length	116.4 Kino units

Figure 6-2 shows the convergence characteristics of the computer simulation. In this figure the cathode current reaches a "steady state" in about 10 iterations and then fluctuates about this "steady state" for time steps 10 through 75. The computer calculated average exiting beam current is 3.62 amps which is near the design value.



(a) Parallel Plane Diode



(b) Long Kino Gun

Figure 6-1. Crossed-Field Beam Configuration to be Studied Using the Three Dimensional Model

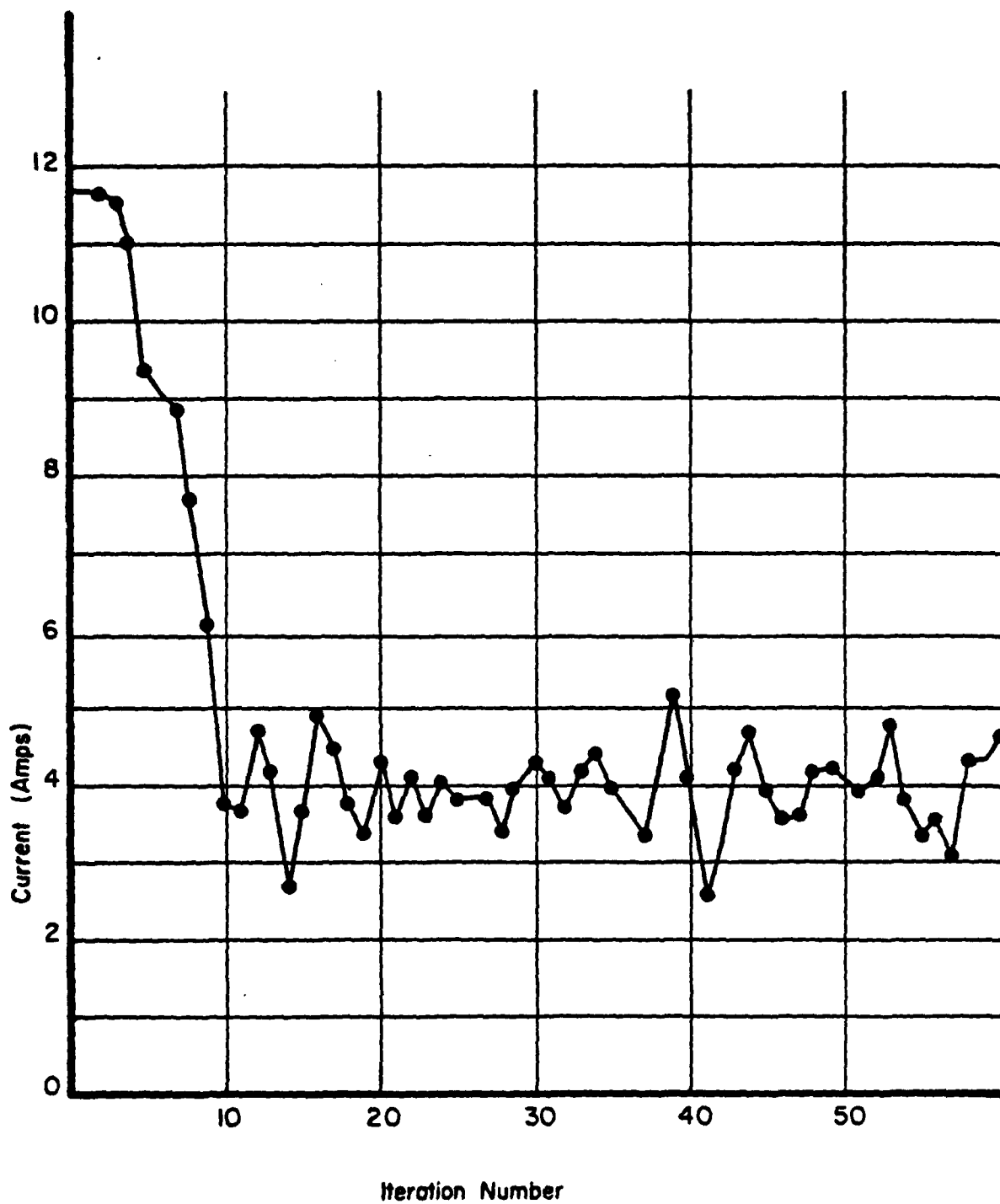


Figure 6-2. Cathode Current in the Long Kino Gun as a Function of Iteration Number.

6.1.1 Current Fluctuation Calculations

Shown in Figure 6-3 is the space charge smoothing factor, Γ , as a function of iteration number for the Long Kino Gun test case with the cathode operating space charge and temperature limited. In the space charge limited case, the current fluctuations are smaller at the beam exit than at the cathode surface. This indicates space charge "smoothing" by the potential minimum and is consistent with the results obtained by Harker.⁽¹⁾ In the temperature limited case the current fluctuations at beam exit are larger than at the cathode surface. In an ideal case of no noise growth mechanisms, the value of Γ for the temperature limited case would be unity. The value of $\Gamma = 1.75$ is due to diocotron noise growth in the beam as it travels from the cathode to the beam exit plane. Space charge smoothing is shown even more clearly in Figure 6-4 where the space charge smoothing factor, Γ^2 , is plotted as a function of the relative current emitted off the cathode. The value of Γ^2 is calculated at a position above the cathode where Γ^2 is minimum. As expected, the space charge smoothing factor is approximately unity in the temperature limited regime and drops dramatically as the cathode is operated space charge limited. Two test cases were run with a small x-directed magnetic field. The value of Γ after 75 iterations are given below:

Case I - No magnetic field in x-direction

$$\begin{aligned} B_z &= .25 \text{ w/m}^2 \\ \Gamma &= .160 \end{aligned}$$

Case II - $B_x = 5\% B_z$

$$\begin{aligned} B_z &= .25 \text{ w/m}^2 \\ \Gamma &= .2005 \end{aligned}$$

Case III - $B_x = 10\% B_z$

$$\begin{aligned} B_z &= .25 \text{ w/m}^2 \\ \Gamma &= .1883 \end{aligned}$$

In both Cases I and III the x-directed magnetic field increases the exiting current fluctuations.

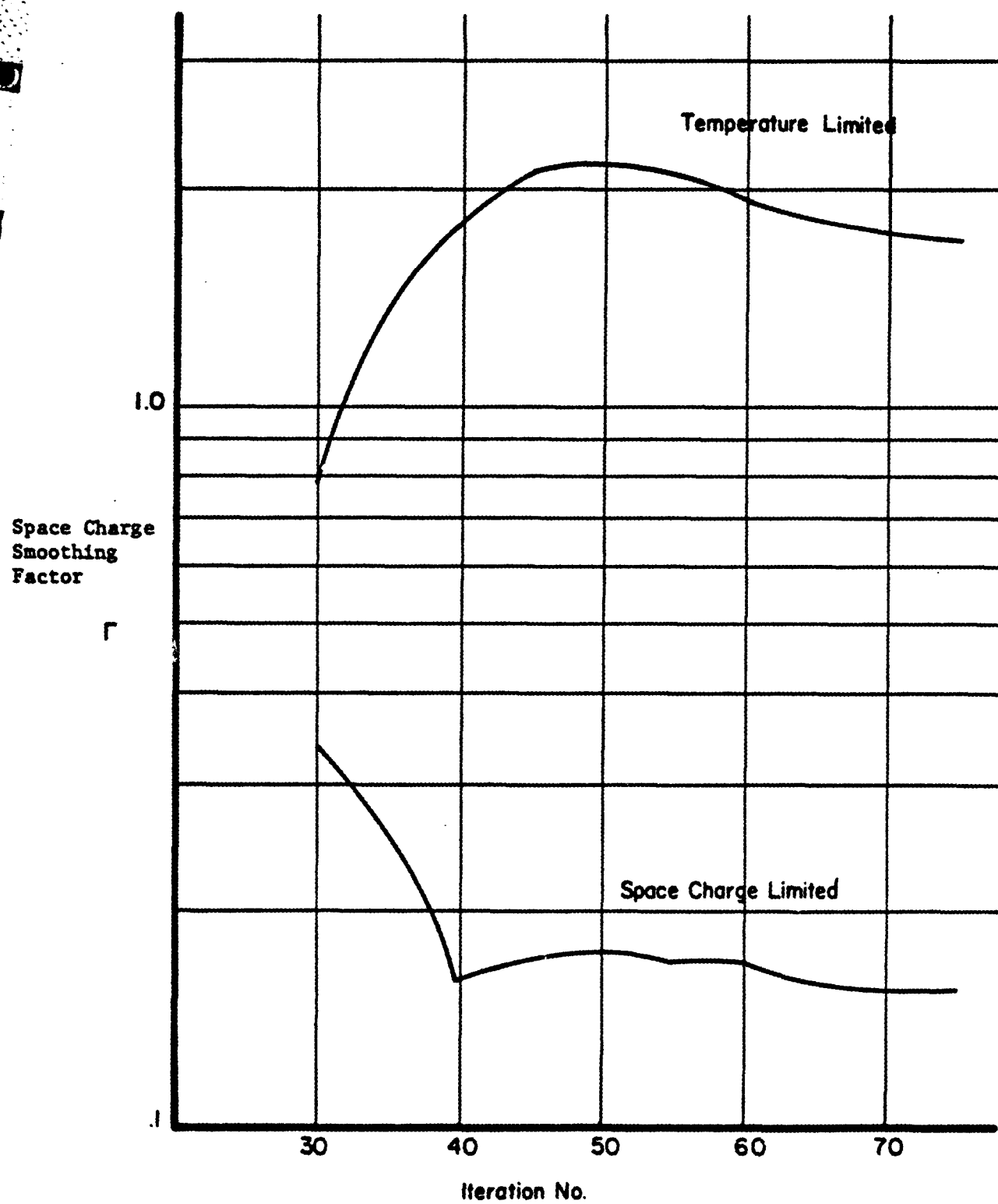


Figure 6-3. Space Charge Smoothing as a Function of Iteration Number for the Long Kino Gun.

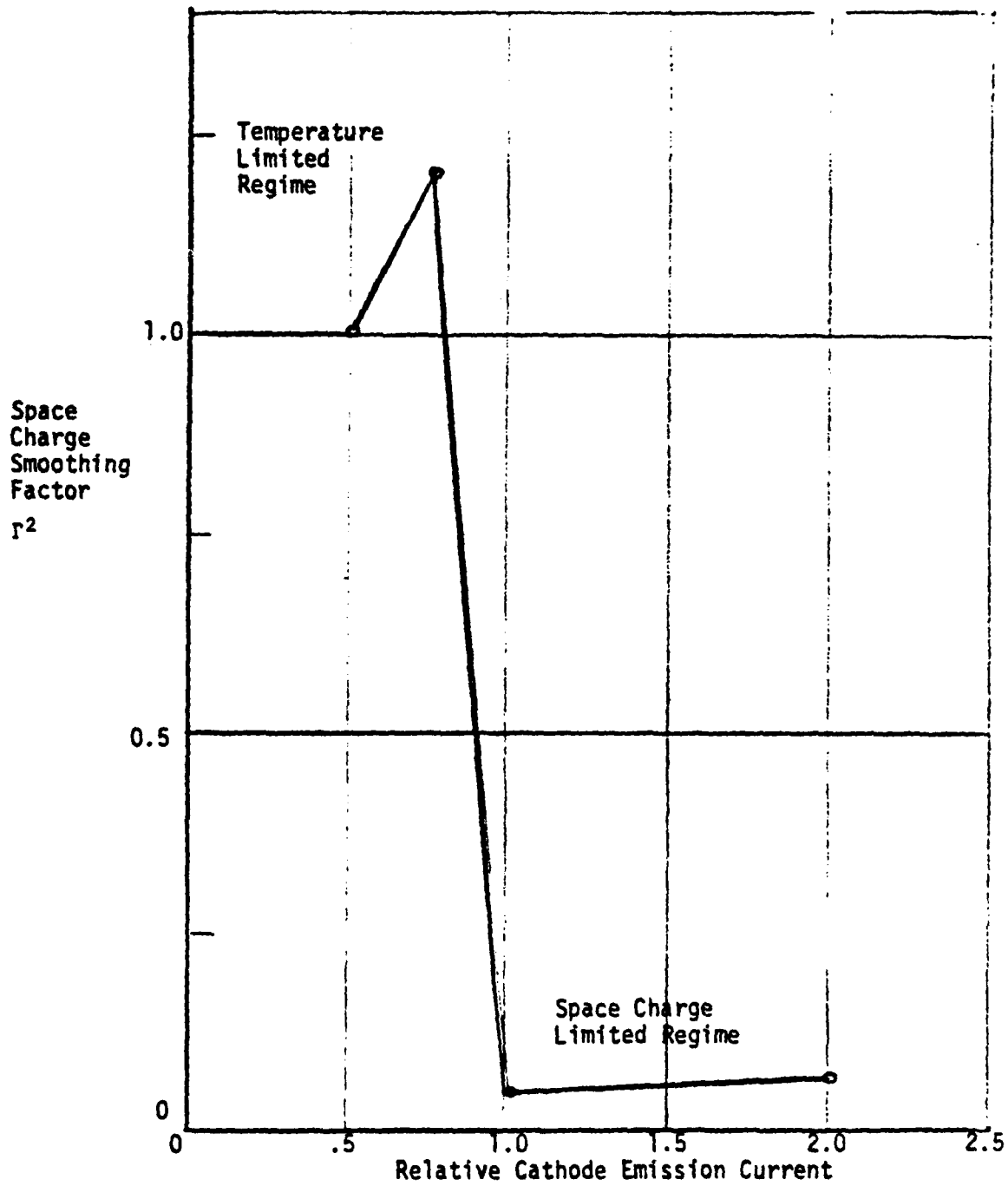


Figure 6-4. Space Charge Smoothing in a Three-Dimension Crossed-Field Gun.

6.1.2 Beam Temperature Calculations

Shown in Figures 6-5, 6-6, and 6-7 is the temperature of the beam as a function of noise region in the x, y, and z planes. Figure 6-5 shows how the beam temperature increases toward the beam exit. This growth appears to be nearly exponential over the cathode surface, drops an order of magnitude at the end of the cathode, and then rises again at the same exponential rate. This exponential growth seems to be due to diocotron noise growth.

Temperature variations as a function of position above the cathode are shown in Figure 6-6. As found in the two-dimensional studies, the top of the beam seems to be noisier than the bottom. This could be due to diocotron growth variations since the electrons on the beam top travel further than those on the bottom.

In Figure 6-7 the variation of beam temperature is given in the direction of the magnetic field for the case of no magnetic field in the x-direction and a small magnetic field in the x-direction. Note that the magnetic field increases the temperature of the beam.

6.2 Three-Dimensional Studies With Grids

As a preliminary test case a three-dimension parallel plane diode was studied using a 16 x 16 x 16 mesh system. The diode had a single grid at -100 volts running the full length of the cathode surface. The grid was simulated using the technique of para. 5.4.1 where the dc potentials are added to the space charge potentials to obtain the total potential for each iteration.

In order to test the effect of grids on the noise in a crossed-field gun, the gridded injected beam gun used by Northrup and discussed by Fontana⁽⁹⁾ was simulated using a 48 x 24 x 16 mesh system. Although the calculation converged in approximately 50 iterations an error in the dc potentials was discovered which prevented the beam from entering the interaction region. Unfortunately time did not permit further calculations on this test case.

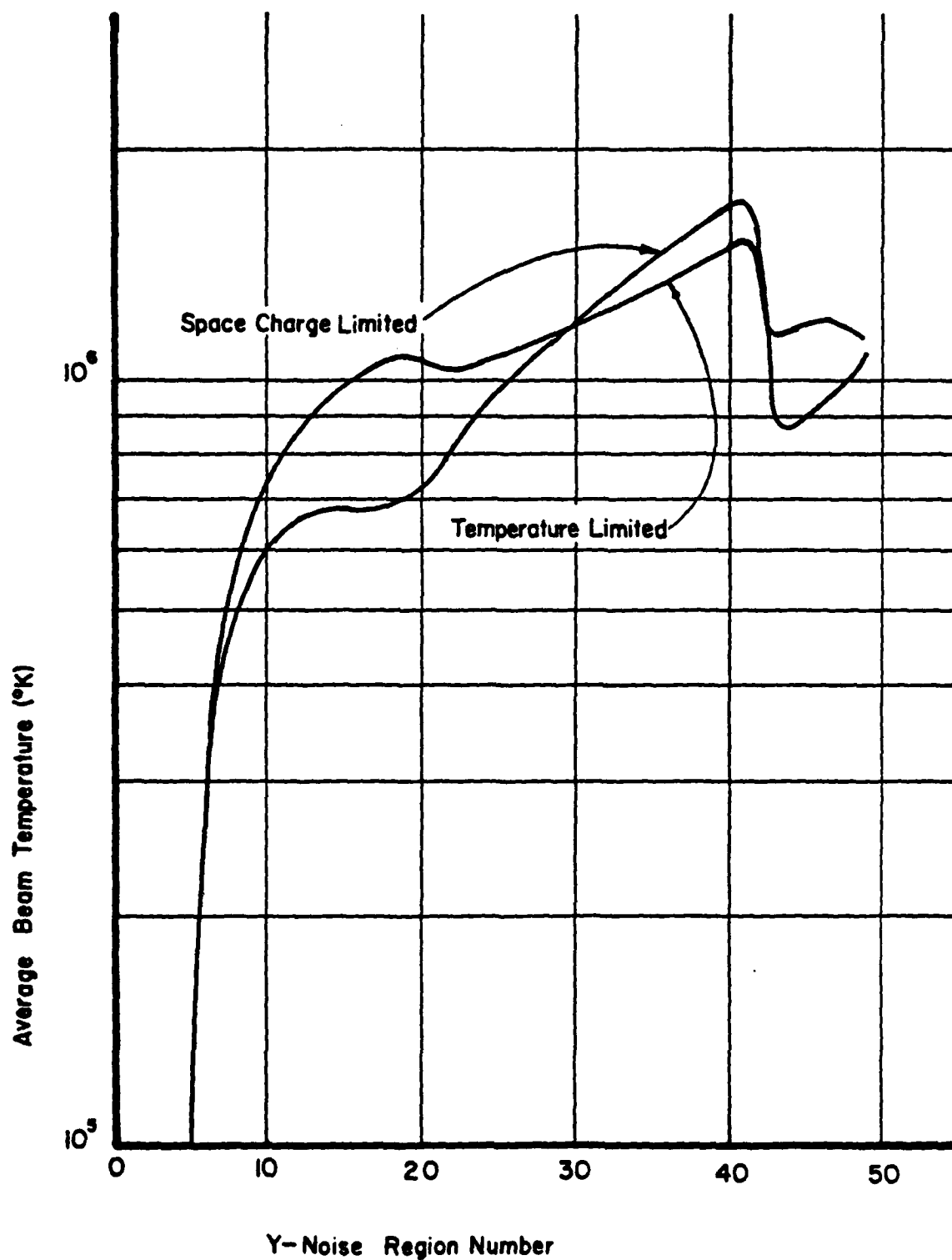


Figure 6-5. Beam Temperature in the x-z Plane.

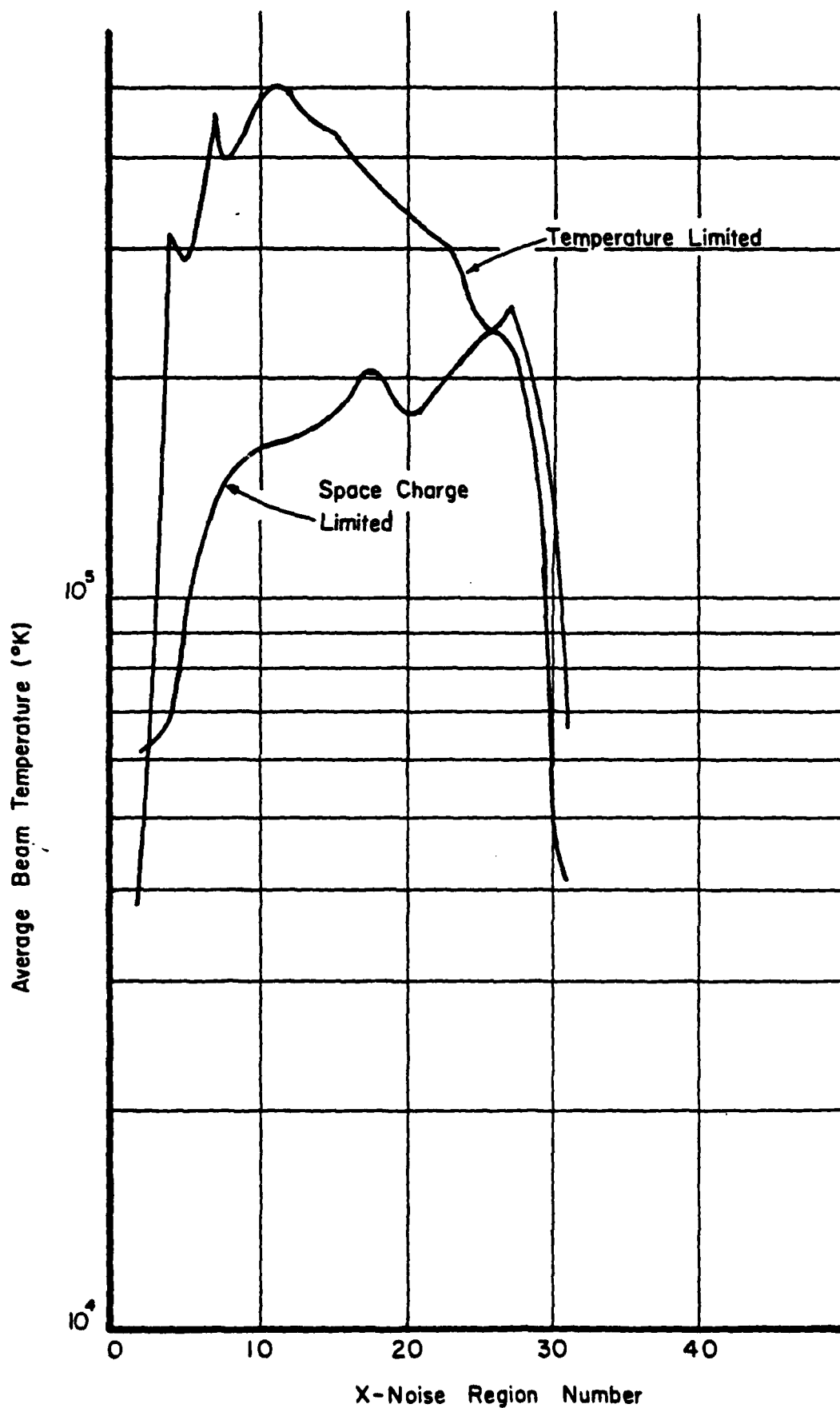


Figure 6-6. Beam Temperature in the y-z Plane.

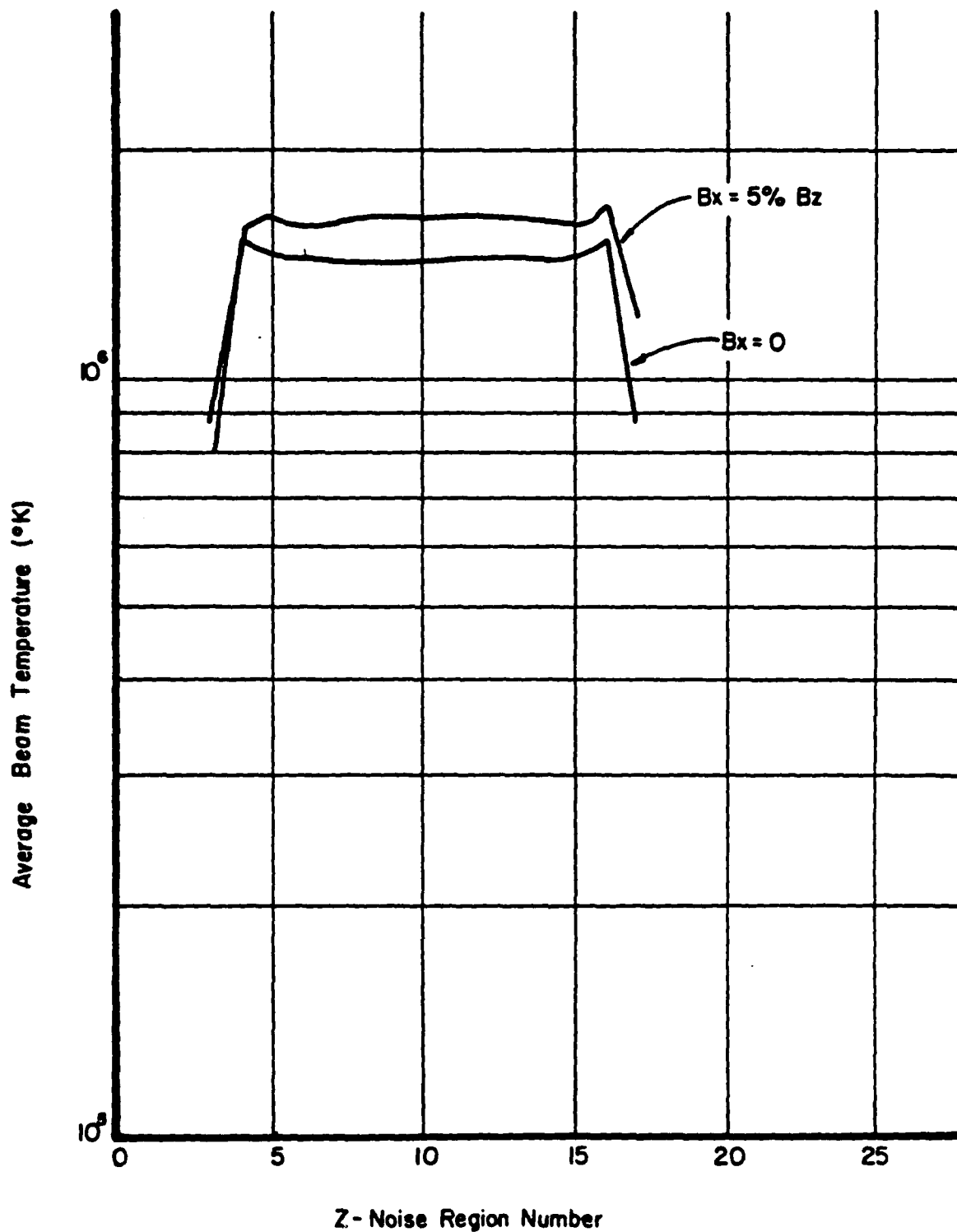


Figure 6-7. Beam Temperature in the x-y Plane.

7.0 ACCURACY AND ERROR CONSIDERATIONS IN COMPUTER SIMULATIONS

The sources of error due to the computer formulation have been identified. These errors can be divided into three categories:

- (1) Truncation errors due to the finite difference approximations used to represent the Lorentz Force Equation (trajectory equations) and Poisson's Equation (potential equation). Such errors are dependent upon the magnitude of the mesh intervals in both time and space.⁽¹⁹⁾ In order to minimize these errors, the finite difference equations have been carried out to second order. The convergence of the calculations indicates that the finite difference procedure is stable.
- (2) Round-off errors due to the inexact representation of floating point numbers in the computer. The error depends on how a number is "rounded off" in the lowest "bits" of a 'word.' The three-dimensional model is solved on an IBM 370/168 using single precision floating point words which have an accuracy of 6 or 7 decimal digits. Clearly any fluctuations in parameters which are approximately 10^{-6} below the average or dc value cannot be calculated accurately. Both the velocity and current fluctuations obtained in the model are approximately two orders of magnitude larger than the round-off values.
- (3) Errors intrinsic to the simulation which arise from the following approximations:
 - (a) Representation of individual electrons by a point charge (big electron) containing many electrons. This approximation results in an exaggerated collision frequency for the electrons.⁽²⁰⁾

- (b) Representation of the space charge assigned to a particular mesh point by a uniform cloud centered on a mesh point or by some other method. This error has been investigated by Hockney⁽²⁰⁾ and Birdsall.⁽²²⁾
- (c) Representation of the functions by finite space and time steps which lead to a lack of energy conservation in the model and thus a "heating" of the electrons. This problem has been investigated by Hockney.⁽²⁰⁾

The magnitude of the errors caused by (a), (b), and (c) above are difficult to estimate. Hockney^(21,22) has investigated various techniques which reduce these errors. Unfortunately, the techniques suggested by Hockney all require increased computer time and thus increase the cost of running the program. One reasonably simple technique called the cloud-in-cell (CIC) approach has proved to be effective in reducing the noise due to (b) and (c) above. Unfortunately, time did not permit the implementation of the cloud-in-cell approach.

- (4) Errors in the model due to the approximation of the exact electrode shapes with planar electrodes.

In the two-dimensional model sketched in Figure 7-1 the space charge contribution to the electric field is found using the idealized rectangular geometry shown by the dotted lines. This results in errors since some of the charges are not imaged in an electrode at the proper distance from the charge.

An estimate of this error can be found by solving for the electric field due to a line charge imaged in a perfect conductor as sketched in Figure 7-2. For this case, the electric field is given by

$$E_{x_0} = \frac{q}{2\pi\epsilon_0} \left(\frac{1}{x-d} - \frac{1}{x+d} \right) \quad (7-1)$$

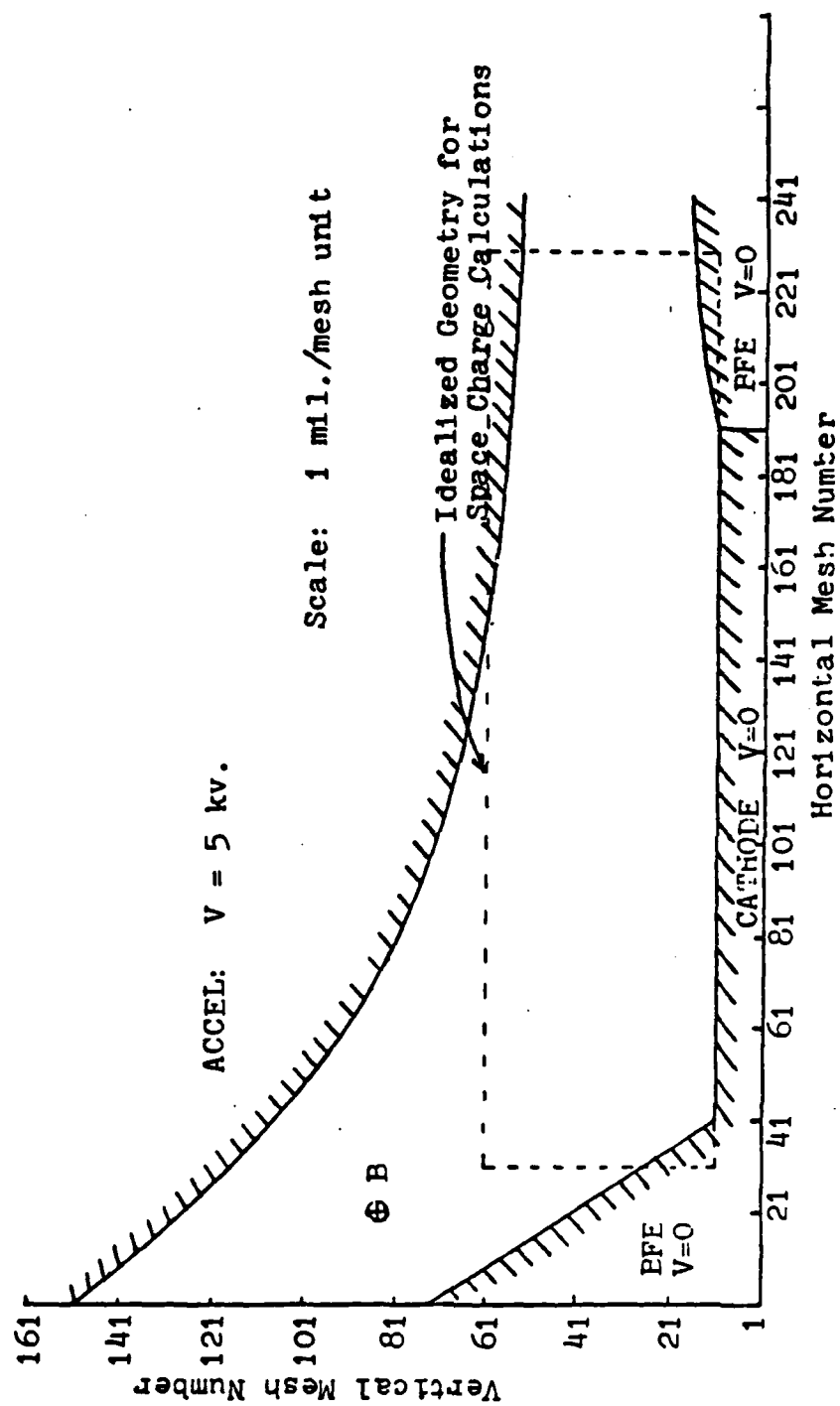


Figure 7-1. Exact Electrode Shapes-Long Klyno Gun Design

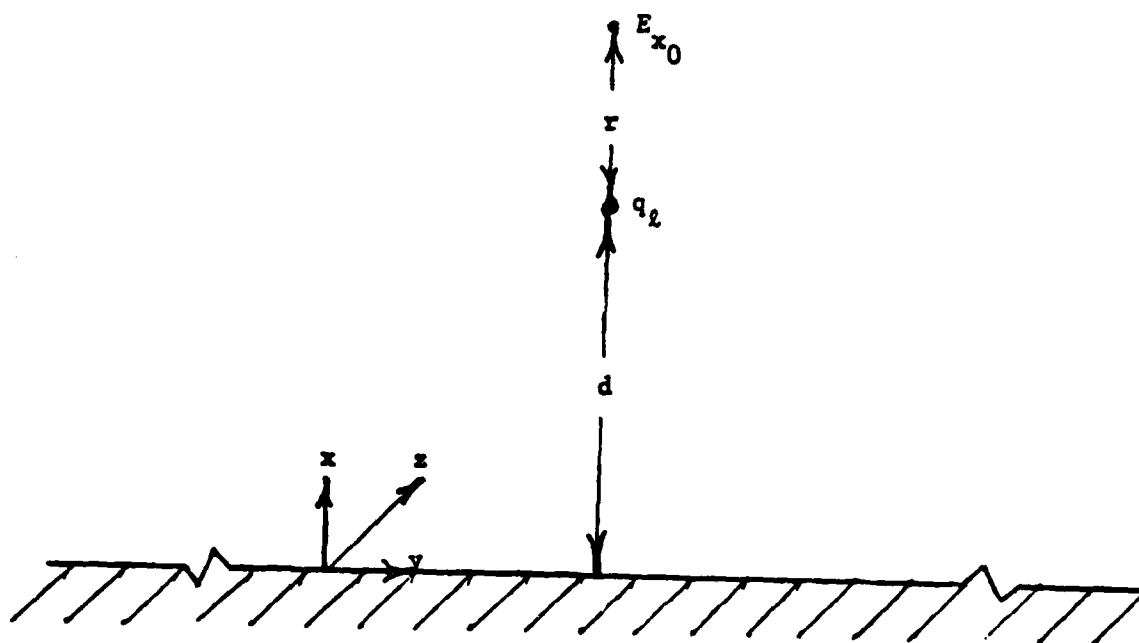


Figure 7-2. A Line Charge Parallel to a
Conducting Plane.

where q is the line charge and d is the distance between the line charge and the conductor. Note that the second term is due to the conductor and reduces the field below that of a "free" line charge.

If d is in error by an amount Δd the above equation becomes

$$E_{x_1} = \frac{q}{2\pi\epsilon_0} \left(\frac{1}{x-d-\Delta d} - \frac{1}{x+d+\Delta d} \right) \quad (7-2)$$

The percent error due to the incorrect position of the conductor is given by

$$\text{Electric Field Error} = \frac{E_{x_1} - E_{x_0}}{E_{x_0}} \times 100\% \quad (7-3)$$

Using Equation (7-1) and (7-2) in Equation (7-3) we obtain

$$\text{Electric Field Error} = \frac{r/d \Delta}{r/d + 2(1+\Delta)} \times 100\%$$

where $r = x-d$, the distance from the line charge to the field point, is kept fixed and $\Delta = \Delta d/d$. This equation is plotted in Figure 7-3 as a function of r/d for various values of Δ as parameters.

We note from Figure 7-3 that as long as the field point is relatively close to the charge ($r/d \ll 1$), the error in the value of the electric field is small even for large errors in the position of the conducting plane ($\Delta \sim 1$).

For the gun of Figure 7-1 the top of the beam is approximately 20 mesh units from the exact electrode and 28 mesh units from the approximate electrode. This gives $\Delta = .4$. The beam thickness is approximately 15 mesh units. Thus, at the middle of the beam $r/d = .33$ and the maximum error in the electric field at the center of the beam would be only 4.2%. In fact, the error in the total field at the center of the beam would be

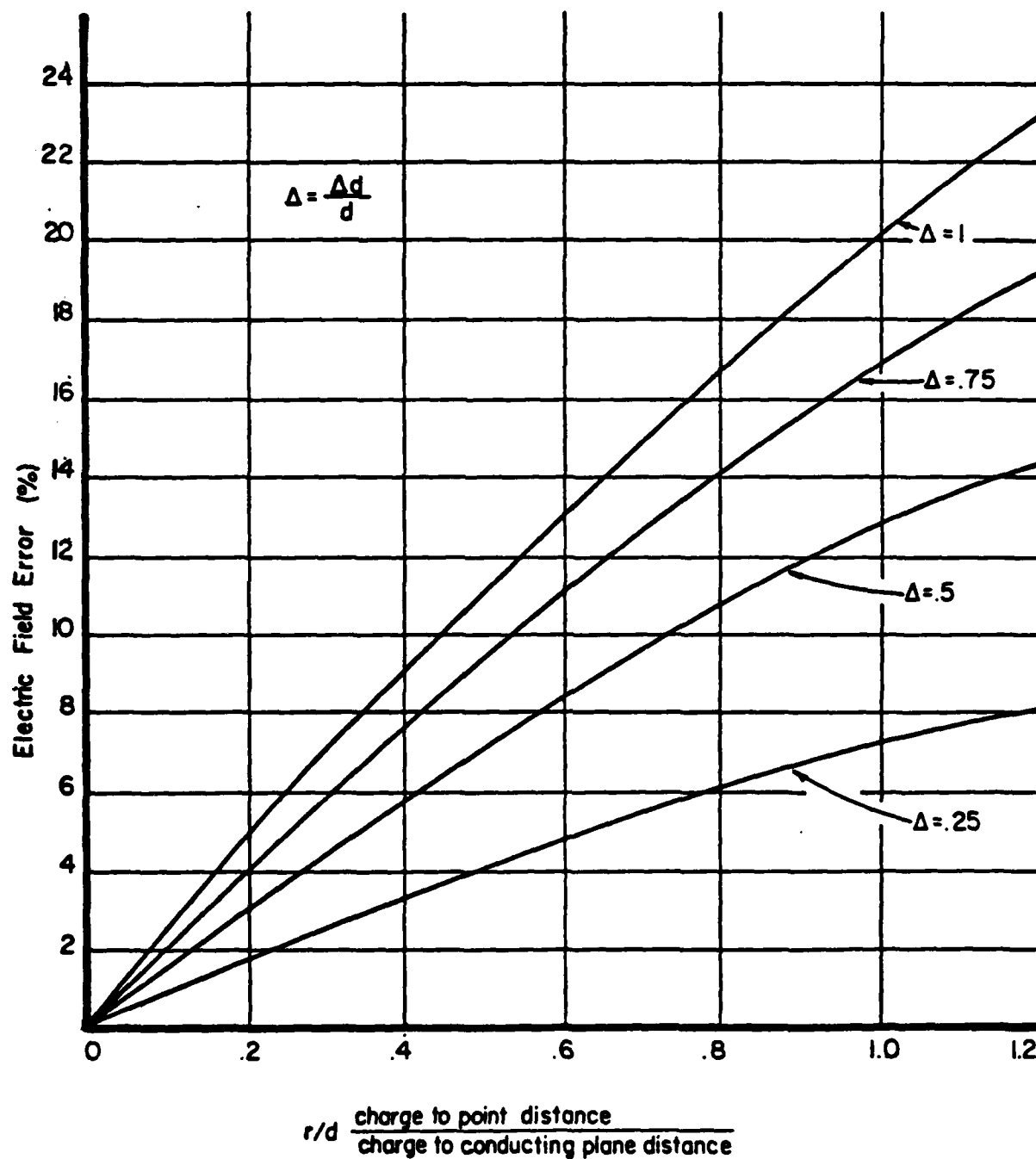


Figure 7-3. Electric Field Error Due to Incorrect Electrode Position.

even less since the field at the center of the beam would be dominated by near charges rather than those at the edge of the beam.

A larger error would occur at the bottom of the beam where at exit the beam is approximately 6 mesh units from the exact electrode and 11 mesh units from the approximate electrode. This gives a value of $\Delta = .833$ and at the center of the beam $r/d = 1.2$. From Figure 7-3 the error is approximately 20.5%.

Again, the actual error would be smaller due to the shielding effects of the nearer charges.

It should be noted that in the critical region of the cathode surface, the idealized and exact gun geometries coincide so there is negligible error in the calculation of electric field near the cathode surface. The field due to charges is not the total field since there is a potential applied between the accelerator and cathode electrodes. This would further reduce the net error in the electric fields.

8.0 CONCLUSIONS AND RECOMMENDATIONS

This study shows that it is possible to model three-dimensional crossed-field beams using computer simulations and to obtain useful information about the beam characteristics from the models.

Further studies of the three-dimensional beams with grids over the cathode would be useful in order to determine the effect of grids on the beam noise and optics.

REFERENCES

1. Harker and Crawford, "Noise in Planar Crossed-field Electron Guns. II," Stanford University Institute for Plasma Research, SU-IPR Report No. 772, Feb. 1979, p. 18.
2. Ho and Van Duzer, IEEE-ED, 15, Feb. 1968, p. 75.
3. MacFarland and Hay, Proc. Phys. Soc., 13-63, 1950, p. 409.
4. Sisodia and Gandhi, Proc. Sixth International Conference on Microwave and Optical Generation and Amplification, Cambridge, England, 1966, p. 214.
5. Wadhwa and Rowe, IEEE-ED, 10, Nov. 1963, p. 378.
6. Pollack and Whinnery, IEEE-ED, 11, Mar. 1964, p. 81.
7. Lele and Rowe, IEEE-ED, 6, Mar. 1969, p. 261.
8. Shkarofsky, "Velocity Noise in a Crossed Field Planar Diode," MPB Tech. Inc., Quebec, MPB Report No. 112-1, Oct. 1978.
9. Fontana, MacGregor, and Rowe, "Simulation of Distributed Emission and Injected-Beam Crossed-Field Amplifiers. Part II. The Injected Beam Crossed-Field Amplifier," Annual Technical Report, Air Force Office of Scientific Research, Mar. 1979.
10. Harker, K. J., Stanford University Institute for Plasma Research, Stanford University, private communication, May 1979.
11. MacGregor, D. M., Harris, SAI Inc., Ann Arbor, Michigan, private communication, Jan. 1980.
12. Davenport and Root, An Introduction to the Theory of Random Signals and Noise, McGraw-Hill, New York, 1958, p. 115.
13. O'Flynn, Stanford Elect. Lab. Report No. 0558-2, June 1964, p. 14.
14. Kooyers, Universal Computer Applications Internal Report, July 1970, p. 69.
15. Abramowitz and Stegun, Handbook of Mathematical Functions, U.S. Government Printing Office, Wash., D.C., 1964, Sec. 26.2.22.
16. Swarztrauber and Sweet, "Efficient FORTRAN Subprograms for the Solution of Elliptic Partial Differential Equations," NCAR Technical Note, NCAR-TN/1A-109, National Center for Atmospheric Research, Boulder, Colorado, July 1975.

17. Christensen and Hockney, "FOUR67, A Fast Fourier Transform Package," Computer Physics Communications, 2, 1971, pp. 127-138.
18. Hockney, R. W., "The Potential Calculation and Some Applications," Meth. Comp. Phys., 9, Academic Press, 1970, p. 162.
19. Potter, D., Computational Physics, John Wiley, 1977, Chapter 2.
20. Hockney, R., Journal of Computational Physics, 8, 1977, p. 19.
21. Hockney, R., Computational Physics, John Wiley, Academic Press, 1970, p. 117.
22. Birdsall and Fuss, Journal of Computational Physics, 8, 1977, p. 19.

APPENDIX A

A SURVEY OF NOISE IN CROSSED-FIELD BEAMS

A.1 Introduction

This survey of papers on noise and noise mechanisms in crossed-field electron beams is not intended to be comprehensive, but rather is intended to be definitive in establishing the current state of knowledge concerning noise mechanisms in crossed-field beams.

Three noise mechanisms have been proposed to account for the noise growth in crossed-field beams: diocotron gain, feedback to the potential minimum and noise enhancement due to electron travel along magnetic field lines (three-dimensional effects). Each of these mechanisms is discussed below, and an effort is made to establish current knowledge concerning each mechanism, noise measurements related to each mechanism and possible methods of noise reduction.

A.2 Diocotron Noise Growth

Below, theoretical calculations, experimental measurements and possible methods of reducing diocotron noise growth are cited from the available literature. It should be noted that accurate and definitive quantitative measurements are difficult to make, which explains in part the lack of experimental measurements. It should also be noted that the theoretical calculations cited are only approximate since the complexity of the problem makes it very difficult to obtain closed form solutions even in the small signal regime where most of the analyses apply. One other problem with the theoretical and experimental results which should be cited is the almost total lack of noise data on high current density "long" guns since most of the experimental laboratory work was done on low current density beams.

A.2.1 Theoretical Calculations and Experimental Results

In an analysis of wave propagation in slipping streams of electrons, MacFarlane and Hay (1949) found that fluctuations in a stream of electrons will grow even without the presence of a slow wave circuit. This effect in crossed-field beams has come to be known as the "diocotron" effect. Gould (1957) developed an equation for the growth rate of signals due to this effect between parallel conducting planes for both centered and non-centered beams. Later, Sasaki and Van Duzer (1966) used coupled mode theory to obtain essentially the same result as Gould. The results of Gould and Sasaki and Van Duzer were limited in that only the three space charge waves were used in the analysis, whereas, in general, there are five possible waves which can propagate on a crossed-field beam. Finally, Mantena (1968) considered all five waves and developed a general transfunction matrix which gives the diocotron growth for a thin, non-accelerating beam in a drift region between parallel conducting boundaries. Unfortunately none of the above results can be applied to the gun region since the beam is accelerating and the electrodes in the gun region are not, in general, parallel. However, numerous experiments have confirmed that the growth of waves due to the diocotron effect does take place and the theoretical results for thin, non-accelerating beams in the small signal regime agree closely with experiment.

Van Duzer (1961) was the first one to try to calculate the growth of fluctuations in the gun region. Using modified Llewellyn-Peterson equations he was able to approximately calculate the growth

rate of velocity, current, and position fluctuations along the beam. Later, Van Duzer (1963) used these results to try to calculate the noise figure of a crossed field amplifier including a gun region, a drift region and an amplifying region. His calculated values were very much higher than those measured on an amplifier operating at a frequency of 1874 MHz. Using an eigenvalue perturbation technique together with Monte Carlo calculations Wadhwa (1964) concluded that the growth of fluctuations in the beam is mainly due to diocotron growth during the latter part of the beam trajectory in the gun region. He also cited some experimental work which seems to confirm the above conclusion. Using the results of his calculations in 1964 for the gun region Wadhwa (1968) calculated the noise figure of an injected beam CFA including both a three and five wave analysis. A comparison of his results with those of Mantens and Van Duzer (1963) shows good correlation between experiment and theory.

A.2.2 Reduction of Diocotron Noise Growth

In order to reduce the growth of fluctuations due to the diocotron effect, various schemes have been proposed. These techniques are reviewed below together with an attempt to evaluate the usefulness of each approach.

A.2.2.1 Modification of beam and geometry design parameters

By examining the gain equation for the diocotron growth, Wadhwa (1964) proposed several design conditions which would reduce the diocotron growth. A low current density, high velocity, high

magnetic field beam would help reduce the diocotron growth. Unfortunately, for practically all of the applications now envisioned for CFA's relatively low velocity, high current density beams are desired with magnetic fields as small as possible in order to reduce the weight of the device.

Two other suggestions of Wadhwa do have merit. First, he proposed eliminating the length of the transition region between the gun and the interaction region. This has been done in all current CFA designs and although no careful quantitative measurements have been made to verify that the noise is reduced, qualitative results would indicate that it is.

Second, he proposed that the beam be positioned asymmetrically between the focusing electrodes in the gun and transition regions. This is a design parameter which is somewhat under the control of the designer.

A.2.2.2 Noise transformer

Wadhwa and Rowe (1963) proposed that a noise transformer somewhat similar to that used in O-type tubes might be useful in reducing the noise output of a crossed field gun. Wadhwa and Van Duzer (1965, 1968) used a noise transformer in an experimental S-band CFA and achieved a 3.5 db noise figure. They attribute the low noise figure obtained to be due, in part, to the noise transformer. Sidhu and Wadhwa (1970) proposed a noise transformer composed of two parallel plate regions and suggest that such a device between the gun and the interaction space would reduce the noise as well as allowing wide dynamic range operation of the gun.

Van Duzer and Harris (1964) found an instability in trajectory calculations they were attempting to make on a long Kino Gun and also proposed a noise mechanism caused by feedback to the potential minimum to account for this space charge instability. Davies and Polter (1965) made noise measurements on a long Kino Gun and were able to identify two types of noise-diocotron noise and noise which could be associated with feedback to the potential minimum. Nunn and Smol (1964) also found that the noise in crossed-field guns increases with the length of the cathode.

Ho and Van Duzer (1968) proposed a feedback model for the potential minimum region of a crossed-field gun which gave at least qualitative agreement with the experimental results cited above. They developed a stability criteria for avoiding excess noise due to feedback to potential minimum of

$$l_k < .6l_c$$

where l_k is the normalized cathode length and l_c is the normalized length of a cycloid in the gun region.

It seems relatively certain that the mechanism of feedback to the potential minimum is causing excess noise in crossed-field guns even though very few quantitative measurements have been made and the theory due to Ho and Van Duzer is only approximate and limited to the small signal regime.

A.2.2.3 Shielded cathode

Theoretical work by Buneman, Levy, and Linson (1966) indicates that a partially shielded gun (shielded from the magnetic field) may have lower diocotron growth than a gun where the magnetic field does not lace the cathode. No experimental work has been reported in the area of shielded cathodes.

A.2.2.4 Non-equipotential cathodes

Pützl (1966) has done some theoretical work on non-equipotential cathodes which is interesting from a theoretical, if not practical, point of view. His calculations indicate that if it were possible to build a non-equipotential cathode, a more stable beam would result with decreased diocotron noise growth. No experimental work has been attempted in the area of non-equipotential cathodes.

A.3 Feedback to the Potential Minimum

A.3.1 Experimental Measurements and Theoretical Calculations

As crossed-field guns were made "longer" in order to give higher current density beams, certain anomalous effects were observed. Epstein (1957) noticed that large values of sole current occurred at certain values of the magnetic field in "long" guns. Arnaud (1964) was able to relate these results to the ratio of the height of the beam above the cathode to the length of the cathode and proposed that feedback to the potential minimum could be the cause of the excess noise.

A.3.2 Reduction of Noise Growth Due to Feedback to the Potential Minimum

Since feedback to the potential minimum is a space charge effect any scheme or method which reduced the space charge in the gun region should also reduce the noise due to feedback. Significant reductions in noise were observed by Arnaud and Doehler (1961) and Arnaud, Diamond, and Epstein (1962) when a grid was added above the gun with the grid wires perpendicular to the direction of the magnetic field and the grid close to the cathode surface. One possible explanation of the reduction in noise due to the grid is the reduction of space charge in the potential minimum (fields from the beam terminating on the grid and thus reducing the space charge fields) and thus a reduction in the feedback noise mechanism. Such a conclusion must be considered tentative since no experimental or theoretical work has been done to determine why or how a grid reduces the noise.

A.4 Three-Dimensional Effects

All of the theoretical analyses which have been made of crossed-field beams have been two dimensional. Variations and fluctuations of the beam in the magnetic field direction have been ignored. Gandhi (1965) made some calculations which indicated that random emission velocities in the direction of the magnetic field may contribute substantially to the noise. Subsequently, Sisodia and Gandhi (1966), Sisodia, Gandhi, and Wadhwa (1967) and Sisodia and Wadhwa (1968) found that large reductions in the noise output of a crossed-field gun could be achieved by either tilting the cathode slightly in the magnetic field direction or by

1

slightly perturbing the magnetic field in the gun region to give small magnetic field components perpendicular to the gun. The noise reduction is believed to be due to smoothing out of the random velocities in the magnetic field direction, although this conclusion must be considered tentative until further three-dimensional theoretical and/or experimental work is completed.

REFERENCES

1. Arnaud, J., (1964), Ann. Radioelect., 19, 3.
2. Arnaud, J., Diamond, F. and Epsztein, B., (1962), Int. Congress on Tubes for Hyperfrequencies, 133.
3. Arnaud, J. and Doehler, A. O., (1961), Proc. IEEE, 49, 234.
4. Buneman, O., Levy, R. H., and Linsen, L., (1966), Research Report 240, Avco Everett Research Laboratory, Everett, Mass.
5. Davies, M. C. et al., (1966), Proc. of the Sixth Int. Conference on Microwave Tubes, Cambridge, England, 209.
6. Epsztein, B., (1957), Instabilite des Faisceaux Electroniques Minces, Thesis, Paris University.
7. Gandhi, O. P., (1965), Int. J. Electron., 19, 315.
8. Gould, R. W., (1957), J. Appl. Phys., 28, 594.
9. Ho, R. Y. C. and Van Duzer, T., (1968), IEEE Trans. on Electron Devices, ED-15, 73.
10. MacFarlane, G. G. and Hay, H. G., (1949), Proc. Phys. Soc. 6313, 409.
11. Mantena, N. R., (1968), IEEE Trans. on Electron Devices, ED-15, 734.
12. Mantena, N. R. and Van Duzer, T., (1963), Proc. IEEE, 51, 315.
13. Nunn, R. A. and Smol, G., (1964), Proc. of the Fifth Int. Congress on Microwave Tubes, Paris, 209.
14. Pötzel, H. et al., (1966), Final Tech. Report European Research Office, Contract No. 91-591-EUC-3589, Institut für Hochfrequenztechnik der Technischen Hochschule Wien.
15. Sasaki, A. and Van Duzer, T., (1966), IEEE Trans. on Electron Devices, ED-13, 494.
16. Sidhu, G. S. and Wadhwa, R. P., (1970), Proc. IEEE, 58, 825.
17. Sisodia and Gandhi, (1966), Proc. Sixth Int. Conference on Microwave and Optical Generation and Amplification, 214.
18. Sisodia, M., Gandhi, O. and Wadhwa, R., (1967), Int. J. Electron., 22, 575.

19. Sisodia, M. L. and Wadhwa, R. P., (1968), Proc. IRE, 56, 94.
20. Van Duzer, T., (1961), IRE Trans. on Electron Devices, ED-8, 78.
21. Van Duzer, T., (1963), IEEE Trans. on Electron Devices, ED-10, 370.
22. Van Duzer, T. and Harris, R. D., (1964), J. Appl. Phys., 35, 1642.
23. Wadhwa, R. P., (1964), Proc. IEEE, 52, 315 and Int. J. Electronics and Control, 17, 258.
24. Wadhwa, R. P., (1968), Int. J. Electronics, 23, 123.
25. Wadhwa, R. P. and Rowe, J. E., (1963), IEEE Trans. on Electron Devices, ED-10, 378.
26. Wadhwa, R. P. and Van Duzer, T., (1965), Proc. IEEE, 53, 425.
27. Wadhwa, R. P. and Van Duzer, T., (1968), Int. J. Electronics, 23, 135.

APPENDIX B

**COMPUTER AIDED DESIGN AND ANALYSIS OF ELECTRON
GUNS FOR INJECTED BEAM CROSSED FIELD AMPLIFIERS**

Elden K. Shaw and Gerald P. Kooyers

**Presented at the 1977 International
Electron Devices Meeting, Washington, D.C.**

COMPUTER AIDED DESIGN AND ANALYSIS OF ELECTRON GUNS FOR INJECTED BEAM CROSSED FIELD AMPLIFIERS

Elden K. Shaw and Gerald P. Kooyers

DCA Systems Incorporated

Palo Alto, California

ABSTRACT

In this paper a self-consistent computer aided CFA gun analysis program is discussed which can be used to solve for the characteristics of "long" crossed field guns with arbitrary electrode shapes and including the effects of space charge. The results of analyzing a "long" Kino gun are presented which show excellent agreement between the theoretical gun parameters and those obtained by the computer analysis. As an example of the design procedure, the results of designing a CFA gun and transition region with the accelerator at anode potential are given. The utility of the model is further illustrated by the results of some preliminary noise calculations made by simulating the noise characteristics of the beam at the cathode surface.

INTRODUCTION

In order to build efficient, high power injected beam crossed field amplifiers it is necessary to be able to design convergent crossed field guns which produce relatively thin laminar beams. The design and analysis of guns for practical CFA's is complicated due to the cycloidal motion of the electrons which leads to trajectory crossings and thus very complicated flow.

In the past CFA guns have been designed using empirical techniques or the design methods suggested by Kino(1) with potential plotting used to match equipotential lines in the transition region between the gun and the interaction region.

A self-consistent CFA gun analysis procedure is discussed below which can be used to solve for the characteristics of "long" crossed field guns with arbitrary electrode shapes. The effects of space charge are included in the analysis. In addition, the analysis procedure discussed below shows promise of being able to be used to study noise mechanisms and noise growth in the gun and transition region.

TWO DIMENSIONAL LAGRANGIAN MODEL

In this approach a large number (up to 6000) rods of charge are used to simulate the beam in the gun and transition regions with rods being released from the cathode consistent with the emission characteristics of the cathode surface.

The approach is discussed below:

- (1) First, the gun and transition region is divided into a rectangular mesh.
- (2) Next, the potentials in the absence of space charge are calculated at each mesh point using a computer code which solves Laplace's equation for arbitrary electrode shapes and potentials. These potentials are then stored for use during the rest of the calculation.
- (3) A relatively large number of rods of charge are released from the cathode with position, density, and velocity consistent with the emission characteristics of the cathode. The beam buildup is followed in time with electrons being emitted from the cathode at equal small increments in time. The beam is allowed to build up to several thousand rods of charge with "new" rods of charge added at the cathode in each time step and "old" rods being removed as they exit the right-hand boundary or are collected on the electrodes.
- (4) The motion of the rods of charge is governed by the Lorentz Force Equation where the electric field is found from the potentials on the mesh points. During each iteration, each rod of charge is allowed to move for a small increment in time with its motion governed by the Lorentz Force Equation. Very accurate finite difference equations are used which have previously been developed and used successfully to solve the Lorentz Force Equation(2).

- (5) Simulating the beam by a large number of rods of charge has not been used in the past as an approach to the design of crossed field guns due to the relatively long computer times required to solve Poisson's Equation by conventional techniques. However, a technique due to R. Hockney(3) has been successfully used to solve Poisson's Equation in less than one second on an IBM 360/168 (compared with approximately one minute for the usual iterative relaxation procedures). This approach is discussed in some detail in a paper by Yu, Kooyers and Buneman(2) and was used successfully with up to four thousand rods of charge in analyzing for the first time the distributed emission CFA. Once the potentials have been calculated including space charge by the Hockney technique for each iteration, "new" rods of charge are released from the cathode and the procedure discussed above is repeated until the beam reaches a "steady state." Steady state or convergence is obtained when the number of rods of charge exiting the gun region averaged over one cyclotron period approaches a constant.

GUN STUDIES USING THE MODEL

Long Kino Gun Analysis

In order to test the accuracy and validity of the model a long Kino gun was designed with the following parameters:

Magnetic Field - $.250 \text{ w/m}^2$
 Cathode Length - $.150 \text{ in.}$
 Normalized Length - 116.4 Kino units
 Accelerator Potential - 5000 volts
 Cathode Current Density - 14 amp/cm^2
 Total Beam Current - 3.34 amp.

Using a time step of $1/20$ of a cyclotron period, the beam buildup characteristics were calculated for 110 iterations. As rods of charge were injected at the cathode surface the beam current as measured by the rods of charge exiting the gun region rapidly built up to an average value of 3.24 amps which differs from the Kino predicted value by less than 3%. The beam thickness and current density of the exiting beam are also in close agreement with the theoretical values given by the Kino theory.

Gun Design with Accelerator at Cathode Potential

The computer model becomes most useful as a design tool for guns when used to design both the gun and transition regions. For a particular dual-mode CFA a gun was required to operate at a magnetic field of $.3 \text{ w/m}^2$ and produce a current of 5 amps .

As a starting point, a Kino gun design was made with the following characteristics:

Current Density - 14 amps/cm^2
 Cathode Length - $.150 \text{ inches}$
 Kino Calculated Current - 3.7 amps
 Anode Potential - 8.2 kv.

Running the accelerator at full anode potential represents an innovation made possible by recognizing that in a gridded gun (this design was made for the eventual inclusion of a grid), grid potential can be used to vary the cathode current. Thus, a separate accelerator is not necessary. Eliminating the accelerator results in three immediate advantages:

- (1) Reduction of the number of required electrode voltages by one.
- (2) Elimination of the gap between the accelerator and the anode, thus reducing the length required for the transition region which in turn reduces diocotron growth and gun noise.
- (3) Elimination of the potential and field matching problems due to the accelerator and anode gap.

Although the cathode current fluctuates, the average value given by the computer model is about 5.0 amps which is only slightly less than that predicted by the Kino theory. However, it must be kept in mind that the accelerator electrode is not the exact Kino shape due to the necessary compromises made to match up the anode and the accelerator and thus it is not expected that the exact Kino current would be obtained.

The beam thickness varies with position, but an average value of about 10 mils is obtained for the exiting beam. This design was reached only after several sols, beam focusing electrode, and anode shapes were analyzed. Only with a computer model which is capable of modeling the complete gun region back to the cathode, can designs such as this be made with any confidence.

Noise Simulation in the Crossed Field Beam

In order to study the noise properties of the beam, it is necessary to simulate the emission properties of the hot cathode surface as accurately as possible. For the computer model this means that the following parameters must be determined at the cathode surface:

- (1) The number of electrons emitted.
- (2) The emission velocities of the electrons.
- (3) The time of emission of the electrons.

The method for calculating each of the above three quantities is summarized below:

(1) Emission Number

It can be shown that the probability of exactly S electrons being emitted from a given cathode spot of length Δy during the time interval Δt is given by

$$f(S) = \frac{e^{-\lambda} \lambda^S}{S!}$$

where λ is the average number of electrons emitted in each Δt . This is recognized to be the Poisson Distribution.

The probability that S or fewer electrons are emitted in the time interval Δt is given by the cumulative distribution function

$$F(S) = \sum_{s=0}^S f(s)$$

and

$$0 < F(S) \leq 1$$

To determine the number of electrons emitted in a time interval, Δt , a uniformly distributed random number between 0 and 1 is generated. The number of electrons emitted is S if

$$F(S-1) < R \leq F(S)$$

When $R \leq F(0)$ no electrons are emitted.

(2) Emission Velocities

A half-Maxwellian distribution is assumed for the x component of emission velocity (the component perpendicular to the cathode). The x velocity is then given by

$$\dot{x} = \left(\frac{2kT}{m} \right)^{1/2} (-\ln R_x)^{1/2}$$

where R_x is a random number uniformly distributed between 0 and 1, T is the cathode temperature, k is Boltzmann's constant, and m is the electron mass.

A full-Maxwellian distribution is assumed for electron velocities in the y direction (parallel to the cathode). The relation giving this velocity is

$$\dot{y} = \left(\frac{2kT}{m} \right)^{1/2} \text{erf}^{-1}(R_y)$$

where R_y is a random number uniformly distributed between 0 and 1.

(3) Emission Times

In order to avoid calculating the positions of the electrons above the cathode for random emission times, it is assumed that all S of the electrons in a given mesh region are emitted at the same time but with a random distribution over the area. The emission points are then given by

$$y = y_0 \pm R_y \frac{\Delta y}{2}$$

where R_y is a random number between 0 and 1 and the sign of R_y is also selected randomly. Thus, to an observer looking at one point on the cathode surface the electrons will appear to come off that spot at random times. Provided the time interval Δt is chosen to be relatively small, the degree of approximation introduced should be small.

Preliminary calculations of beam "noisiness" as measured by velocity variance and noise power spectral density calculations have led to the following preliminary observations:

- (1) Operation of a CFA gun in the temperature limited regime leads to a marked increase in beam noise. Observation of the beam shape and trajectories during temperature limited operation shows a deterioration of the gun optics which may explain the increased noise.
- (2) The noise grows approximately exponentially with distance in the direction of beam flow. This result is not unexpected since amplification of the noise due to the diocotron effect would be expected to be approximately exponential.
- (3) The upper edge of the beam (nearest the anode) is noisier than the lower edge of the beam.

References

- (1) G. S. Kino, "A Design Method for Crossed-Field Electron Guns," IRE Trans. on El. Dev., Vol. ED-7, pp. 179-185: Jul. 1960.
- (2) S. P. Yu, O. Buneman, and G. P. Kooyers, "Time Dependent Computer Analysis of Electron-Wave Interaction in Crossed-Fields," J. Appl. Phys., Vol. 36, p. 2250: Aug. 1965.
- (3) R. Hockney, Methods in Computational Physics, Vol. 9, Academic Press Inc., New York: 1969.

APPENDIX C

COMPUTER-AIDED DESIGN OF ELECTRON GUNS
FOR INJECTED-BEAM CROSSED-FIELD AMPLIFIERS

Elden K. Shaw and Gerald P. Kooyers

Published in the IEEE Transactions on Electron Devices
Vol. ED-26, No. 7, July 1979, pp. 1100-1102

Computer-Aided Design of Electron Guns for Injected-Beam Crossed-Field Amplifiers

ELDEN K. SHAW AND G. P. KOOYERS

Abstract—A two-dimensional self-consistent computer-aided CFA gun analysis program is discussed which can be used to solve for the characteristics of "long" crossed-field guns with arbitrary electrode shapes and including the effects of space charge. The results of analyzing a "long" Kino gun show excellent agreement between the theoretical gun parameters and those obtained by the computer analysis. The model shows promise of also being useful in the analysis of noise in CFA guns.

I. TWO-DIMENSIONAL LAGRANGIAN MODEL

In this approach a large number (up to 6000) of rods of charge are used to simulate the beam in the gun and transition regions with rods being released from the cathode consistent with the emission characteristics of the cathode surface.

The approach is summarized below:

- 1) First, the gun and transition region is divided into a rectangular mesh.
- 2) Next, the potentials in the absence of space charge are calculated at each mesh point using a computer code which solves Laplace's equation for arbitrary electrode shapes and potentials. These potentials are then stored for use during the rest of the calculation.
- 3) A number of rods of charge are released from the cathode with position, density, and velocity consistent with the emission characteristics of the cathode. The beam buildup is followed *in time* with electrons being emitted from the

Manuscript received February 6, 1978. This work was supported in part by the United States Army Electronics Command, Fort Monmouth, NJ, and in part by the United States Air Force Office of Scientific Research, Bolling Air Force Base, Washington, DC.

The authors are with UCA Systems, Inc., Palo Alto, CA 94304.

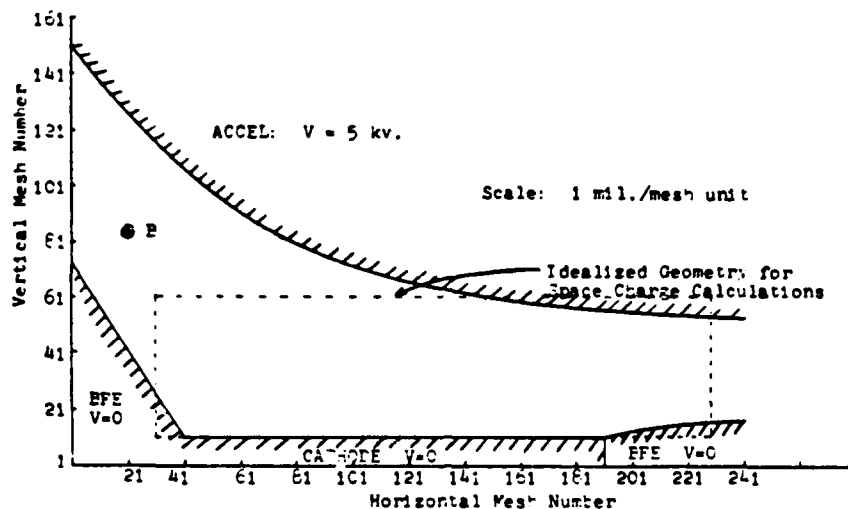


Fig. 1. Exact electrode shapes for "long" Kino gun design.

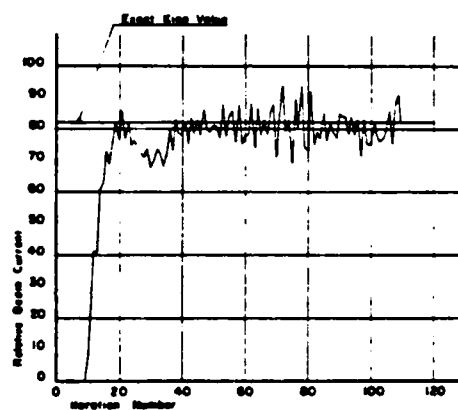


Fig. 2. Computer-calculated beam current exiting the gun region as a function of time.

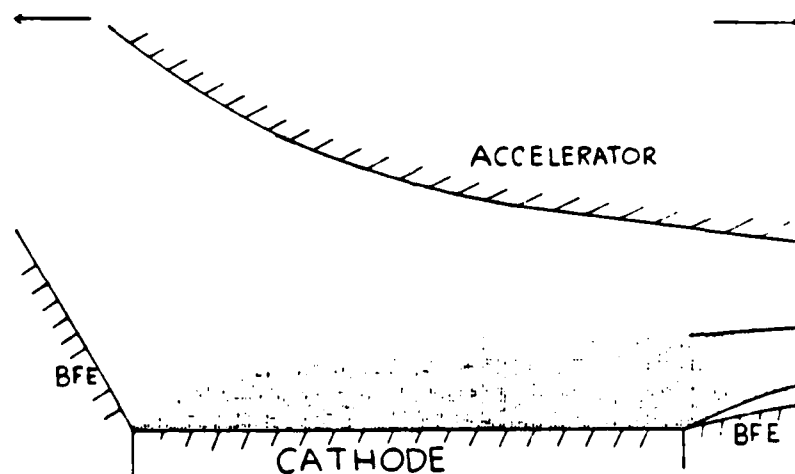


Fig. 3. Beam density profile for the "long" Kino gun. Notes: 1) There are 2555 rods of charge simulating the beam. 2) 152 rods of charge are injected at each time step; only an average of 21 exit the gun region. 3) The current exiting to the right differs from the Kino calculated value by only 5 percent. 4) Random electron thermal velocities are included in this calculation. 5) Electron shapes are from Kino gun theory.

cathode at equal small increments in time. The beam is allowed to build up to *several thousand* rods of charge with "new" rods of charge added at the cathode in each time step and "old" rods being removed as they exit the right-hand boundary or are collected on the electrodes.

4) The motion of the rods of charge is governed by the Lorentz force equation where the electric field is found from the potentials on the mesh points. During each iteration, each rod of charge is allowed to move for a small increment in time with its motion governed by the Lorentz force equation.

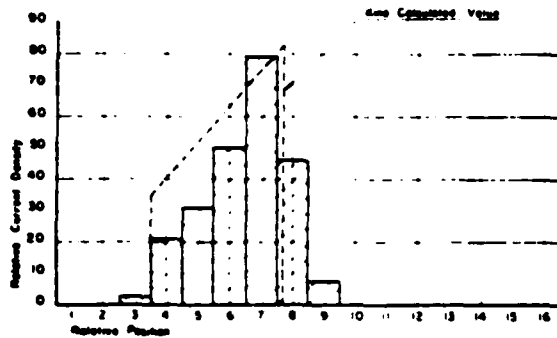


Fig. 4. Calculated current density at gun exit compared to theoretical beam density profile.

5) Simulating the beam by a large number of rods of charge has not been used in the past as an approach to the design of crossed-field guns due to the relatively long computer times required to solve Poisson's equation by conventional techniques. However, a technique due to Hockney [1]–[3] has been successfully used to solve Poisson's equation in less than 1 s on an IBM 370/168 (compared with approximately 1 min for the usual iterative relaxation procedures). This approach is discussed in some detail in a paper by Yu, Kooyers, and Buneman [4] and was used successfully in analyzing for the first time the distributed emission CFA. Once the potentials have been calculated including space charge by the Hockney technique for each iteration, "new" rods of charge are released from the cathode and the procedure discussed above is repeated until the beam reaches a "steady state." Steady state or convergence is obtained when the number of rods exiting the gun region averaged over one cyclotron period approaches a constant.

II. ANALYSIS OF A LONG KINO GUN

In order to determine the validity of the computer model, the "long" Kino gun [5] shown in Fig. 1 was analyzed. The parameters of this gun are:

total beam current	3.34 A
cathode length	0.150 in
magnetic field	0.2500 W/m ²
current density	14 A/cm ²
accelerator potential	5000 V
normalized cathode length	116.4 Kino units.

Current exiting the gun region as a function of time step is shown in Fig. 2. For this case the current rises rapidly and then fluctuates about a mean value which is close to the Kino predicted value. In this case, the cathode is operating space-charge-limited with only a fraction of the total emitted rods exiting the gun region. Shown in Fig. 3 is the exact Kino beam shape compared to that obtained by plotting the individual charge positions from the computer program. Again, the agreement between the computer-calculated results and the Kino theory is good. In Fig. 4 the computer-calculated current density is compared to the "exact" values calculated using the Kino equations.

REFERENCES

- [1] R. W. Hockney, *J. Assoc. Comput. Mach.*, vol. 12, p. 95, 1965.
- [2] —, *Methods in Computational Physics*, vol. 9. New York: Academic Press, 1969, pp. 135–211.
- [3] —, *Computational Physics*. New York: Academic Press, 1970, p. 17.

- [4] S. P. Yu, G. P. Kooyers, and O. Buneman, "Time dependent computer analysis of electron wave interaction in crossed-fields," *J. Appl. Phys.*, vol. 36, p. 2550, 1965.
- [5] G. S. Kino, "A design method for crossed-field electron guns," *IRE Trans. Electron Devices*, vol. ED-7, pp. 179–185, July 1960.

APPENDIX D

SOLVING POISSON'S EQUATION
IN THREE DIMENSIONS

D.1 Solving Poisson's Equation in Three Dimensions

We want to solve Poisson's Equation in the region sketched in Figure D-1 with a constant potential, ϕ_C , on the z boundaries.

First, the potential, ϕ_C , is subtracted from all boundary potentials since this results in simpler boundary conditions (i.e., two boundaries at zero potential rather than one). The modified boundary conditions are shown in Figure D-1.

A coordinate grid system is introduced with l segments in the x -direction, m in the y -direction, and n in the z -direction as sketched in Figure D-1.

For the mesh system defined above the boundary conditions are now given by

$$\phi_{1,j,1} = \phi_{1,j,n+1} = 0$$

$$\phi_{1,j,k} = -\phi_C$$

$$\phi_{l+1,j,k} = \phi_A - \phi_C = \phi_B \quad (D-1)$$

$$\phi_{1,0,k} = \phi_{1,2,k}$$

$$\phi_{1,m,k} = \phi_{1,m+2,k} \quad \frac{\partial \phi}{\partial n} = 0$$

The five point difference approximation to Poisson's Equation is:

$$\begin{aligned} & \frac{1}{\Delta x^2} \phi_{i-1,j,k} - 2\phi_{i,j,k} + \phi_{i+1,j,k} + \\ & \frac{1}{\Delta y^2} \phi_{i,j-1,k} - 2\phi_{i,j,k} + \phi_{i,j+1,k} + \\ & \frac{1}{\Delta z^2} \phi_{i,j,k-1} - 2\phi_{i,j,k} + \phi_{i,j,k+1} = \frac{\rho_{i,j,k}}{\epsilon_0} \end{aligned} \quad (D-2)$$

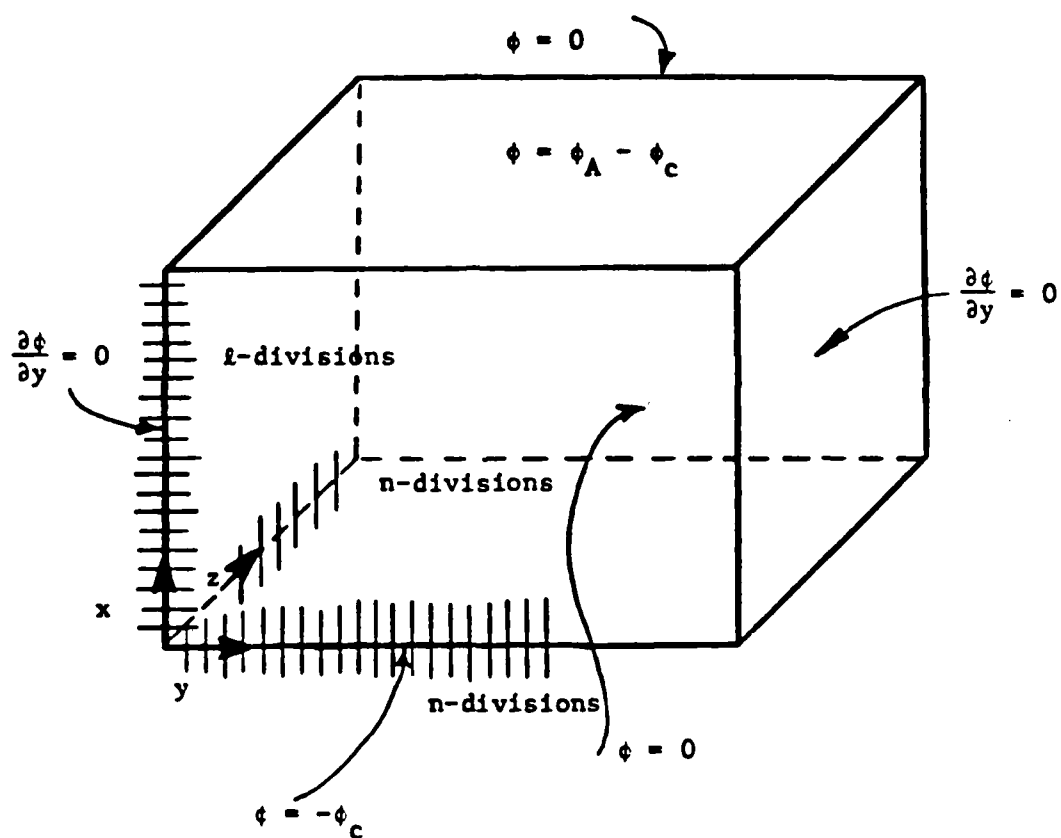


Figure D-1. Three-Dimensional Geometry with Modified Boundary Conditions for the Case of Constant Potential on z-Boundary.

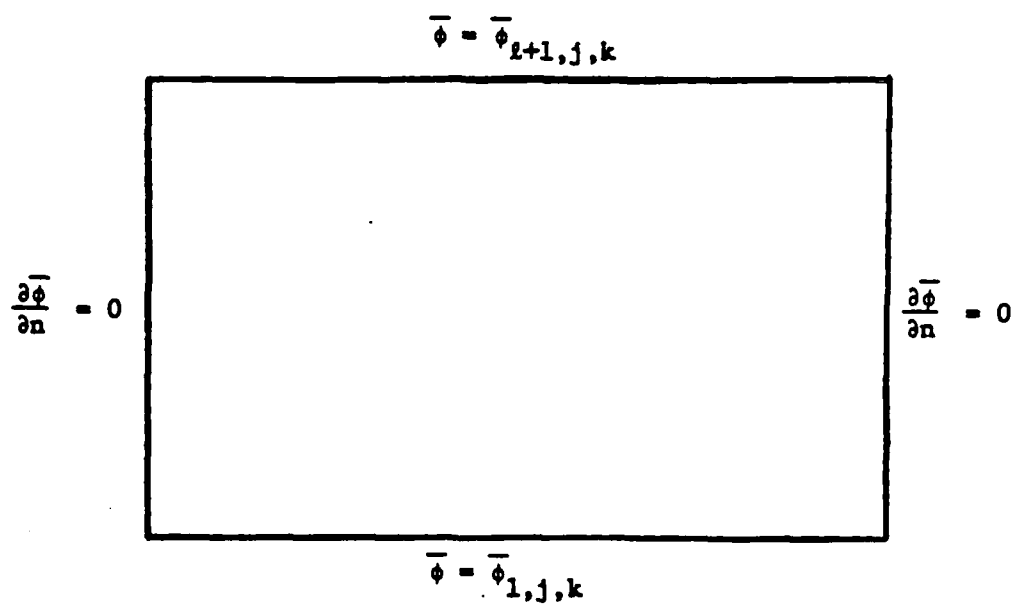


Figure D-2. Boundary Conditions for the Two-Dimensional Helmholtz Equation.

where the subscripts i, j , and k refer to the point (x_i, y_j, z_k) such that

$$\begin{aligned}x_i &= (i-1)\Delta x \\y_j &= (j-1)\Delta y \\z_k &= (k-1)\Delta z\end{aligned}\tag{D-3}$$

and

$$\begin{aligned}\Delta x &= \frac{a}{l} \\\Delta y &= \frac{b}{m} \\\Delta z &= \frac{c}{n}\end{aligned}$$

We now take the finite Fourier expansion of $\phi_{i,j,k}$ in the k (i.e., z) direction with the boundary conditions

$$\phi_{i,j,1} = \phi_{i,j,n+1} = 0.$$

For $1 \leq k \leq n-1$ we have

$$\bar{\phi}_{i,j,k+1} = \sum_{s=1}^{n-1} \phi_{i,j,s+1} \sin \frac{\pi s k}{n}\tag{D-4}$$

where $\bar{\phi}$ is the Fourier transform of ϕ and

$$\phi_{i,j,k} = \frac{2}{n} \sum_{s=1}^{n-1} \bar{\phi}_{i,j,s+1} \sin \frac{\pi s (k-1)}{n}\tag{D-5}$$

$k = 2, 3, \dots, n$.

Substituting the expression for ϕ into the three-dimensional five point difference equation, simplifying and equating the sine components, we obtain the equation

$$\begin{aligned} \bar{\rho}_{i,j,s+1} = & \frac{1}{\Delta x^2} \bar{\phi}_{i-1,j,s+1} - 2\bar{\phi}_{i,j,s+1} + \bar{\phi}_{i+1,j,s+1} \\ & + \frac{1}{\Delta y^2} \bar{\phi}_{i,j-1,s+1} - 2\bar{\phi}_{i,j,s+1} + \bar{\phi}_{i,j+1,s+1} + \frac{2}{\Delta z^2} \cos \frac{\pi s}{n} - 1 \\ & \bar{\phi}_{i,j,s+1} \end{aligned} \quad (D-6)$$

where we have also used the sine expansion for ρ . We note that this is just the finite difference approximation to the Helmholtz equation in two dimensions for each value of s . Thus, in order to solve the three-dimensional Poisson Equation, we use the following procedure:

- (1) Calculate $\bar{\rho}_{i,j,k}$ for all i,j by analyzing $\rho_{i,j,k}$ along k .

$$\bar{\rho}_{i,j,k+1} = \sum_{s=1}^{n-1} \rho_{i,j,s+1} \sin \frac{\pi s(k-1)}{n} \quad (D-7)$$

with the $\rho_{i,j,k}$'s being known.

This will require applying a Fourier Analysis program (l-1)x(m-1)x(n-1) times. To accomplish this analysis, an efficient computer program called FOUR67 is used.

- (2) Knowing the $\bar{\rho}$'s we then solve the two-dimensional Helmholtz equation

$$\nabla^2 \bar{\phi} + K^2 \bar{\phi} = \bar{\rho}$$

for each of the $n-1$ values of K . This two-dimensional problem is solved using a computer program called PWSCRT.

In order to solve the Helmholtz equation the boundary conditions of the transformed potentials must be known. We note that since

$$\phi_{1,j,k} = -\phi_C$$

$$\text{and } \phi_{l+1,j,k} = \phi_A - \phi_C$$

$$\text{then } \bar{\phi}_{1,j,k} = -\phi_C \sum_{s=1}^{n-1} \sin \frac{\pi s(k-1)}{n} \quad (D-8)$$

$$\text{and } \bar{\phi}_{l+1,j,k} = (\phi_A - \phi_C) \sum_{s=1}^{n-1} \sin \frac{\pi s(k-1)}{n} \quad (D-9)$$

The boundary conditions at $j=1$ and $j=m+1$ are

$$\frac{\partial \phi}{\partial y} = 0$$

$$\text{or } \phi_{1,0,k} = \phi_{1,2,k}$$

$$\text{and } \phi_{1,m,k} = \phi_{1,m+1,k}$$

which give

$$\frac{\partial \bar{\phi}_{1,m+1,k}}{\partial y} = \frac{\partial \bar{\phi}_{1,1,k}}{\partial y} = 0 \quad (D-10)$$

These boundary conditions are sketched in Figure D-2 for the k -th row in the z -direction.

- (3) Given the $\bar{\phi}_{1,j,k}$ we then use the inverse Fourier Transform (Synthesis)

$$\phi_{1,j,s+1} = \frac{2}{n} \sum_{k=1}^{n-1} \bar{\phi}_{1,j,k+1} \sin \frac{(\pi s k)}{n} \quad (D-11)$$

to obtain the potentials on all of the interior points. The efficient computer program FOUR67 is used to perform the above synthesis on the $(l-1) \times (m-1) \times (n-1)$ potential points.

APPENDIX E

FINITE DIFFERENCE EQUATIONS OF
MOTION IN THREE DIMENSIONS

E.1 EQUATIONS OF MOTION

In order to find the motion of the charges, it is necessary to solve the equation

$$m \frac{d\vec{v}}{dt} = q(\vec{E} + \vec{v} \times \vec{B}) .$$

Assuming both electric and magnetic field components in the x, y, and z directions, the components of the above equation become

$$\ddot{x} = \frac{q}{m} (E_x + \dot{y} B_z - \dot{z} B_y) \quad (E-1)$$

$$\ddot{y} = \frac{q}{m} (E_y + \dot{z} B_x - \dot{x} B_z) \quad (E-2)$$

$$\ddot{z} = \frac{q}{m} (E_z - \dot{y} B_x + \dot{x} B_y) \quad (E-3)$$

Assuming that the electric and magnetic fields are constant in the interval of integration, the above equations can be integrated once to obtain:

$$\dot{x}(t) - \dot{x}(0) = \frac{q}{m} \left[E_x t + (y(t) - y(0)) B_z - (z(t) - z(0)) B_y \right] \quad (E-4)$$

$$\dot{y}(t) - \dot{y}(0) = \frac{q}{m} \left[E_y t + (z(t) - z(0)) B_x - (x(t) - x(0)) B_z \right] \quad (E-5)$$

$$\dot{z}(t) - \dot{z}(0) = \frac{q}{m} \left[E_z t - (y(t) - y(0)) B_x + (x(t) - x(0)) B_y \right] \quad (E-6)$$

Using the Laplace Transform on Eqs. E-4, E-5 and E-6, we obtain the linear equations

$$s\tilde{x} - \omega_{cz}\tilde{y} + \omega_{cy}\tilde{z} = \eta \frac{E_x}{s^2} + \frac{1}{s} (\omega_{cy}z_0 - \omega_{cz}y_0 + \dot{x}_0) + x_0 \quad (E-7)$$

$$\omega_{cz} \tilde{x} + s\tilde{y} - \omega_{cx} \tilde{z} = \eta \frac{E_y}{s^2} + \frac{1}{s} (\omega_{cz} x_0 - \omega_{cx} z_0 + \dot{y}_0) + y_0 \quad (E-8)$$

$$- \omega_{cy} \tilde{x} + \omega_{cx} \tilde{y} + s\tilde{z} = \eta \frac{E_z}{s^2} + \frac{1}{s} (\omega_{cx} y_0 - \omega_{cy} x_0 + \dot{z}_0) + z_0 \quad (E-9)$$

where $\omega_{cx} = \eta B_x$

$$\omega_{cy} = \eta B_y$$

$$\omega_{cz} = \eta B_z$$

$$\eta = \frac{q}{m}$$

$$x_0 = x(0) \quad \dot{x}_0 = \dot{x}(0)$$

$$y_0 = y(0) \quad \dot{y}_0 = \dot{y}(0)$$

$$z_0 = z(0) \quad \dot{z}_0 = \dot{z}(0)$$

and $\tilde{x}, \tilde{y}, \tilde{z}$ are the Laplace Transforms of $x(t), y(t), z(t)$.

Equations E-7, E-8 and E-9 can be solved simultaneously for $\tilde{x}, \tilde{y}, \tilde{z}$ and then inverse transformed to obtain

$$\begin{aligned} x - x_0 &= \frac{\dot{x}_0}{\omega_c} \left[\sin \tau + \frac{\omega_{cx}^2}{\omega_c^2} (\tau - \sin \tau) \right] + \\ &\frac{\dot{y}_0}{\omega_c} \left[\frac{\omega_{cz}}{\omega_c} (1 - \cos \tau) + \frac{\omega_{cx}}{\omega_c} \frac{\omega_{cy}}{\omega_c} (\tau - \sin \tau) \right] \\ &+ \frac{\dot{z}_0}{\omega_c} \left[\frac{\omega_{cy}}{\omega_c} (1 - \cos \tau) + \frac{\omega_{cx}}{\omega_c} \frac{\omega_{cz}}{\omega_c} (\tau - \sin \tau) \right] \end{aligned}$$

AD-A125 951

NOISE PHENOMENA IN CROSSED-FIELD ELECTRON BEAMS(U) UCA
SYSTEMS INC PALO ALTO CA G P KOOVERS ET AL. 15 APR 80
AFOSR-TR-83-0132 F49620-77-C-0061

2/2

UNCLASSIFIED

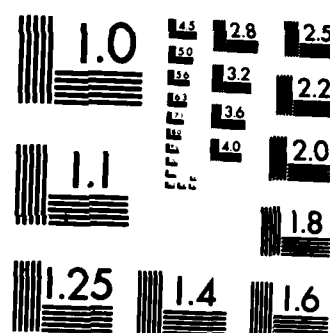
F/G 9/1

NL



END

FILED
21
070



MICROCOPY RESOLUTION TEST CHART
NATIONAL BUREAU OF STANDARDS-1963-A

$$\begin{aligned}
& + \frac{\eta E_x}{\omega_c^2} \left[\frac{\omega_{cx}^2}{\omega_c^2} \left(-1 + \frac{\tau^2}{2} + \cos \tau \right) \right] \\
& + \frac{\eta E_y}{\omega_c^2} \left[\frac{\omega_{cx}}{\omega_c} \frac{\omega_{cy}}{\omega_c} \left(-1 + \frac{\tau^2}{2} + \cos \tau \right) + \frac{\omega_{cz}}{\omega_c} (\tau - \sin \tau) \right] \\
& + \frac{\eta E_z}{\omega_c^2} \left[\frac{\omega_{cx}}{\omega_c} \frac{\omega_{cz}}{\omega_c} \left(-1 + \frac{\tau^2}{2} + \cos \tau \right) - \frac{\omega_{cy}}{\omega_c} (\tau - \sin \tau) \right]
\end{aligned}
\tag{E-10}$$

$$\text{where } \omega_c^2 = \omega_{cx}^2 + \omega_{cy}^2 + \omega_{cz}^2$$

$$\text{and } \tau = \omega_{ct}.$$

Equations for y and z are not given since they are easily obtained from Equation E-10 by permuting the coordinates as given below:

$$x \rightarrow y$$

$$y \rightarrow z$$

$$z \rightarrow x$$

In the finite difference procedures used in the computer program, the x , y , and z positions of the particles are found at $t + \Delta t$ using Equation E-7 and the similar equations for y and z . Equations E-4, E-5, and E-6 are then used to find the x , y , and z velocities at $t + \Delta t$.

APPENDIX F

**SAMPLE COMPUTER CALCULATED OUTPUT
FROM THE THREE-DIMENSIONAL PROGRAM**

***** TEST CASE FOR GUNED 7/5/79

-----GEOMETRY PARAMETERS-----

NO. OF MESH DIVISIONS IN THE X-DIRECTION = 32.0000
NO. OF MESH DIVISIONS IN THE Y-DIRECTION = 48.0000
NO. OF MESH DIVISIONS IN THE Z-DIRECTION = 16.0000
HEIGHT OF THE GUN IN THE X-DIRECTION IN INCHES = 0.0320
LENGTH OF THE GUN IN THE Y-DIRECTION IN INCHES = 0.1920
WIDTH OF THE GUN IN THE Z-DIRECTION IN INCHES = 0.2470

-----TRAJECTORY PARAMETERS-----

THE X-DIRECTED MAGNETIC FIELD = 0.0 THE Z-DIRECTED MAGNETIC FIELD = 0.2500
THE NUMBER OF TIME STEPS PER CYCLOTRON PERIOD = 10.0000
OUTPUT TRAJECTORY NORMALIZATION PARAMETER = 1.0000 THE MAXIMUM NUMBER OF PARTICLES = 10000.0000
THIS CALCULATION PROCEEDS FOR 76.0000 ITERATIONS

-----CATHODE EMISSION PARAMETERS-----

BEGINNING Y-MESH POINT OF CATHODE = 5.0000 ENDING Y-MESH POINT OF CATHODE = 42.0000
BEGINNING Z-MESH POINT OF CATHODE = 3.0000 ENDING Z-MESH POINT OF CATHODE = 17.0000
NUMBER OF CATHODE SEGMENTS IN Y-DIRECTION = 10.0000 NUMBER OF CATHODE SEGMENTS IN Z-DIRECTION = 10.0000
CATHODE TEMPERATURE IN DEGREES KELVIN = 1323.0000 NUMBER OF PARTICLES EMITTED PER MESH REGION = 4.0000
RANDOM NUMBER PARAMETER = 1.0000 RANDOM POSITION PARAMETER = 1.0000
RANDOM VELOCITY PARAMETER = 1.0000

-----POTENTIAL AND SPACE CHARGE PARAMETERS-----

THE NUMBER OF PARTICLES IN THE DRILLQUIN BEAM IS = 0.3000E+05 THE SPACE CHARGE CALCULATION PARAMETER IS 0.0
ARRAY OF BOUNDARY POTENTIALS AT X=A
0.9050E+03 0.1154E+04 0.1364E+04 0.1495E+04 0.1639E+04 0.1756E+04 0.1853E+04 0.1938E+04 0.1996E+04 0.2069E+04 0.2137E+04 0.2201E+04
.2263E+04 0.2322E+04 0.2380E+04 0.2439E+04 0.2498E+04 0.2550E+04 0.2617E+04 0.2676E+04 0.2733E+04 0.2788E+04 0.2843E+04 0.2896E+04
.2947E+04 0.2997E+04 0.3045E+04 0.3090E+04 0.3132E+04 0.3172E+04 0.3209E+04 0.3243E+04 0.3275E+04 0.3305E+04 0.3334E+04 0.3363E+04
.3391E+04 0.3418E+04 0.3443E+04 0.3466E+04 0.3483E+04 0.3495E+04 0.3502E+04 0.3506E+04 0.3510E+04 0.3515E+04 0.3521E+04 0.3528E+04
--.3538E+04
THE Z-BOUNDARY POTENTIAL = 0.0
POTENTIAL NORMALIZATION CONSTANT = 0.1409E+00 CHARGE NORMALIZATION CONSTANT = 0.1270E+10

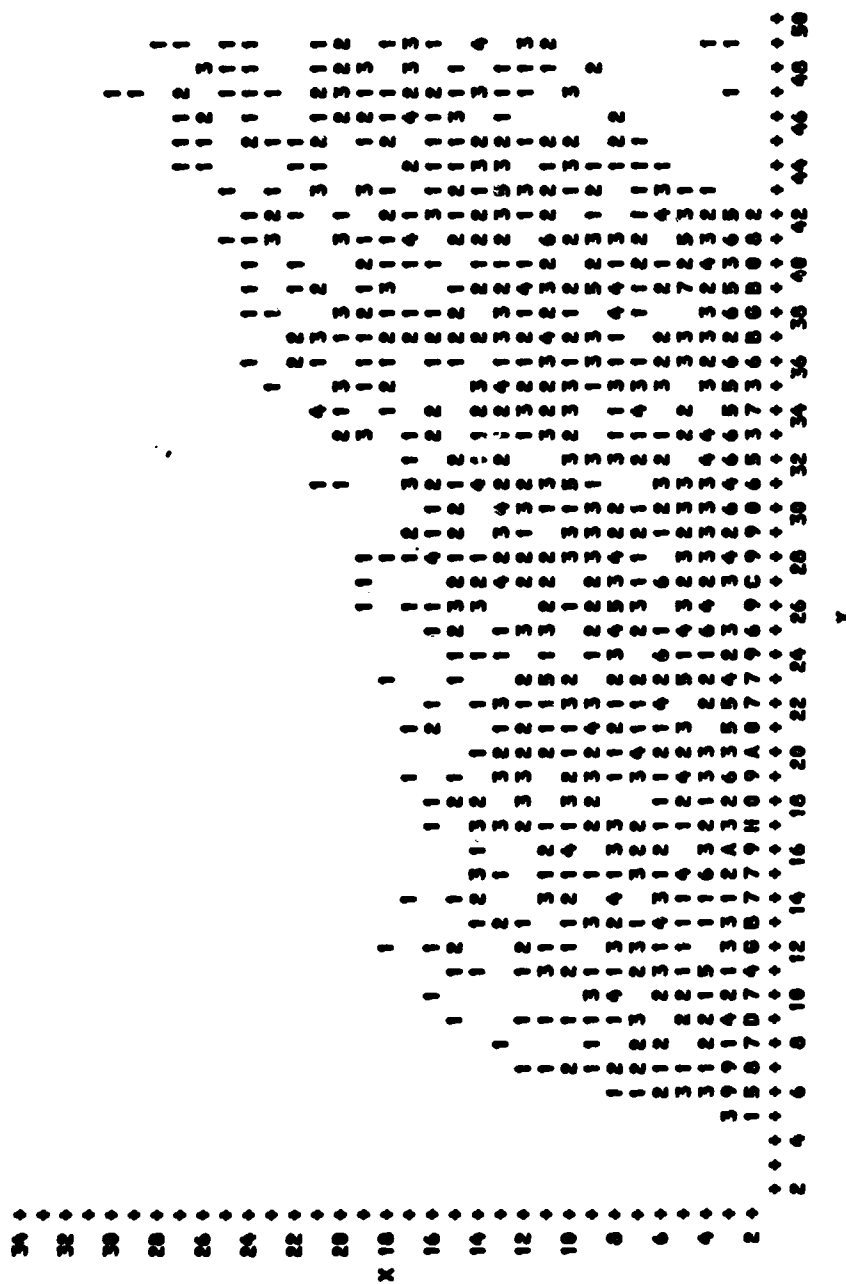
-----PARTICLE EXIT PARAMETERS-----

MAXIMUM NUMBER OF EXITING TRAJECTORIES SAVED FOR EACH BOUNDARY 20.0000 20.0000 20.0000 20.0000 20.0000 20.0000

-----PRINT PARAMETERS-----

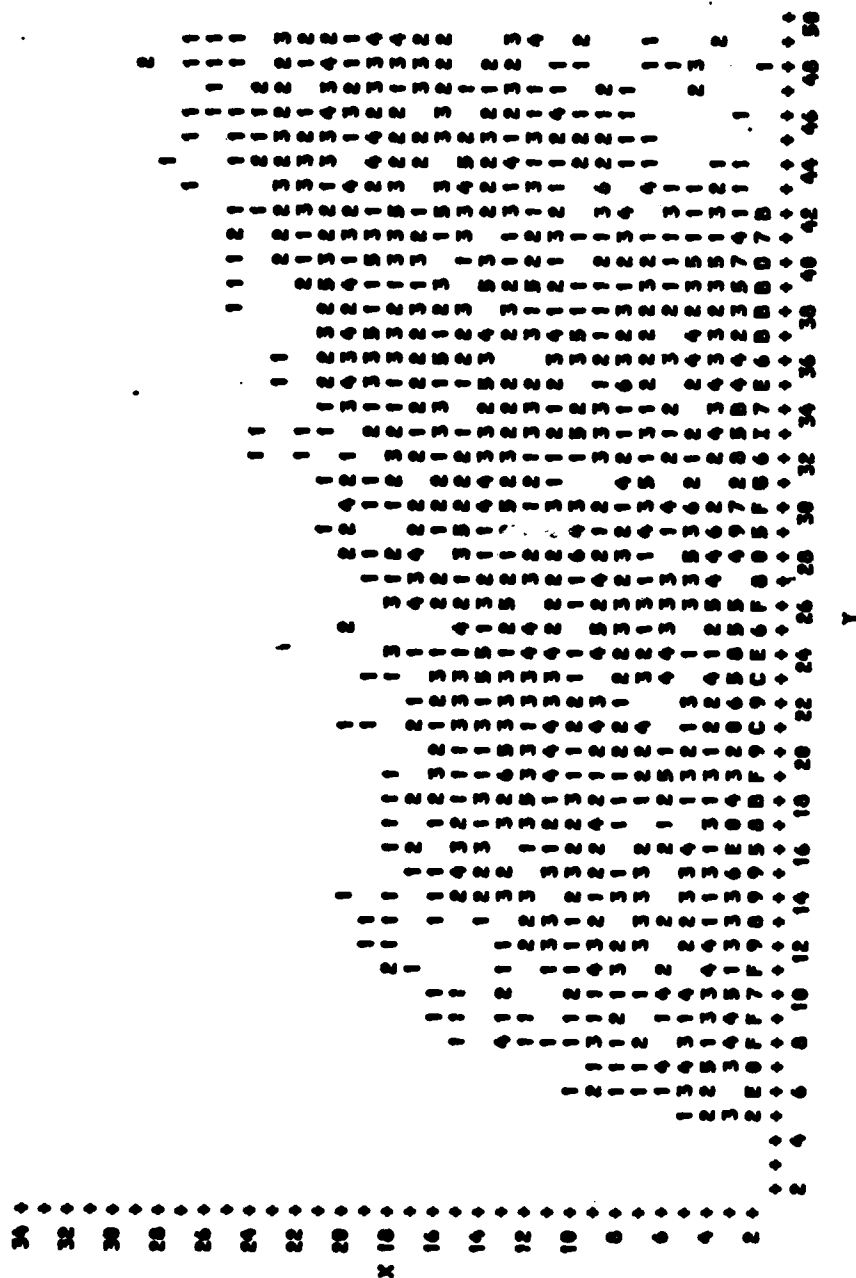
TRAJECTORY INFORMATION WILL BE PRINTED OUT EVERY 20.0000-TH TIME STEP FOR EVERY 100.0000-TH PARTICLE

BEAM PROFILE PLOT FOR ITERATION NO. 75 AT THE Z-MEM POINT 4 WITH Z-THICKNESS OF 2

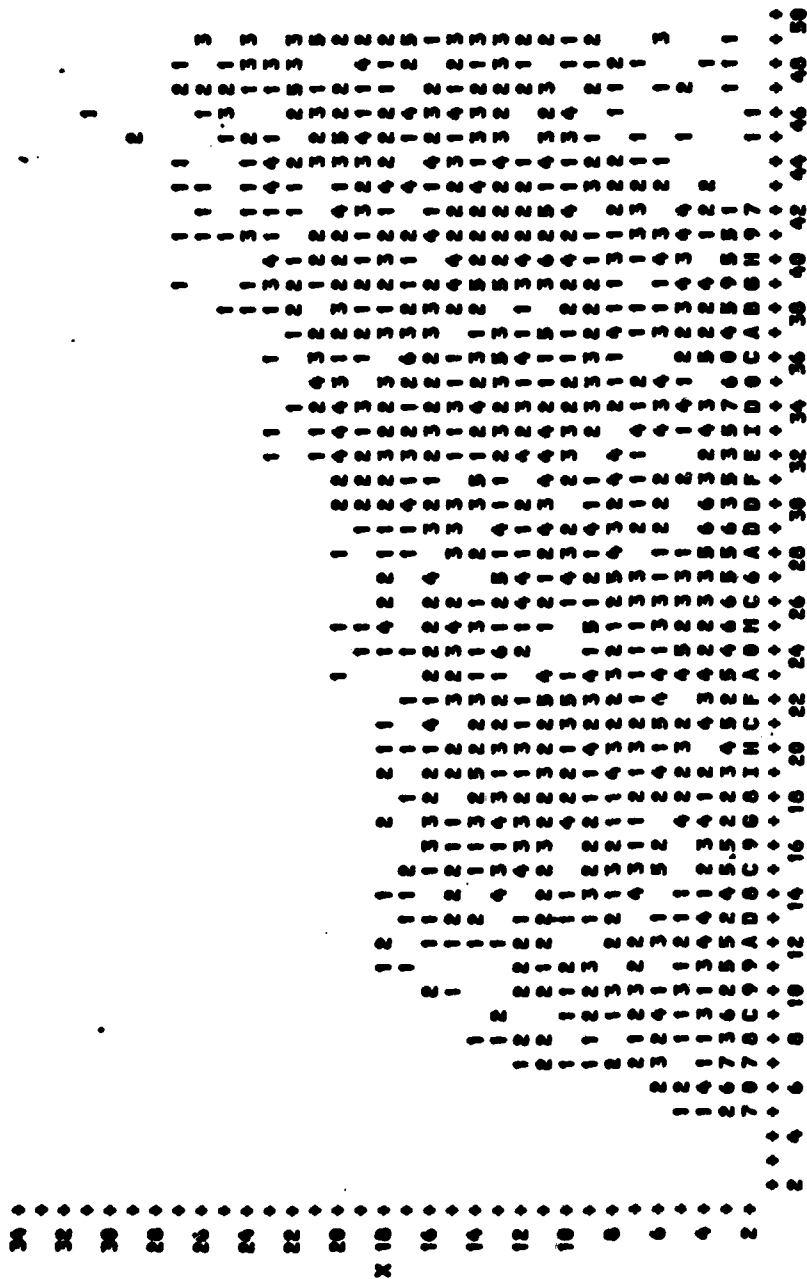


Y

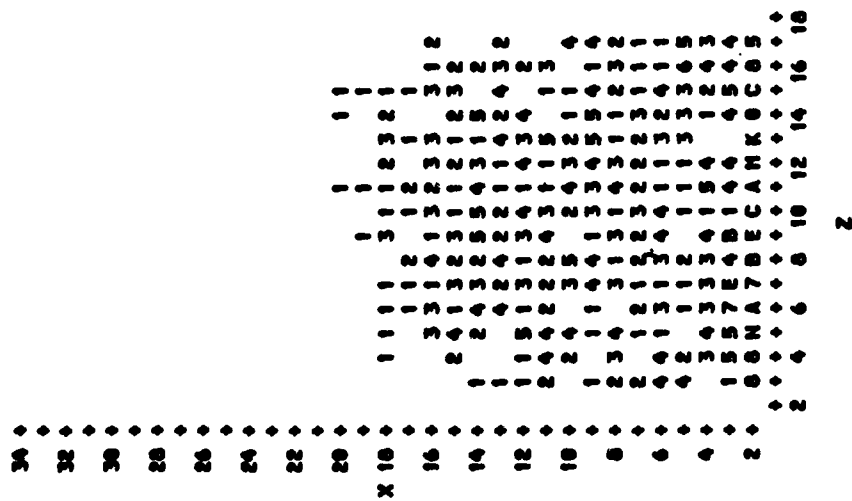
MEAN PROFILE PLOT FOR ITERATION NO. 75 AT THE Z-MESH POINT 10 WITH Z-THICKNESS OF 2



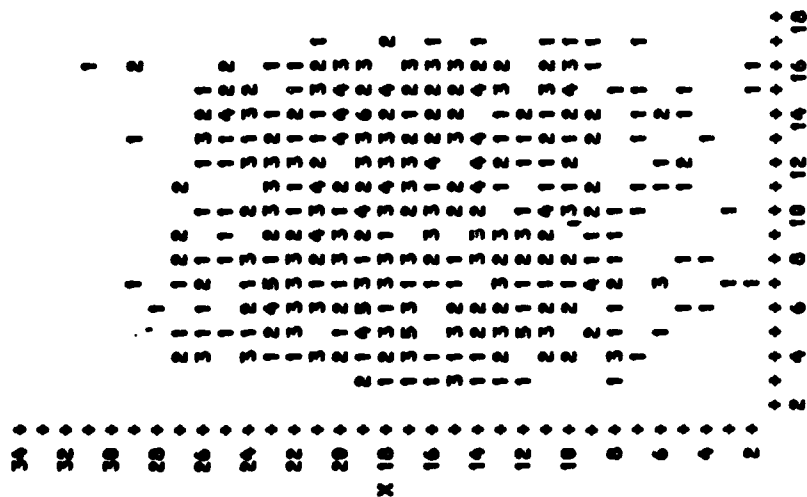
BEAM PROFILE PLOT FOR ITERATION NO. 75 AT THE Z-MESH POINT 16 WITH Z-THICKNESS OF 2



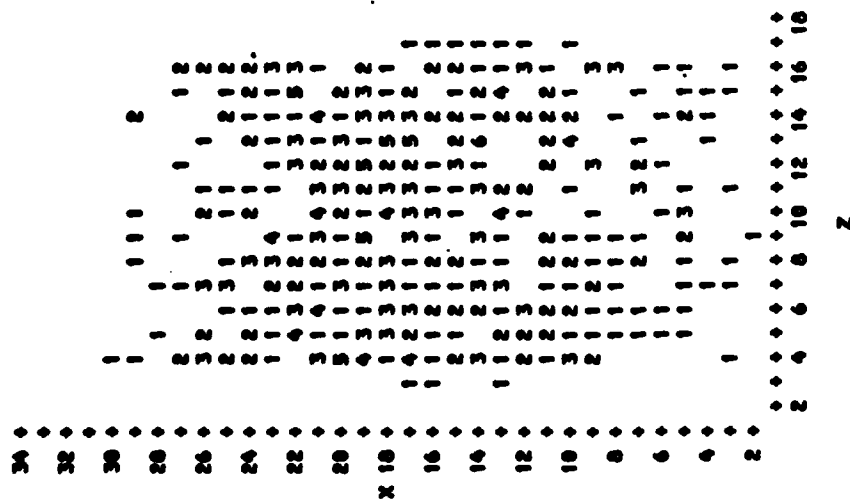
BEAM PROFILE PLOT FOR ITERATION NO. 75 AT THE Y-HEM POINT 24 WITH Y-THICKNESS OF 2



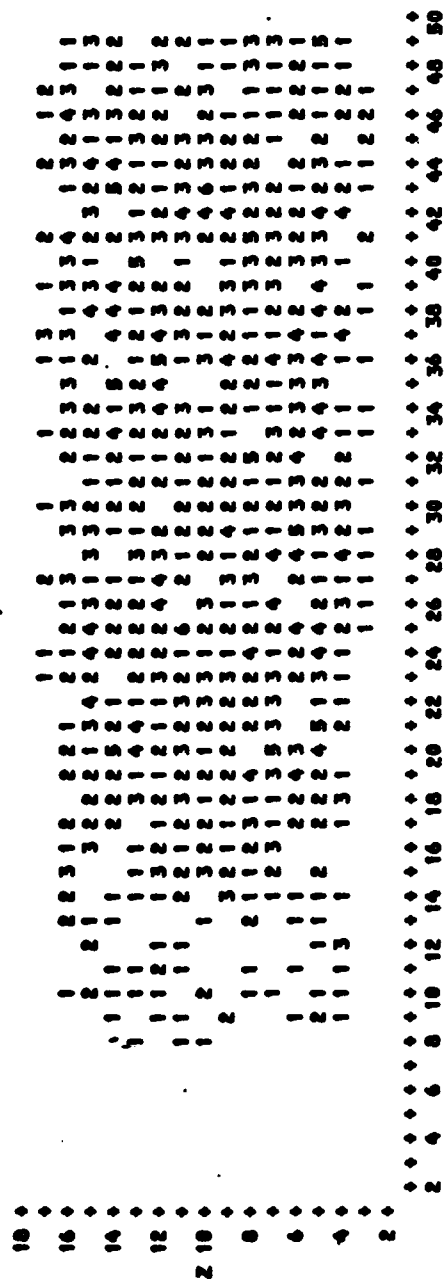
BEAM PROFILE PLOT FOR ITERATION NO. 75 AT THE Y-MESH POINT 46 WITH Y-THICKNESS OF 2



BEAM PROFILE PLOT FOR ITERATION NO. 75 AT THE Y-HEEN POINT 40 WITH Y-THICKNESS OF 2



BEAM PROFILE PLOT FOR ITERATION NO. 75 AT THE X-MESH POINT 16 WITH X-THICKNESS OF 2



THE TOTAL NUMBER OF PARTICLES FOR ITERATION NUMBER 75 IS 15494 THE MAXIMUM NUMBER OF PARTICLES USED = 15674

- PARTICLE NO. 12 WITH AGE 1 EXITS THE LOWER BOUNDARY WITH XN = 0.2064E+01 YN = 0.4154E+02 ZN = 0.1274E+02
VXN = -0.1722E+01 VYN = -0.9301E-01 VZN = -0.2367E-02
- PARTICLE NO. 13 WITH AGE 1 EXITS THE LOWER BOUNDARY WITH XN = 0.2244E+01 YN = 0.4162E+02 ZN = 0.1342E+02
VXN = -0.9628E+00 VYN = -0.1002E-01 VZN = -0.1272E-02
- PARTICLE NO. 14 WITH AGE 1 EXITS THE LOWER BOUNDARY WITH XN = 0.2037E+01 YN = 0.4167E+02 ZN = 0.1268E+02
VXN = -0.1568E+01 VYN = -0.1010E+00 VZN = 0.9837E-02
- PARTICLE NO. 16 WITH AGE 1 EXITS THE LOWER BOUNDARY WITH XN = 0.2453E+01 YN = 0.4202E+02 ZN = 0.1249E+02
VXN = -0.2998E+00 VYN = -0.8166E-01 VZN = -0.5232E-02
- PARTICLE NO. 32 WITH AGE 1 EXITS THE LOWER BOUNDARY WITH XN = 0.2195E+01 YN = 0.4178E+02 ZN = 0.1243E+02
VXN = -0.1040E+01 VYN = -0.7694E-01 VZN = 0.1171E-01
- PARTICLE NO. 135 WITH AGE 1 EXITS THE LOWER BOUNDARY WITH XN = 0.2346E+01 YN = 0.4174E+02 ZN = 0.8870E+01
VXN = -0.5984E+00 VYN = -0.2968E-01 VZN = 0.8326E-02
- PARTICLE NO. 136 WITH AGE 1 EXITS THE LOWER BOUNDARY WITH XN = 0.2492E+01 YN = 0.4225E+02 ZN = 0.8658E+01
VXN = -0.1346E+00 VYN = -0.2054E-01 VZN = -0.1223E-01
- PARTICLE NO. 160 WITH AGE 1 EXITS THE LOWER BOUNDARY WITH XN = 0.2338E+01 YN = 0.4178E+02 ZN = 0.8468E+01
VXN = -0.6847E+00 VYN = -0.1356E-01 VZN = -0.3844E-02
- PARTICLE NO. 173 WITH AGE 1 EXITS THE LOWER BOUNDARY WITH XN = 0.1482E+01 YN = 0.4194E+02 ZN = 0.4829E+01
VXN = -0.3212E+01 VYN = -0.2338E+00 VZN = 0.5171E-02
- PARTICLE NO. 182 WITH AGE 1 EXITS THE LOWER BOUNDARY WITH XN = 0.1668E+01 YN = 0.4179E+02 ZN = 0.4831E+01
VXN = -0.2809E+01 VYN = -0.2459E+00 VZN = 0.1150E-01

PARTICLE NO. 106 WITH AGE 1 EXITS THE LOWER BOUNDARY WITH XN = 0.2286E+01 YN = 0.4211E+02 ZN = 0.5112E+01
VXN = -0.0367E+00 VTN = -0.9145E-01 VZN = 0.1552E-01

PARTICLE NO. 107 WITH AGE 1 EXITS THE LOWER BOUNDARY WITH XN = 0.1035E+01 YN = 0.4220E+02 ZN = 0.4920E+01
VXN = -0.0202E+01 VTN = -0.1634E+00 VZN = -0.7395E-02

PARTICLE NO. 199 WITH AGE 1 EXITS THE LOWER BOUNDARY WITH XN = 0.1730E+01 YN = 0.4173E+02 ZN = 0.4462E+01
VXN = -0.0486E+01 VTN = -0.1702E+00 VZN = -0.3770E-02

PARTICLE NO. 212 WITH AGE 3 EXITS THE LOWER BOUNDARY WITH XN = 0.2227E+01 YN = 0.4140E+02 ZN = 0.5972E+01
VXN = -0.0030E+00 VTN = -0.1019E+00 VZN = 0.0964E-02

PARTICLE NO. 216 WITH AGE 4 EXITS THE LOWER BOUNDARY WITH XN = 0.2013E+01 YN = 0.4100E+02 ZN = 0.6010E+01
VXN = -0.3707E+00 VTN = -0.5013E-01 VZN = 0.2610E-02

PARTICLE NO. 221 WITH AGE 1 EXITS THE LOWER BOUNDARY WITH XN = 0.2304E+01 YN = 0.4112E+02 ZN = 0.1746E+02
VXN = -0.4766E+00 VTN = -0.7611E-01 VZN = 0.9505E-02

PARTICLE NO. 270 WITH AGE 7 EXITS THE LOWER BOUNDARY WITH XN = 0.2362E+01 YN = 0.4247E+02 ZN = 0.0045E+01
VXN = -0.1050E+01 VTN = 0.2435E+00 VZN = 0.1769E-01

PARTICLE NO. 299 WITH AGE 1 EXITS THE LOWER BOUNDARY WITH XN = 0.2360E+01 YN = 0.4072E+02 ZN = 0.1570E+02
VXN = -0.4404E+00 VTN = -0.1301E-01 VZN = -0.1313E-01

PARTICLE NO. 300 WITH AGE 1 EXITS THE LOWER BOUNDARY WITH XN = 0.2495E+01 YN = 0.4090E+02 ZN = 0.1536E+02
VXN = -0.3494E-01 VTN = -0.1929E-01 VZN = 0.7343E-02

PARTICLE NO. 441 WITH AGE 5 EXITS THE LOWER BOUNDARY WITH XN = 0.1970E+01 YN = 0.4074E+02 ZN = 0.1203E+02
VXN = -0.2517E+01 VTN = -0.0001E-01 VZN = -0.5667E-02

PARTICLE NO. 92 WITH AGE 11 EXITS THE RIGHT BOUNDARY WITH XN = 0.1600E+02 YN = 0.5195E+02 ZN = 0.1523E+02
VXN = -0.1570E+00 VTN = 0.4260E+01 VZN = -0.2901E-01

PARTICLE NO. 192 WITH AGE 11 EXITS THE RIGHT BOUNDARY WITH XN = 0.1501E+02 YN = 0.5139E+02 ZN = 0.1391E+02
VXN = -0.3448E+00 VTN = 0.4261E+01 VZN = -0.3245E-01

PARTICLE NO. 210 WITH AGE 11 EXITS THE RIGHT BOUNDARY WITH XN = 0.1402E+02 YN = 0.5121E+02 ZN = 0.1327E+02
VXN = -0.1543E+01 VTN = 0.3090E+01 VZN = -0.3617E-01

PARTICLE NO. 200 WITH AGE 13 EXITS THE RIGHT BOUNDARY WITH XN = 0.1136E+02 YN = 0.5044E+02 ZN = 0.7027E+01
VXN = -0.7371E+00 VTN = 0.3296E+01 VZN = -0.5945E-02

PARTICLE NO. 357 WITH AGE 11 EXITS THE RIGHT BOUNDARY WITH XN = 0.1425E+02 YN = 0.5123E+02 ZN = 0.9307E+01
VXN = 0.3052E+00 VTN = 0.3594E+01 VZN = 0.2451E-01

PARTICLE NO. 496 WITH AGE 0 EXITS THE RIGHT BOUNDARY WITH XN = 0.1170E+02 YN = 0.5095E+02 ZN = 0.3972E+01
VXN = -0.0372E+00 VTN = 0.2942E+01 VZN = 0.1706E+00

PARTICLE NO. 499 WITH AGE 0 EXITS THE RIGHT BOUNDARY WITH XN = 0.1211E+02 YN = 0.5044E+02 ZN = 0.4060E+01
VXN = -0.3379E+00 VTN = 0.3000E+01 VZN = 0.7419E-01

PARTICLE NO. 501 WITH AGE 13 EXITS THE RIGHT BOUNDARY WITH XN = 0.1606E+02 YN = 0.5070E+02 ZN = 0.1290E+02
VXN = 0.1600E+00 VTN = 0.4270E+01 VZN = 0.3601E-02

PARTICLE NO. 516 WITH AGE 0 EXITS THE RIGHT BOUNDARY WITH XN = 0.1526E+02 YN = 0.5027E+02 ZN = 0.4023E+01
VXN = 0.2077E+01 VTN = 0.3747E+01 VZN = 0.6763E-01

PARTICLE NO. 530 WITH AGE 11 EXITS THE RIGHT BOUNDARY WITH XN = 0.1350E+02 YN = 0.5000E+02 ZN = 0.5255E+01
VXN = 0.3113E+00 VTN = 0.3249E+01 VZN = 0.1314E-01

PARTICLE NO. 576 WITH AGE 11 EXITS THE RIGHT BOUNDARY WITH XN = 0.1031E+02 YN = 0.5090E+02 ZN = 0.1600E+02
 VXN = 0.1017E+01 VYN = 0.4196E+01 VZN = 0.1051E-01

PARTICLE NO. 611 WITH AGE 11 EXITS THE RIGHT BOUNDARY WITH XN = 0.1050E+02 YN = 0.5029E+02 ZN = 0.1457E+02
 VXN = -0.2407E+01 VYN = 0.2954E+01 VZN = -0.1226E-01

PARTICLE NO. 643 WITH AGE 13 EXITS THE RIGHT BOUNDARY WITH XN = 0.1047E+02 YN = 0.5240E+02 ZN = 0.4097E+01
 VXN = 0.5231E-01 VYN = 0.4320E+01 VZN = 0.0579E-01

PARTICLE NO. 644 WITH AGE 13 EXITS THE RIGHT BOUNDARY WITH XN = 0.1374E+02 YN = 0.5027E+02 ZN = 0.1653E+02
 VXN = -0.1249E+01 VYN = 0.3399E+01 VZN = -0.3696E-01

PARTICLE NO. 648 WITH AGE 13 EXITS THE RIGHT BOUNDARY WITH XN = 0.7005E+01 YN = 0.5003E+02 ZN = 0.1666E+02
 VXN = -0.2266E+01 VYN = 0.2400E+01 VZN = 0.0095E-02

PARTICLE NO. 675 WITH AGE 13 EXITS THE RIGHT BOUNDARY WITH XN = 0.1039E+02 YN = 0.5061E+02 ZN = 0.1356E+02
 VXN = 0.2669E+00 VYN = 0.4530E+01 VZN = -0.2594E-01

PARTICLE NO. 677 WITH AGE 11 EXITS THE RIGHT BOUNDARY WITH XN = 0.1763E+02 YN = 0.5202E+02 ZN = 0.1340E+02
 VXN = -0.0470E+00 VYN = 0.4622E+01 VZN = -0.3055E-01

PARTICLE NO. 700 WITH AGE 13 EXITS THE RIGHT BOUNDARY WITH XN = 0.1978E+02 YN = 0.5133E+02 ZN = 0.1207E+02
 VXN = 0.0402E+00 VYN = 0.4094E+01 VZN = -0.3297E-02

PARTICLE NO. 801 WITH AGE 15 EXITS THE RIGHT BOUNDARY WITH XN = 0.1397E+02 YN = 0.5075E+02 ZN = 0.1191E+02
 VXN = -0.1045E+01 VYN = 0.3612E+01 VZN = 0.3331E-01

PARTICLE NO. 800 WITH AGE 8 EXITS THE RIGHT BOUNDARY WITH XN = 0.1206E+02 YN = 0.5082E+02 ZN = 0.1214E+02
 VXN = 0.0000E-01 VYN = 0.3370E+01 VZN = -0.5235E-02

MATRIX OF NET CATHODE PARTICLE EMISSION FOR ITERATION NUMBER 75
 THE CATHODE IS DIVIDED INTO 10 SEGMENTS IN Y AND 10 SEGMENTS IN Z

	1	2	3	4	5	6	7	8	9	10
NRGZ = 1	12	10	5	-1	4	10	4	15	10	-1
NRGZ = 2	13	14	14	-2	0	-10	14	15	12	15
NRGZ = 3	15	-1	-3	1	4	16	0	10	1	17
NRGZ = 4	10	11	6	3	7	-15	1	9	3	0
NRGZ = 5	19	24	13	1	-11	-3	12	11	10	19
NRGZ = 6	4	10	6	-3	0	-1	6	9	7	10
NRGZ = 7	5	11	-2	2	3	-9	17	-1	6	2
NRGZ = 8	13	2	-6	-11	-3	-1	0	0	-6	10
NRGZ = 9	11	11	10	17	-9	-9	-2	-6	12	2
NRGZ = 10	20	2	13	19	4	10	13	10	20	16

MATRIX OF AVERAGE CATHODE CURRENT DENSITY IN AMPS PER CM² FOR ITERATION NUMBER 75
 THE CATHODE IS DIVIDED INTO 10 SEGMENTS IN Y AND 10 SEGMENTS IN Z

	1	2	3	4	5	6	7	8	9	10
NRGZ = 1	64.20	59.55	51.60	52.55	50.59	21.99	24.62	27.40	30.65	34.01

NREGZ = 2	30.90	22.48	17.70	15.03	11.60	13.00	17.59	19.61	20.00	26.90
NREGZ = 3	31.26	21.78	19.18	16.48	13.04	16.66	21.13	24.66	23.03	32.23
NREGZ = 4	32.30	23.33	20.05	19.04	16.67	16.15	20.37	22.39	25.05	29.96
NREGZ = 5	32.30	23.29	19.25	17.02	14.75	16.69	21.96	24.00	24.77	32.74
NREGZ = 6	32.74	22.14	19.25	17.23	14.93	15.32	20.30	23.04	24.62	31.47
NREGZ = 7	32.45	21.05	20.41	17.49	14.42	17.31	20.44	23.11	24.95	31.76
NREGZ = 8	32.56	21.56	19.79	16.40	13.04	15.06	20.90	23.04	24.37	30.00
NREGZ = 9	31.07	20.44	18.09	15.39	11.54	15.15	19.34	20.15	21.70	24.84
NREGZ = 10	37.42	29.46	20.91	26.93	27.51	29.24	32.01	30.79	32.66	30.83

-----EXITING CURRENT FOR ITERATION NUMBER 75-----

THE NET CURRENT OFF THE CATHODE = 3.0169
 THE CURRENT EXITING THE LOWER X-BOUNDARY = -3.6472
 THE CURRENT EXITING THE UPPER X-BOUNDARY = 0.0
 THE CURRENT EXITING THE LEFT Y-BOUNDARY = 0.0
 THE CURRENT EXITING THE RIGHT Y-BOUNDARY = 3.6020
 THE CURRENT EXITING THE FRONT Z-BOUNDARY = 0.0
 THE CURRENT EXITING THE BACK Z-BOUNDARY = 0.0

THE NUMBER OF PARTICLES EXITING THE LOWER X-BOUNDARY = -645
 THE NUMBER OF PARTICLES EXITING THE UPPER X-BOUNDARY = 0
 THE NUMBER OF PARTICLES EXITING THE LEFT Y-BOUNDARY = 0
 THE NUMBER OF PARTICLES EXITING THE RIGHT Y-BOUNDARY = 637
 THE NUMBER OF PARTICLES EXITING THE FRONT Z-BOUNDARY = 0
 THE NUMBER OF PARTICLES EXITING THE BACK Z-BOUNDARY = 0

-----NOISE CALCULATIONS FOR ITERATION NUMBER 75-----

THE AVERAGE CURRENT OFF THE CATHODE = 3.9437
 THE INSTANTANEOUS CURRENT OFF THE CATHODE = 3.0169
 THE INSTANTANEOUS CATHODE CURRENT FLUCTUATION SQUARED = 0.0161
 THE AVERAGE CATHODE CURRENT FLUCTUATION SQUARED = 0.2253
 THE AVERAGE EXITING CURRENT = 3.6639
 THE INSTANTANEOUS EXITING CURRENT = 3.6020
 THE INSTANTANEOUS EXITING CURRENT FLUCTUATION SQUARED = 0.0030
 THE AVERAGE EXITING CURRENT FLUCTUATION SQUARED = 0.0057
 THE INSTANTANEOUS RMS FLUCTUATION CURRENT RATIOS = 0.4805
 THE AVERAGE RMS FLUCTUATION CURRENT RATIOS = 0.1596

NOISE PARAMETERS FOR THE X-NOISE REGIONS

REGION	INSTANTANEOUS NUMBER OF PARTICLES	INSTANTANEOUS TEMPERATURE	AVERAGE TEMPERATURE	INSTANTANEOUS CHARGE FLOW	INSTANTANEOUS CURRENT FLUCTUATIONS	RMS NOISE CURRENT RATIOS	AVERAGE CURRENT
I = 2	0.3633E+04	0.6022E+05	0.6107E+05	-0.1490E+04	0.1911E+00	0.0560E+00	-0.0034E+01
I = 3	0.1505E+04	0.6960E+05	0.6455E+05	0.6570E+03	0.3402E-02	0.4925E+00	0.3656E+01
I = 4	0.0760E+03	0.6750E+05	0.6753E+05	0.6310E+03	0.4047E-02	0.4561E+00	0.3432E+01
I = 5	0.6810E+03	0.9946E+05	0.8944E+05	0.6490E+03	0.6306E-02	0.3603E+00	0.3590E+01
I = 6	0.5740E+03	0.1124E+06	0.1121E+06	0.6400E+03	0.1496E-01	0.2646E+00	0.3542E+01
I = 7	0.5640E+03	0.1220E+06	0.1332E+06	0.6500E+03	0.5504E-01	0.3311E+00	0.3464E+01
I = 8	0.5760E+03	0.1301E+06	0.1478E+06	0.6040E+03	0.1795E-04	0.2570E+00	0.3411E+01
I = 9	0.5950E+03	0.1520E+06	0.1557E+06	0.5020E+03	0.2410E-02	0.2516E+00	0.3340E+01
I = 10	0.5540E+03	0.1670E+06	0.1629E+06	0.5920E+03	0.1043E-01	0.3035E+00	0.3245E+01

REGION	INSTANTANEOUS NUMBER OF PARTICLES	INSTANTANEOUS TEMPERATURE	AVERAGE TEMPERATURE	INSTANTANEOUS CHARGE FLOW	INSTANTANEOUS CURRENT FLUCTUATIONS	RMS NOISE CURRENT RATIOS	AVERAGE CURRENT
J = 11	0.5940E+03	0.1630E+06	0.1640E+06	0.530E+03	0.1951E-01	0.3134E+00	0.3140E+01
J = 12	0.6100E+03	0.1700E+06	0.1680E+06	0.4760E+03	0.1124E+00	0.3009E+00	0.3027E+01
J = 13	0.6410E+03	0.1699E+06	0.1677E+06	0.5120E+03	0.1224E-03	0.2557E+00	0.2906E+01
J = 14	0.6110E+03	0.1747E+06	0.1741E+06	0.4900E+03	0.1005E-02	0.2310E+00	0.2762E+01
J = 15	0.5440E+03	0.1815E+06	0.1798E+06	0.4600E+03	0.1152E-03	0.2347E+00	0.2612E+01
J = 16	0.4890E+03	0.1931E+06	0.1898E+06	0.4070E+03	0.2087E-01	0.2439E+00	0.2446E+01
J = 17	0.4310E+03	0.2154E+06	0.2005E+06	0.370E+03	0.2776E-01	0.2356E+00	0.2270E+01
J = 18	0.3600E+03	0.2603E+06	0.2303E+06	0.3160E+03	0.8252E-01	0.2441E+00	0.2074E+01
J = 19	0.3420E+03	0.1947E+06	0.1909E+06	0.3190E+03	0.5499E-02	0.2008E+00	0.1678E+01
J = 20	0.3010E+03	0.1720E+06	0.1786E+06	0.2940E+03	0.3557E-04	0.1996E+00	0.1660E+01
J = 21	0.2670E+03	0.1831E+06	0.1811E+06	0.2700E+03	0.1427E-01	0.1944E+00	0.1453E+01
J = 22	0.1800E+03	0.1734E+06	0.1920E+06	0.2300E+03	0.6270E-02	0.1666E+00	0.1221E+01
J = 23	0.1440E+03	0.1624E+06	0.2011E+06	0.1620E+03	0.7361E-02	0.1520E+00	0.1002E+01
J = 24	0.1100E+03	0.2002E+06	0.2128E+06	0.1300E+03	0.3183E-02	0.1259E+00	0.7915E+00
J = 25	0.8000E+02	0.2180E+06	0.2305E+06	0.1060E+03	0.2159E-04	0.1043E+00	0.6040E+00
J = 26	0.4900E+02	0.3181E+06	0.2368E+06	0.6200E+02	0.7729E-02	0.8842E-01	0.4385E+00
J = 27	0.3600E+02	0.3008E+06	0.2513E+06	0.4300E+02	0.1421E-02	0.4776E-01	0.1105E+00
J = 28	0.9000E+01	0.1593E+06	0.2259E+06	0.2600E+02	0.6616E-03	0.3052E-01	0.1047E+00
J = 29	0.1400E+02	0.2397E+06	0.2037E+06	0.1500E+02	0.1579E-03	0.2585E-01	0.5533E-01
J = 30	0.3600E+01	0.1633E+06	0.1515E+06	0.1200E+02	0.1304E-03	0.2585E-01	0.2251E-01
J = 31	0.1000E+01	0.3967E+01	0.6771E+05	0.6000E+01	0.2764E-05	0.1390E-01	0.7310E-02
J = 32	0.0	-0.4825E+01	0.3583E+05	0.1000E+01	0.3983E-05	0.7487E-02	0.1996E-02
J = 33	0.0	0.1059E+05	0.1051E+04	0.0	0.1104E-06	0.2553E-02	0.3326E-03
J = 34	0.0	0.0	0.0	0.0			

NOISE PARAMETERS FOR THE Y-NOISE REGIONS

REGION	INSTANTANEOUS NUMBER OF PARTICLES	INSTANTANEOUS TEMPERATURE	AVERAGE TEMPERATURE	INSTANTANEOUS CHARGE FLOW	INSTANTANEOUS CURRENT FLUCTUATIONS	RMS NOISE CURRENT RATIOS	AVERAGE CURRENT
J = 2	0.0	0.0	0.0	0.0	0.0	0.0	0.0
J = 3	0.0	0.0	0.0	0.0	0.0	0.0	0.0
J = 4	0.0	0.0	0.0	0.0	0.0	0.0	0.0
J = 5	0.8200E+02	0.1680E+06	0.1035E+06	0.0	0.4802E-19	0.4513E-02	0.2191E-09
J = 6	0.2050E+03	0.2867E+06	0.2841E+06	0.5200E+02	0.1129E-02	0.0696E-01	0.2604E+00
J = 7	0.2540E+03	0.4266E+06	0.4266E+06	0.7400E+02	0.8076E-04	0.1043E+00	0.4095E+00
J = 8	0.2340E+03	0.5274E+06	0.5143E+06	0.9200E+02	0.1910E-03	0.9581E-01	0.5341E+00
J = 9	0.2630E+03	0.4966E+06	0.5543E+06	0.1100E+03	0.9631E-03	0.8134E-01	0.6530E+00
J = 10	0.2460E+03	0.6011E+06	0.6161E+06	0.1340E+03	0.1672E-04	0.8029E-01	0.7618E+00
J = 11	0.2810E+03	0.6306E+06	0.6412E+06	0.1590E+03	0.1252E-02	0.8495E-01	0.8637E+00
J = 12	0.2800E+03	0.6691E+06	0.6766E+06	0.1750E+03	0.3944E-03	0.1804E+00	0.9697E+00
J = 13	0.2960E+03	0.6266E+06	0.6721E+06	0.1900E+03	0.1439E-03	0.1137E+00	0.1042E+01
J = 14	0.2780E+03	0.6869E+06	0.6808E+06	0.2020E+03	0.7439E-04	0.7730E-01	0.1151E+01
J = 15	0.3210E+03	0.7394E+06	0.6806E+06	0.2260E+03	0.1086E-02	0.9876E-01	0.1245E+01
J = 16	0.3330E+03	0.6813E+06	0.6785E+06	0.2540E+03	0.1338E-01	0.1034E+00	0.1321E+01
J = 17	0.3680E+03	0.6750E+06	0.6747E+06	0.2430E+03	0.5831E-03	0.8861E-01	0.1390E+01
J = 18	0.3240E+03	0.7270E+06	0.6833E+06	0.2520E+03	0.2239E-02	0.1883E+00	0.1472E+01
J = 19	0.3780E+03	0.6776E+06	0.6952E+06	0.2620E+03	0.3730E-02	0.1125E+00	0.1543E+01
J = 20	0.3610E+03	0.6946E+06	0.7130E+06	0.2820E+03	0.6700E-04	0.9430E-01	0.1603E+01
J = 21	0.3560E+03	0.7681E+06	0.7511E+06	0.3010E+03	0.1560E-02	0.1178E+00	0.1663E+01
J = 22	0.3500E+03	0.7487E+06	0.7992E+06	0.2990E+03	0.8362E-03	0.1376E+00	0.1720E+01
J = 23	0.3730E+03	0.8912E+06	0.8501E+06	0.3010E+03	0.5032E-02	0.1302E+00	0.1773E+01
J = 24	0.3000E+03	0.8672E+06	0.9000E+06	0.3290E+03	0.8259E-03	0.1330E+00	0.1832E+01
J = 25	0.3900E+03	0.1043E+07	0.9649E+06	0.3280E+03	0.1157E-02	0.1211E+00	0.1889E+01
J = 26	0.4080E+03	0.1019E+07	0.1014E+07	0.3400E+03	0.4162E-04	0.1073E+00	0.1961E+01
J = 27	0.3900E+03	0.1043E+07	0.1040E+07	0.3630E+03	0.3194E-03	0.1108E+00	0.2035E+01
J = 28	0.3910E+03	0.1152E+07	0.1106E+07	0.4040E+03	0.2947E-01	0.1459E+00	0.2113E+01
J = 29	0.4190E+03	0.1179E+07	0.1154E+07	0.3980E+03	0.2310E-02	0.1151E+00	0.2202E+01

J = 30	0.4890E+03	0.1190E+07	0.1800E+07	0.4130E+03	0.1540E-02	0.1397E+00	0.2294E+01
J = 31	0.3710E+03	0.1220E+07	0.1236E+07	0.4100E+03	0.5003E-02	0.1381E+00	0.2395E+01
J = 32	0.1305E+07	0.1305E+07	0.1277E+07	0.4490E+03	0.1514E-02	0.1440E+00	0.2500E+01
J = 33	0.1310E+07	0.1329E+07	0.1329E+07	0.4550E+03	0.1574E-02	0.1376E+00	0.2613E+01
J = 34	0.4300E+03	0.1466E+07	0.1371E+07	0.4700E+03	0.3299E-03	0.1460E+00	0.2721E+01
J = 35	0.4200E+03	0.1344E+07	0.1421E+07	0.5090E+03	0.2223E-02	0.1368E+00	0.2831E+01
J = 36	0.4260E+03	0.1506E+07	0.1407E+07	0.5290E+03	0.1624E-02	0.1640E+00	0.2949E+01
J = 37	0.4430E+03	0.1503E+07	0.1525E+07	0.5430E+03	0.1702E-04	0.1285E+00	0.3066E+01
J = 38	0.4350E+03	0.1506E+07	0.1502E+07	0.5610E+03	0.7439E-04	0.1482E+00	0.3181E+01
J = 39	0.4600E+03	0.1630E+07	0.1640E+07	0.5810E+03	0.2402E-03	0.1450E+00	0.3301E+01
J = 40	0.4600E+03	0.1656E+07	0.1700E+07	0.5900E+03	0.1792E-02	0.1332E+00	0.3424E+01
J = 41	0.4650E+03	0.1701E+07	0.1716E+07	0.6100E+03	0.1170E-01	0.1306E+00	0.3550E+01
J = 42	0.4100E+03	0.1503E+07	0.1509E+07	0.6600E+03	0.1153E-02	0.1543E+00	0.3732E+01
J = 43	0.3350E+03	0.9353E+06	0.9549E+06	0.6610E+03	0.2804E-03	0.1470E+00	0.3721E+01
J = 44	0.2700E+03	0.8434E+06	0.8647E+06	0.6640E+03	0.1667E-02	0.1344E+00	0.3714E+01
J = 45	0.2596E+03	0.8596E+06	0.8829E+06	0.6550E+03	0.8819E-05	0.1000E+00	0.3707E+01
J = 46	0.2520E+03	0.8965E+06	0.9185E+06	0.6490E+03	0.5887E-03	0.1261E+00	0.3694E+01
J = 47	0.2320E+03	0.9209E+06	0.9720E+06	0.6510E+03	0.2466E-04	0.1760E+00	0.3686E+01
J = 48	0.2490E+03	0.1031E+07	0.1023E+07	0.6670E+03	0.7813E-02	0.1119E+00	0.3683E+01
J = 49	0.2500E+03	0.1030E+07	0.1066E+07	0.6430E+03	0.1496E-02	0.1610E+00	0.3675E+01
J = 50	0.0	0.0	0.0	0.5190E+03	0.1241E-02	0.1316E+00	0.2970E+01

NOISE PARAMETERS FOR THE Z-NOISE REGIONS

REGION	INSTANTANEOUS NUMBER OF PARTICLES	INSTANTANEOUS TEMPERATURE	AVERAGE TEMPERATURE	INSTANTANEOUS CHARGE FLOW	INSTANTANEOUS CURRENT FLUCTUATIONS	RMS NOISE CURRENT RATIOS	AVERAGE CURRENT
K = 2	0.0	0.0	0.0	0.0	0.0	0.0	0.0
K = 3	0.5410E+03	0.8354E+06	0.8834E+06	-0.1000E+01	0.1775E-04	0.1753E-01	-0.1441E-02
K = 4	0.1070E+04	0.1561E+07	0.1535E+07	0.3000E+02	0.7870E-03	0.6260E-01	0.1068E+00
K = 5	0.1121E+04	0.1446E+07	0.1466E+07	0.3000E+02	0.4150E-02	0.4051E-01	0.1052E+00
K = 6	0.1097E+04	0.1435E+07	0.1451E+07	-0.2000E+01	0.1567E-02	0.3920E-01	0.2827E-01
K = 7	0.1110E+04	0.1444E+07	0.1454E+07	0.1000E+01	0.2300E-04	0.2434E-01	0.1053E-01
K = 8	0.1151E+04	0.1511E+07	0.1448E+07	0.5000E+01	0.4872E-03	0.2982E-01	0.8994E-02
K = 9	0.1800E+04	0.1402E+07	0.1433E+07	0.2000E+01	0.9092E-04	0.2680E-01	0.1774E-02
K = 10	0.1071E+04	0.1472E+07	0.1461E+07	-0.3000E+01	0.3765E-03	0.2919E-01	0.2439E-02
K = 11	0.1104E+04	0.1450E+07	0.1449E+07	0.3000E+01	0.2953E-03	0.2583E-01	-0.2217E-03
K = 12	0.1145E+04	0.1450E+07	0.1466E+07	0.0	0.2601E-04	0.3379E-01	-0.5100E-02
K = 13	0.1101E+04	0.1401E+07	0.1459E+07	-0.1000E+01	0.5035E-04	0.3615E-01	-0.1275E-01
K = 14	0.1151E+04	0.1484E+07	0.1440E+07	-0.3000E+01	0.4253E-03	0.3355E-01	-0.3759E-01
K = 15	0.1113E+04	0.1454E+07	0.1470E+07	-0.1000E+02	0.1701E-02	0.4965E-01	-0.9779E-01
K = 16	0.1075E+04	0.1477E+07	0.1530E+07	-0.3500E+02	0.1776E-04	0.5654E-01	-0.1937E+00
K = 17	0.5540E+03	0.8954E+06	0.8842E+06	-0.2000E+01	0.1712E-03	0.1361E-01	0.1774E-02
K = 18	0.0	0.0	0.0	0.0	0.0	0.0	0.0

4-8
DT